Università degli studi di Padova

SCUOLA DI INGEGNERIA

CORSO DI LAUREA IN INGEGNERIA MECCANICA

Dipartimento di Ingegneria Industriale

Master Thesis

Evaluation of Compressor Blade Profiles characteristics at different operating conditions

Supervisor
Ch.mo Prof. Giorgio Pavesi

Supervisor
Prof. Friedrich-Karl Benra

Assistant Supervisor
Eng. Jan Philipp Schnitzler

Student
Luca Crosato

17 April, 2014

La struttura alare del calabrone, in relazione al suo peso,
non è adatta al volo, ma lui non lo sa e vola lo stesso
A. Einstein

Abstract

In order to analyze the performances of an axial compressor (or a turbomachine in general), the CFD analysis is widely used, especially for the investigation of the entire machine by 3-D simulations. This approach can require high computational time, thus in order to save it 2-D techniques like the streamline curvature method are even more used in order to study the machine by decreasing simulation time. In this method the meridian channel of the machine is cut in more slices in order to study a 2-D domain.

The achievement of this research is to analyze the performances of an axial compressor with four stages and IGV blades leveraging two-dimensional technique in order to define loss coefficient, flow deflection and flow angles (Inlet and Outlet) of each blade profile. This piece of information as well as for the performance analysis also serves to the setting of a new streamline curvature program. The ANSYS-CFX investigation is carried out deeply in detail for a dry operating condition and a primary analysis of wet operating condition is also considered.

Because of the high number of the blade profiles and the wide variability range of the working conditions, the entire simulation process from Meshing phase, to Pre and Post-Processing phases is processed through automatic Matlab scripts. Only one blade profile is analyzed for each simulation leveraging the steady-state approach by changing every time the inlet Mach number and the Incidence angle value.

The graphic results of loss coefficient and flow deflection, extracted from the dry condition investigation, are closer to those in literature, demonstrating the dependence from the initial condition setting, the geometry definition (shape of profile) and from the type of the blade (rotor, stator or IGV). Moreover the graphics show the good performance of the profiles and in the loss coefficient it is possible to investigate also the operating range, different for every working condition. Instead the wet situation is studied starting from the dry simulation results by the introduction of the water spray action. The trajectories of the water droplets injected upstream of the blade are investigated into the flow domain without resolving the flow field again leveraging the Euler-Lagrangian theory and also without considering the evaporation process. This kind of analysis shows the dependence of the performances of the compressor in two-phase flow condition by the investigation of the water mass fraction present at the Outlet of the domain, necessary to set the investigations considering the evaporation condition. With the final results it is also possible to evaluate the impact of the water droplet on the blade walls mostly in function of Incidence angle and diameter size of the particles.

Acknowledgments

I would like to express my sincer gratitude to my Supervisor Prof. Giorgio Pavesi from University of Padova for introducing me to the topic of this Thesis and for giving me the opportunity to get in touch with the Turbomachinery Institute at University of Duisburg-Essen. I would like to thank the German Supervisor Prof. Friedrich-Karl Benra and all the staff who work at the department of Turbomachinery in Duisburg for the knowledge, patience and hospitality given to me in this six months of research. In particular I am very grateful to Eng. Jan Philipp Schnitzler for his technical support and for his professionalism, without him this Master Thesis would not have been completed.

A special thanks to my family for the moral and financial support during my university carrier especially for the last six months in Germany. Their presence for me was what sustained me in these years. Furthermore I would like to thank my girlfriend Giulia for her love and for encouraging me to leave for a new experience abroad.

Last but for sure not least, I would like to thank all my friends always present in this course and also those which have allowed me to spend an unforgettable Erasmus experience in Germany.

Contents

1 Turbomachine **1**
1.1 Characterization of Turbomachinery . . . 1
1.1.1 Classification of the machines . . . 1
1.2 Brief history of Turbomachinery . . . 4
1.2.1 Root Blowers and Compressors . . . 4
1.2.2 Gas Turbine and Turbojet . . . 5
1.3 Theory of Turbomachinery . . . 7
1.3.1 Specific work and velocity components . . . 8
1.3.2 Efficiency definition . . . 10

2 Compressor theory **11**
2.1 Axial-Flow Compressor . . . 11
2.1.1 Velocity diagrams . . . 13
2.1.2 Dimensionless group . . . 14
2.1.3 Compressor design Approach . . . 15
2.2 Performance of a compressor . . . 16
2.2.1 Compressor map . . . 16
2.2.2 Surge and Chocking Conditions . . . 16
2.3 Streamline Curvature . . . 18

3 2D Cascade Theory **21**
3.1 Introduction . . . 21
3.2 Profile characteristics and parameters of the cascade . . . 23
3.2.1 General nomenclature . . . 24
3.2.2 Cascade Characteristics . . . 25
3.3 Aerodynamic behaviours . . . 26
3.3.1 Lift and Drag Coefficient . . . 27
3.4 Incidence and Deflection . . . 28
3.4.1 Loss Coefficient . . . 29
3.4.2 Incidence and Mach Number effects . . . 31
3.4.3 Deflection . . . 32

4 TGrid file generation **35**
4.1 Heavy Duty Multi-stage Axial Compressor . . . 35
4.1.1 Introduction . . . 35
4.1.2 Multi-stage Axial Compressor . . . 36
4.1.3 Blade shape . . . 37
4.2 Automatic Scripting of Profile . . . 38
4.2.1 Export profile points . . . 38

4.2.2 Scale of the blade . . . 40
4.2.3 Control volume definition . . . 40
4.2.4 TurboGrid File Definition . . . 42
4.3 Profile Meshing . . . 42
4.3.1 Validation Code . . . 45
4.3.2 Automatized of meshing process . . . 46

5 Single Phase Simulations 49
5.1 Operating Range . . . 49
5.1.1 Mach number . . . 49
5.1.2 Incidence Angle . . . 50
5.2 CFX Pre-Solver setting . . . 51
5.2.1 Basic Equations . . . 52
5.2.2 Domain analysis . . . 54
5.2.3 Solver setting . . . 55
5.3 Automatic scripting Pre-Solver files . . . 56
5.3.1 Computational details . . . 58
5.4 CFX Post Processing . . . 58
5.4.1 Evaluating of simulations . . . 59
5.4.2 Reference planes positions . . . 60
5.4.3 How to calculate the results . . . 62
5.5 Automatic Scripting of results . . . 64
5.5.1 Cleaning results . . . 65

6 Two-Phase Flow 67
6.1 Introduction . . . 67
6.1.1 Overview of spray action . . . 67
6.2 Axial Compressor wet condition . . . 68
6.2.1 Achievements of the work . . . 69
6.3 Two-Phase Simulation . . . 71
6.3.1 Analysis Conditions . . . 72
6.4 Simulation setting . . . 73
6.4.1 Pre-Solver Setting . . . 74
6.4.2 Solver Setting . . . 78
6.4.3 Post-Processing . . . 78
6.5 Automatic Scripting of the Simulations . . . 79

7 Results 81
7.1 Single Phase Flow Results . . . 81
7.1.1 IGV Results . . . 82
7.1.2 Rotor Results . . . 88
7.1.3 Stator Results . . . 98
7.2 Two-Phase Flow Results . . . 105
7.2.1 Diameter size influence . . . 105
7.2.2 Incidence angle influence . . . 106
7.2.3 Mach number influence . . . 110

8 Conclusion 113
8.1 Conclusion . . . 113

A Geometry construction and Mesh definition **117**
A.1 General Script 117
A.1.1 Extraction profile points 118
A.1.2 Mesh Definition 120

B ANSYS Pre and Post Processing **121**
B.1 General Script 121
B.1.1 ANSYS CFX Pre Setting 122
B.1.2 ANSYS CFD Post Processing 123

C Wet condition ANSYS Pre **125**
C.1 ANSYS CFX Pre Setting 125

Chapter 1

Turbomachinery

1.1 Characterization of Turbomachinery

In the Field of Turbomachinery are described machines which can exchange energy from Fluid to Rotor or from Rotor to Fluid. In other words, these devices can transfer energy by the dynamic action of the blades of the rotor with the flow field (liquid or gas). This interaction produces a positive or negative work (it depends on the machine). Due to this work the stagnation enthalpy of the fluid moving into the flow duct changes and it can increase (case of a compressor) or decrease (turbine). The goal of this kind of machines is to obtain the maximum energy transmission or output power with minimum losses, both hydraulic and thermodynamic. The achievement of the designers is to find the best configurations for a turbine or a pump, i.e., to provide the optimum working conditions with a wide range of operation. This range can be found with the analysis of the Loss Coefficient and the Deflection of the Flow. These two aspects will be studied and discussed in this work, and the whole argument will be analyzed more in detail in the next Chapters.

1.1.1 Classification of the machines

Turbomachinery can be divided in two big classes by the direction of the energy exchange:

- Absorb power: the machine gives energy to the fluid field, in order to increase the head or fluid pressure (compressors, pumps and ducted fans).
- Produce power: the device expands fluid to a lower pressure in order to give the power to a machine's shaft for an electric generator or for a generic engine (gas, steam and hydraulic turbines).

Another subdivision of turbomachinery can be made according to the geometry of the flow trough the rotor (fig. 1.1):

- Axial flow: the flow has the same direction or is parallel to the rotational axis.
- Radial (or Centrifugal) flow: when the flow has a radial direction, therefore the fluid's direction is fully (or mainly) perpendicular of the rotational axis.
- Mixed flow: when a prevalent direction cannot be identified and both velocity components (axial or radial) are significantly present.

Another categorization can be imposed by the characterizing different approaches in the exchange of energy i.e.: if the pressure only changes in the stator or in the entire stage of the machine:

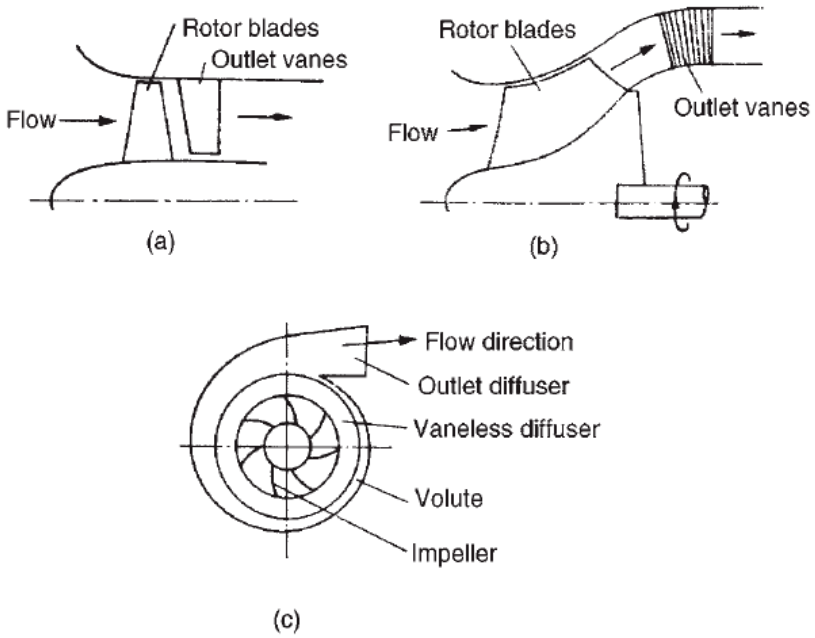

Figure 1.1: Different type of turbomachines: a)Axial Flow, b)Mixed Flow, c)Radial Flow [5]

- Impulse machines: the level of pressure changes only through the stator components (or nozzles) of the machines, then the fluid is directed to the rotor. This effects depends on the shape of the blades.
- Reaction machines: here the pressure changes in part through the stator and in part through the rotor.

This last characterization is especially applied in the turbines field in particular the type called Impulse machines, can operate with high value of rotational velocity but, also for this reason, with high frictional losses. Normally impulse blades are used for the first stage of a turbine, where an high efficiency is required, to the contrary of the last stages of the machine, where it is possible to use the reaction type to minimize losses.

Turbomachinery can transfer energy through one or more stages. A single stage is formed from one row of rotor blades and another row of stationary blades, the shape will be totally different on the basis of the design conditions as well. Through the rotating part there is the exchange of energy while the stationary part of the machine, that it is introduced upstream or downstream (it depends on the machine), generates the swirling of the flow, or introduces the fluid into the rotor in a straight flow, or also decreases the axial component of the absolute velocity to increase the specific work done (as it will be possible to observe in the following paragraphs). However the specific work is only exchanged through the rotor; the task of the stator is to transform the energy, i.e., from thermal to kinetic or from kinetic to thermal. More stages are usually found on high power machines in order to transfer energy, but this imply high costs to produce the device. Depending on the pressure additional stages may be required complying with the structural requirements.

Another category should be mentioned, this is not in function on the type of the machine, but it depend on the flow condition:

- Incompressible: the flow can be studied with the normal equations of the ideal gas

and the basic equations of thermodynamic.

- Compressible: the flow must be studied with the gas-dynamic theory implemented with ideal gas thermodynamic equations.

A short list of machines will be reported in order to better understand the field covered from turbomachinery, depending on the task required. As it is written at the beginning the first category is Absorb power machines. This is the field of compressors (axial or centrifugal), pumps, and blowers. These devices are used in a wide range of industrial applications and processing.

Power producing machines are the second category and this is the world of turbines and turbojet (or turbofan: aeronautic engines). The turbines have a wide range of applications for power production, starting from many different types of primary energy (thermal, hydraulic or wind energy). In thermal applications it is possible to find gas or steam turbines; for hydraulic uses the known machines are Francis, Pelton, and Kaplan turbines.

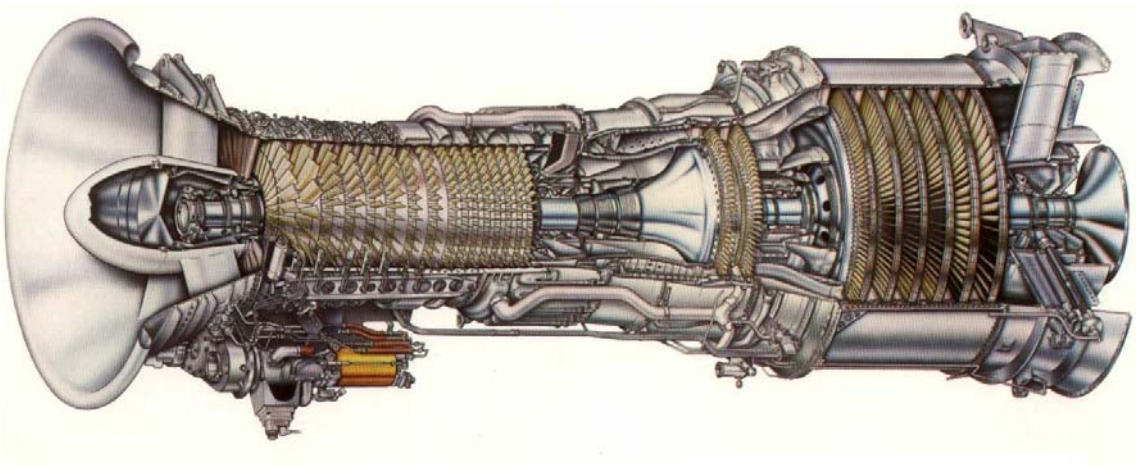

Figure 1.2: Example of turbomachinery: gas turbine type LM 2500 by General Electric. From left to right: compressor, combustor, and turbine

As any machine, in order to provide the best possible design in accordance to its working field a turbomachine should be engineered by the means of the thermo-fluid dynamic. Fundamental analytical laws are:

- Equation of Continuity
- First Law of Thermodynamics (for steady flow system)
- Newton's Second Law
- Second Law of Thermodynamics
- Dimensional analysis
- Laws of Aerodynamics or Hydrodynamics

With the first four laws it is possible to define the entire stage of the machine. Therefore, it is possible to solve the problem of compressible and incompressible flow and the thermo-fluid dynamic behavior of Turbomachinery.

Efficiency is deeply affected by the design of the blades which must be engineered with special attention to the internal dynamic of the flow. At the end, in order to specify the material to build the blades, it is necessary to involve the dimensional analysis.

1.2 Brief history of Turbomachinery

Nowadays the state of the art of Turbomachinery is represented by modern turbofan engine (or fanjet), which is found in aircraft propulsion, or the modern turbo-compressors, which are used in combined cycles or cogeneration plants, in order to produce electricity. In the next paragraph this kind of devices will be explained in detail. Even if humanity as always tried to take advantage of natural power sources the cutting edge technology that is involved in the engineering of nowadays turbomachinery is only been capitalized with computational codes and computer aided design.

After a strong struggle the creation of an optimization process for new manufacturing was made possible, and create also a database of experimental testing to include in simulation programs in order to describe the real machines behaviours was created. Experimental data have also been included in the metallurgical field in order to develop high temperature performing materials.

A short evolution of the machines will be reported from the work of Meher-Homji, just as an example. He documented the increasing power in aircraft engines in the paper *The historical evolution of Turbomachinery* [18]; in 1925 an aircraft engine had 350 hp and with new approaches and studies, in 1945 the engines increased their power to 3500 hp, hence approximately ten times more. After that there was a radical revolution of technology, due to a strong industrial competition in the half of the twentieth century, hence the research started to aim at the highest performance possible.

In the further paragraphs, the attention will concentrate on the compressor development, gas turbine and turbojet history.

1.2.1 Root Blowers and Compressors

The development of compressors or turbocompressors mainly occurred in the second half of the nineteenth hundreds, together with the evolution of the steam turbine. The firsts pioneers of this kind of turbomachinery came from Indiana [18], they were P.H.Roots and F.M.Roots. They needed a method to exploit the force of the water stream from a canal, in order to produce mechanical energy for driving a line shafts. They wanted to use an hydraulic turbine, hence at first, they made a new device with a metal sheet shell and wooden impeller. As it is possible to understand, the big problem was the wood for the rotor, but after some adjustments they could build the first Roots Blower in 1859 [18], an ancient lobe pump used for mine ventilation. Nowadays this machine is used as positive displacement blower or as air blower commonly used in car engines. This was an ancestor of compressors like they are known today.

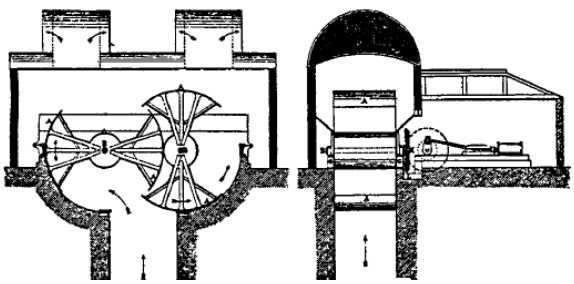

Figure 1.3: The first Roots Blower [18]

The field of compressors, is divided instead in two big categories: Axial or Centrifugal.

The first examples of centrifugal machines were built around the end of the fifteenth century without any knowledge about aerodynamic conditions and only with the basic equations of the ideal gas. However, the most important development was achieved at the end of the nineteenth century, when designers started to appreciate the force of compressors.

One of the first compressor was designed from Rateau [18], who soon became the major designer of compressors, because his machines could work in a large operating range contrarily to the previous. Furthermore he tried to match an high speed steam turbine and his compressor and this was the most important goal, because it was the first form of fan (today turbofan) and it was used in many different applications, i.e., for ventilation service and several others. Rateau made another important discovery, the multi-stage compressor; that could achieve an higher efficiency.

The first axial flow compressor was designed from Sir Charles Parson (1884) [18], this was a low-pressure compressor with an efficiency of 55% and that because of the stall of the blades [5]. Some years later he designed an 80-stages axial flow compressor with an adiabatic efficiency of around 70-80 percent, and further he could build a 41-stage axial flow with the same high efficiency. However the problem was always the same, he could not have aerodynamics knowledge and it wasn't solved until the half of the twentieth century (1926), with a new approach of design and later with the birth of computers aided codes. After that period different studies started to develop the axial multi-stage compressors implementing the airfoil theory for turbines as well.

Indeed, A.A. Griffith and his team at the Royal Aircraft Establishment, Farnborough [18], discovered that was possible to achieve an efficiency of around 90% with small stages.

Since the second half of the twentieth century, the achievements for the designers are to obtain compact and light engines. One of the first high performances compressor has been designed a single shaft 15-stages axial compressor (pressure ratio 12.1 and mass flow 27.3 kg/s [5]) for electric production (6 MW) used in industrial gas turbines. In this new compressor was considered the possibility of changing the stagger angle of the stator blade (in order to control the flow through the machine and the stall effects).

Today the state of the art is represented by multi-stages axial compressors with maximum efficiency of 90.9%, with pressure ratio 1.804 and lower rotational speed [5]. The last factor means less friction losses and less power required to move the shaft, hence in a turbocompressor used in a combined cycle i.e., more power generated and less required from the compressor.

1.2.2 Gas Turbine and Turbojet

Producing gas from the fuel was an idea arrived at the end of the eighteenth century, with John Barber [18] who discovered the main concept of gas turbines. One hundred years later, Dr. J. F. Stolze built the first real gas turbine (1872) which included some concepts of caloric and hot-air engines. This device, called hot air turbine, consisted in a multistage axial compressor and multistage reaction turbine together. But, as mentioned before, a lack of understanding of fluids dynamics affected the performances. Together with compressor and turbine a rudimentary coal gasifier was used in order to produce gas from fuel, and that was an ancient kind of combustor used today in a general type of gas turbine. Here below are reported the main characteristics of the machine in order to show the design level [fig. 1.4]:

- single shaft machine
- single silo combustor

- 10 stages axial flow compressor
- 15 stages reaction turbine (inlet temperature 400°C)
- alternator able to produce 150 kW.

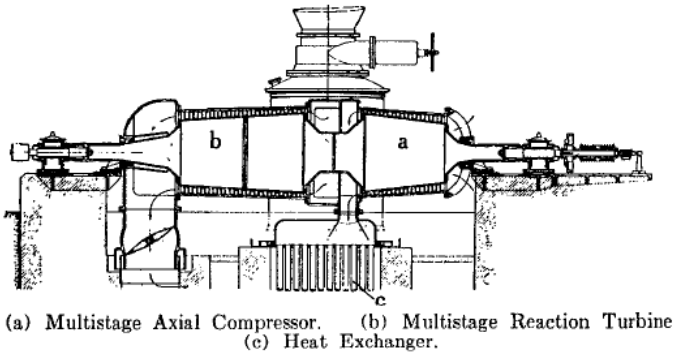

Figure 1.4: Scheme of Stolze Gas Turbine [18]

The invention of constant-volume gas turbine (developed by Dr. Holzworth [18]) at the beginning of the twentieth century revolutionized the world of gas turbines. The most important aspect was that the hot air from the compressor was directed into a small fuel chamber. The mix of hot air and fuel burst and this created an increase of pressure of more than four times the inlet value. Only a small part of the power produced by the turbine was required to cool its blades (by water) and to drive the compressor. The exhaust smokes from the turbine were still hot (or relatively hot) and Dr. Aurel Stodola, immediately before the second world war, suggested to use those fumes to produce steam. That was the first approach at the world of combined cycle.

Between the two World Wars great powers recognized the importance of the airborne weapon and largely funded research in this field. The most important turbojet revolution occurred in England due to Sir Frank Whittle and in Germany thanks to Hans von Ohain. They wanted to develop an engine able to fly up to 30000 ft (up to 9100m) and increase the speed to around 500 mph (ca. 800 km/h) [18]. They initially started to build their engines without any help from governments or big companies.

The main idea of *Whittle's work* was to produce a new concept of single shaft turbojet using an axial-centrifugal compressor, tubular combustor, and two stages turbine. That was simple, robust and it had a rapid development capacity, indeed most companies offered him money to buy his patent and also Rolls Royce adopted, some years later, the Whittle type's jet engines.

On the other side, *Von Ohnain's work* consisted of using a centrifugal compressor and a radial inflow turbine in order to reducing the problem of the matching. At this earlier date he arrived very closer to the fixed achievement with this rudimentary machine. Only in a second time he changed the layout using a radial compressor. After Heinkel bought his design Von Ohnain began to develop an even more efficient engine.

Today, the state of the art of turbofans is represented by centrifugal or axial compressors and turbines with one or more shafts. The convenience of a centrifugal compressor resides in the pressure ratio, since it is possible to obtain a ratio of 4-6 (or more), while with axial devices the pressure ratio is lower, around 1-2 (2 in transonic condition) [20]. Anyway, the axial compressor has an higher efficiency and it can work with high mass flows.

1.3 Theory of Turbomachinery

According to the first paragraph, one of the most important laws for Turbomachinery is the Newton's second law of motion. The equation shows the equilibrium of the forces acting in a specific direction. However, in a turbomachine it is also possible to consider the moments which those forces generates respect to the rotational axis in order to directly find the total moment or shaft torque. The following picture shows [1.5] a general machine rotor, without geometric details and blades. The rotor into the control volume is considered without rotational motion, [5] and the flow is stationary. The inlet velocity is called **c1** (absolute velocity) and the outlet one is **c2**. These are the general velocities in inlet and outlet surfaces generally directed.

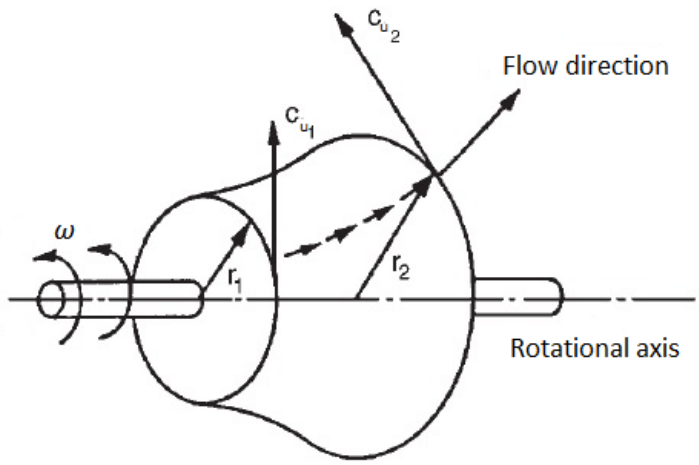

Figure 1.5: Control volume for a generalized turbomachine [5]

The variation of moment of momentum of the fluid respect to the rotational axis can be compared to the moments of all the external forces in the same axis. This is Newton's second law for Turbomachinery [2]:

$$M = \dot{m}(r_2 c_{u2} - r_1 c_{u1}) \tag{1.1}$$

In the equation [1.1] all the forces applied in the control volume are considered and can be divided in two types:

- pressure forces: work on the rotor's walls and on the inlet and outlet sections
- viscosity forces: work only on the rotor's walls

A big percentage of the moment rate **M**, depends on the work of the pressure forces, and in a minimum percentage on the presence of the other types of forces. The previous equation (1.1) is written for an absorbing power machine, where the fluid increases heat or pressure (the subscript 1 is for inlet and 2 is for outlet section). Otherwise, in an power producing machine the subscripts are inverted as it is written in the next equation, because the machine produces energy from the fluid:

$$M = \dot{m}(r_1 c_{u1} - r_2 c_{u2}) \tag{1.2}$$

Another important law is the Euler's equation which defines the power transfer of the rotor. As an example, the equation for a compressor is:

$$P = M * \omega = \dot{m}(u_2 c_{u2} - u_1 c_{u1}) \tag{1.3}$$

where ω is the angular velocity that can be derived from the tangential velocity $u = \omega * r$.

In a monodimensional case, the specif work can be defined in two different way, it depends on the type of turbomachine. For a compressor (absorbing power machine [1.4]) the work is done on the fluid. While, for a turbine (producing power machine [1.5]) the work is done on the rotor. In each case the specific work is always positive:

$$L = \frac{P}{\dot{m}} = (u_2 c_{u2} - u_1 c_{u1}) > 0 \tag{1.4}$$

$$L = \frac{P}{\dot{m}} = (u_1 c_{u1} - u_2 c_{u2}) > 0 \tag{1.5}$$

Without the monodimensional theory the Euler's law is still true. Indeed, it can be shown that instead of considering the entire domain, an elementary control volume is taken under exam and only the mass flow rate in that domain is considered. The equation is the same and for a compressor will be [5]:

$$dM = d\dot{m} = (r_2 c_{u2} - r_1 c_{u1}) \tag{1.6}$$

There are many different ways to solve the integral problem in order to find the amount of the momentum and thus the power of the machine. For example, the integral could be solved by the calculation of tangential velocity at the inlet section and at the outlet section, it is also possible to find a mass flow integral average. Hence, the equation of moment of momentum (1.2) and the Euler's equation (1.4) are always valid in the monodimensional theory. Indeed, if the fluid flow has a casual direction at the inlet or outlet section, the problem is resolved by calculating the average integral of the mass flow.

1.3.1 Specific work and velocity components

In order to describe the path of a general fluid particle through the rotor, it is possible to divide the motion in two different reference systems:

- absolute: it is fixed with the stationary part of the machine
- relative: it is fixed on the machine's rotor and it has a specific angular velocity

The velocity, in the first reference system is called, "absolute velocity" **c**. While the velocity in the second reference system is called "relative" **w**. There is a relation between these two velocities [2]:

$$c = w + u \tag{1.7}$$

This equation describes a vectorial triangular construction and the correlation between the velocities is called velocity triangle or velocity diagram, and it is a geometrical representation of the vectorial components of the velocities in a turbomachine. These triangles should be drawn in inlet and outlet section in order to define, as is written before, the condition (efficiency, specific work and other significant values) of the machine. The velocity components are also calculated to find the angles conditions that will be important, as it will be written below, to design the correct bending of the blades.

From the first law of thermodynamic, the total enthalpy h_1^0 at the stagnation point is defined as a sum of specific enthalpy and the absolute velocity value [2]:

$$h_1^0 = h_1 + \frac{c_1^2}{2} \tag{1.8}$$

this equation is always true, also for not ideal gas.

After some rearranging of the first law of thermodynamic (1.8) and the Euler's law (1.3), a new equation of the specific work has been found, and it is valid for steady, adiabatic and irreversible flow [2]:

$$L = u_2 c_{u2} - u_1 c_{u1} = h_2 + \frac{c_2^2}{2} - h_1 - \frac{c_1^2}{2} = h_2^0 - h_1^0 \tag{1.9}$$

Otherwise, a new physical quantity has been defined to study the flow in a rotating system. This is called Rothalpy **I**, and this is a contraction of rotational stagnation enthalpy [5] defined as is written below:

$$I = h_2 + \frac{w_2^2 - u_2^2}{2} = h_1 + \frac{w_1^2 - u_1^2}{2} \tag{1.10}$$

This value is the same between inlet and outlet sections, hence it should be constant in a flow line in this volume (only for rotor or moving duct), as well as it is for the total enthalpy in a stator.

According to the thermodynamic laws, it is also possible to write another equation for the specific work. Thus combining both previous equations ((1.9) (1.10)) the specific work is so defined [2]:

$$L = \frac{c_2^2 - c_1^2}{2} + \frac{u_2^2 - u_1^2}{2} + \frac{w_1^2 - w_2^2}{2} \tag{1.11}$$

This function uses the differences of the velocity components and it is useful in order to compare the amount of action work (dynamic size) respect to the reaction work (static size):

- Action work: comes from the acceleration of the absolute flow through the rotor:

  $$L_a = \frac{c_2^2 - c_1^2}{2} \tag{1.12}$$

  this work must be considered in the fluid dynamics losses

- Reaction work: it depends from the centrifugal effects and from the deceleration of the relative flow:

  $$L_r = \frac{u_2^2 - u_1^2}{2} + \frac{w_1^2 - w_2^2}{2} \tag{1.13}$$

  the first term considers the centrifugal effects and it won't be considered in the losses calculation. The other term measures the deceleration of the flow and must be considered as a function of the fluid dynamics losses, as well as the acceleration of the absolute flow.

Hence the final definition of the specific work can be written as below:

$$L = L_a + L_r \tag{1.14}$$

The previous equations are written for absorbing power machines, but could be also used for producing power machine. The only difference is that the indexes 1 and 2 must be inverted in order to change the sign of the specific work [2]:

$$L = \frac{c_1^2 - c_2^2}{2} + \frac{u_1^2 - u_2^2}{2} + \frac{w_2^2 - w_1^2}{2} \tag{1.15}$$

1.3.2 Efficiency definition

The *Efficiency* of a turbomachine is the comparison between the real quantity of energy transferred and the ideal thermodynamic process. For example, in an absorbing power machine, the ideal specific work is less then the real specific work. Conversely, for a producing power machine, the real energy produced is less than the ideal one (this is because of the increase of the entropy) [20]:

$$\eta_{ab} = \frac{L_{id}}{L} \tag{1.16}$$

$$\eta_{prod} = \frac{L}{L_{id}} \tag{1.17}$$

A wide treatment of the Efficiency is included in the literature of turbomachinery, but for the purposes of this thesis it is enough to know that there are two types of Efficiency.

One is the *Isentropic Efficiency* calculated with the isentropic work L_{is}. This value represents the exchanged work if the process occurs without losses, in other words without the increase of entropy. Below are written the formulations for compression and expansion [20]:

$$Compression\ \eta_c = \frac{L_{is}}{L} = \frac{h^0_{2is} - h^0_1}{h^0_2 - h^0_1} \tag{1.18}$$

$$Expansion\ \eta_e = \frac{L}{L_{is}} = \frac{h^0_1 - h^0_2}{h^0_1 - h^0_{2is}} \tag{1.19}$$

The isentropic efficiency is not very useful to define the technological level of a turbomachine. This because of the irreversibility of the flow and the efficiency depending on the inlet/outlet pressures. Indeed, for a multistage turbomachine, the isentropic efficiency is less than a single stage machine (because of the entropy losses increase). The efficiency directly depends on the pressure ratio [20]:

$$\pi_c = \frac{p^0_2}{p^0_1} \tag{1.20}$$

and also on the final temperatures (first law of thermodynamic). Hence as pressure ratio grows higher isentropic efficiency decreases.

For these reasons another function has been adopted in order to evaluate the technological level of the machine, without considering the pressure ratio. This is called small stage or *Polytropic Efficiency*. This is the efficiency of an adiabatic thermodynamic process where the pressure ratio is around one. It means that the difference of the inlet and outlet pressure is an infinitesimal value and generally it is also possible to define this polytropic efficiency as [20]:

$$\eta_{pol} = \frac{dh_{is}}{dh} = \frac{dp/\rho}{c_p dT} \tag{1.21}$$

In the literature it is possible to find a correlation between isentropic efficiency, polytropic efficiency, and pressure ratio. Through those graphics it is possible to understand the performances of machine, or to make the first steps in a design approach.

Chapter 2

Axial Flow Compressor

2.1 Axial-Flow Compressor

The main purposes of a compressor hence of an axial compressor as well, are to increase the pressure of the gas flow given in inlet and provide the volume or mass flow rate requests. According to the first Chapter, the compressor is an absorbing power machine thus it needs power to transfer the energy from the rotor to the fluid. This process should happen with the maximum isentropic efficiency and the minimum energy required. The machine is formed by a rotating blades row before the stator blades.

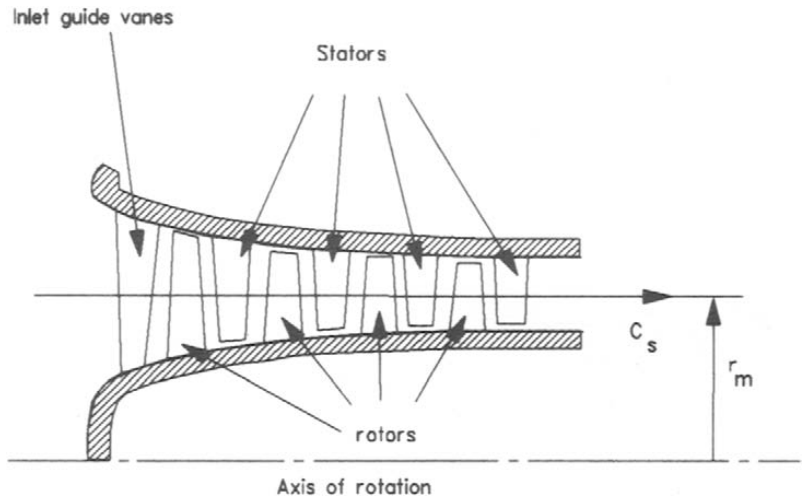

Figure 2.1: Scheme of axial flow compressor with IGV blades and four stages (1 stage=rotor+stator) [17]

Most of the time, in multi-stage machines another kind of blades is also present (stator blades) [fig. 2.1], these are called in different ways in function on the working conditions:

- IGV (Inlet Guide Vanes): stator blades, at the beginning of the compressor. Their task is to deflect the flow in order to accelerate the absolute velocity, hence the kinetic energy of the flow is increased. The goal is to decrease the relative inlet Mach number at the entrance of the first stage, thus it is possible to obtain a lower blade loading.

- OGV (Outlet Guide Vanes): stator blades, at the end of the machine. This type of blades is used in order to increase the resistance of the outer casing of the compressor

and to reduce the tangential component of absolute velocity after the last stator blades.

The IGV or OGV are mounted in a variable pitch angle system in order to increase the performance of the compressor in on and off design condition due to the flow control.

The aim of rotating blades is to convert the mechanic energy coming from the shaft to fluid enthalpy. This is possible with the raise of temperature (static and total), pressure and absolute velocity and with the reduction of the relative one. Otherwise, the task of the stator blades is to decrease the absolute velocity in order to increase the value of the static pressure. This phenomenon can be observed in the picture below (fig. 2.2) where the variations of the most important parameters as mass flow rate, pressure ratio, and rotational velocity are reported, describing the thermo and fluid dynamics behaviours of the compressor.

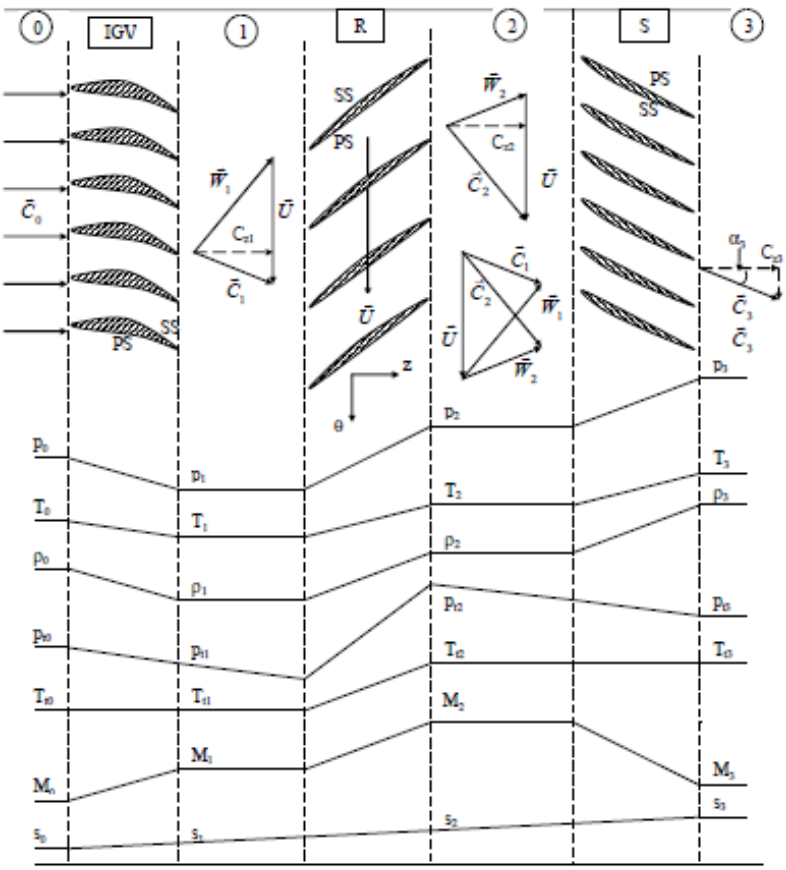

Figure 2.2: Behaviour of the quantity through a single stage of an axial flow compressor [2]

The graphics *h-s* (fig. 2.3), describe the entire compression process in a general stage, where 1-2 show the compression in the rotor blades and 2-3 describe the process through the stator. The known inlet conditions normally are pressure (total or static), temperature (total or static), and sometimes velocity. Hence, it is possible to define point 1, static and stagnation conditions (total), in that graphic. Furthermore, from the pressure ratio and the isentropic specific work, the real work done is defined. In order to track the trend of the process in that graphic, for the rotor the conservation of the Rothalpy must be considered [Chapter 1], so point 2 is also totally defined. To define the process through the stator it is necessary to consider the conservation of the total enthalpy between the points 2 and 3.

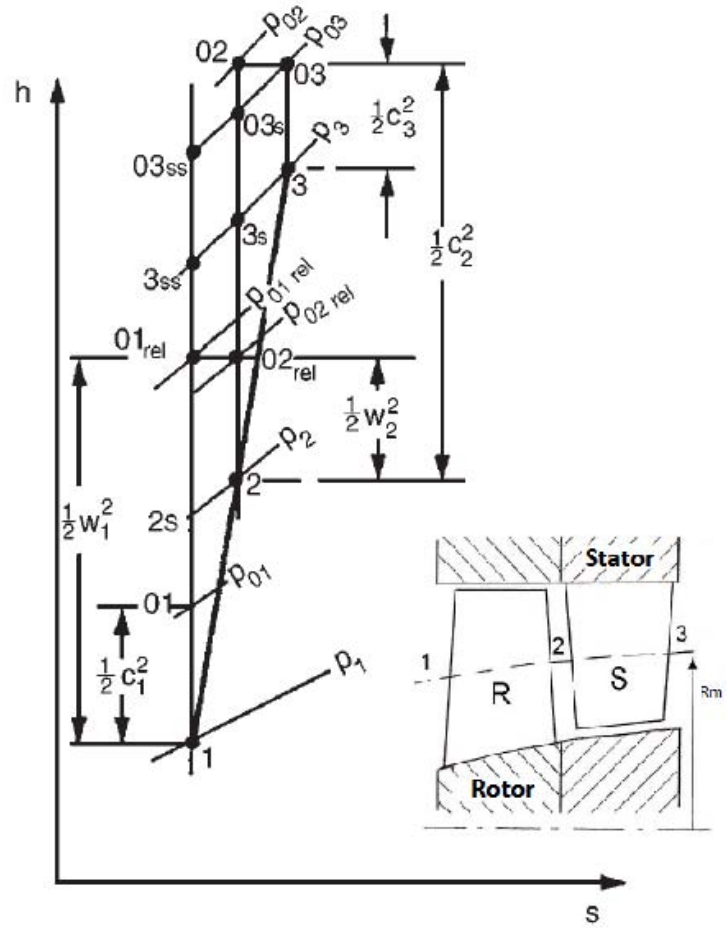

Figure 2.3: Mollier graphic of the entire compressor process [5], and in the bottom, the particular of a single stage of the machine [2]

Now the process is wholly described and it is possible to analyze the parameters affecting the total-to-total efficiency of an axial compressor [2]:

$$\eta_{TT} = \frac{Total\ Enthalpy\ Ideal\ Stage}{Total\ Enthalpy\ Real\ Process} = \frac{h^0_{3s} - h^0_1}{h^0_3 - h^0_1} \tag{2.1}$$

As it is reported in the graphic (fig. 2.3) and as it has already been written in the first Chapter, there is an increase of entropy level at the end of the process. This is because the general frictional losses are not considered in the isentropic compression hence, the final temperature T_3 will be higher than the temperature in a ideal stage T^0_3 [17].

2.1.1 Velocity diagrams

The convention of the velocity diagrams is reported in the picture (fig. 2.4) and it is possible to see how velocity changes in the generic stage of an axial compressor. Obviously, for the rotor blade the velocity considered is the relative value, instead for the stator it is necessary to evaluate the absolute one. As in literature, in order to calculate the thermodynamic condition of the rotor blade (or in general the condition of the stage), the angle considered for the calculation is called β and this is the angle between the meridional and relative

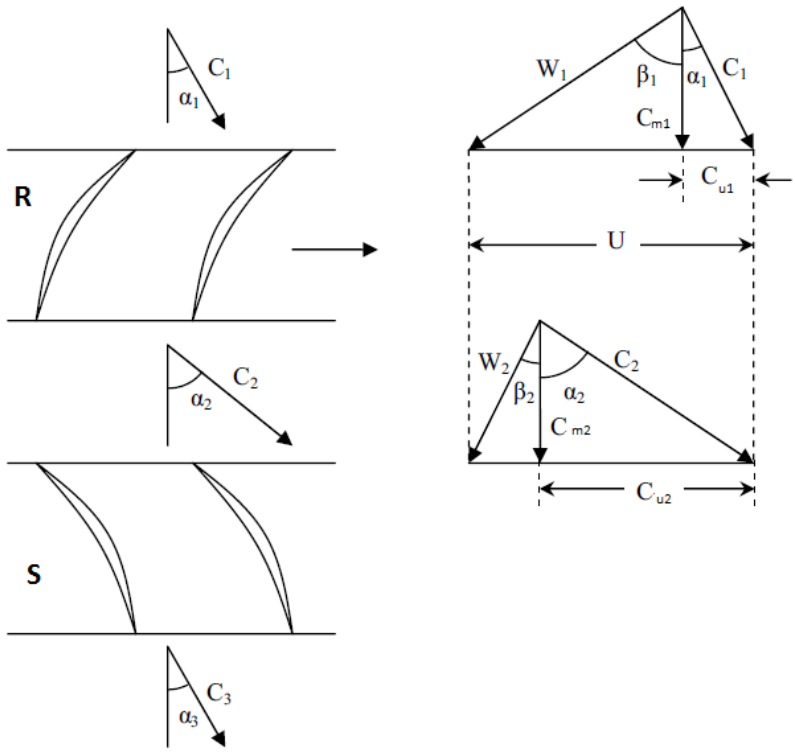

Figure 2.4: Velocity triangles for a generic stage of a compressor [6]

velocity. Instead, α is the angle between the meridional and absolute velocity and this is calculated for the stator blade row. The flow coming from the IGV arrives at the Inlet section of the rotor oriented with a defined angle (β), as it is already known the relative velocity decreases and the absolute increases (see the behaviour of the parameters fig. 2.2). Thus, the flow arrives to the Inlet section of the stator with a specific angle (α) and then trough the duck the absolute velocity decreases [5] [17] [2].

It is possible to call *normal* stage of a compressor, which has the absolute velocity at the rotor inlet equal in value and direction with the stator outlet one ($C_3 = C_1$). In this way, the design of the compressor is easier because it can be possible to repeat the same configuration for all the stages. The diffusion of the velocities is one of the most important point in the design or in the performance analysis of a compressor for the iteration with the calculation of the specific work and the losses evaluation.

2.1.2 Dimensionless group

In this Thesis the dimensionless group theory is not reported because there are many papers in literature about this argument, and this is not the focus of this work. Here, a general view of the main variables that have a big interaction with the performances of the compressor will be reported. An explicit description of these variables has been found in literature [17] with the explanation of the physical quantity taken under exam:

$$\eta_{TT} = f(\phi,\ \psi,\ R,\ w_1,\ c_2,\ M_1,\ M_2,\ Re,\ \zeta_R,\ \zeta_S) \tag{2.2}$$

Those variables could be divided in a dimensionless groups as follows:

- Thermodynamics conditions: duty coefficients (ϕ, ψ) are the first parameters in a design process of a compressor and it could give the general shape of the velocity

triangles. Flow coefficient ϕ, is a ratio between the meridional velocity and tangential velocity. Instead, the work input coefficient ψ is the ratio of the stagnation enthalpy rise and the tangential velocity squared. It is also possible to define the reaction degree R as a ratio between the specific enthalpy rise through the rotor and the specific enthalpy rise through the entire stage.

- Velocity triangles: the most important velocities to study are the relative one for rotor and the absolute one for stator.

- Mach Numbers: this is the ratio between the velocity (absolute or relative) and the speed of sound. This parameter should be controlled in a design or testing process because the working condition (subsonic, transonic, and supersonic) depends on the mach number.

- Flow Properties: this is in function on the stage Reynolds number, calculated at middle span (middle radius), and it depends on the flow condition (dynamic viscosity)

- Losses (rotor and stator): there are two different approaches for discussion about the losses, one is with two-dimensional view (this is the focus of the present work) and the other is with 3D system, in order to declare the performance of the entire blade.

In a design process, i.e., only the flow coefficient, inlet work condition, or reaction stage degree can be fixed in order to predict the performance of the compressor. The usual values of ϕ are between 0,45-0,6 for a good design, in order to obtain a velocity triangle proportioned between relative and absolute velocities to minimize the losses. The typical values of ψ should be less than 0,45 in order to be far from the stall zone (read next paragraph) and decrease the blade loading. The stage reaction degree depends on the type of the blades (first or last stage) and the usual values are between 0,5-0,65 [2].

2.1.3 Compressor design Approach

In order to design or obtain a high performance axial compressor there are other important aspects to take into account as the best practice known today as the state of the art.

Since few years ago different types of blades profile from NACA-65 have been adopted in function on the application field of the compressor [20]. First of all because the sonic or supersonic conditions are increasingly required especially in the aviation engines, secondly because today the compressors are used in a lot of different applications (electric generation, industrial purposes, etc.) and in different working conditions. Hence highly performances and highly operation ranges are required. Nowadays, instead of NACA-65 profiles, it is possible to find shape profile like DCA (double arc circle) or special profiles optimized for the specific application [15] [24].

The blades can be built in titanium or aluminum alloys or also in nickel superalloys. The titanium alloys heve good performances and resistances until 600^oC, instead the nickel superalloys could be used with higher temperatures (700^oC) [20]. Also the compressor dimensions are very important in particular the hub radius (where the rotary blades are fixed) and the shroud radius (at the tip of the rotary blades). The ratio between these values cannot be too high because the efficiency of the compressor drop down, otherwise, it cannot be too low as well, because the solicitation at root of the blade could be unsustainable for the material resistance. In this last configuration the blades result overly twisted and it is not possible to study the flow as two dimensional anymore (hard to design and analyze) and also the manufacture should be more difficult (more expensive).

Some values have been found in literature and for the first stages of the compressor it is possible to find a ratio between 0,5-0,6, while for the last stages between 0,8-0,85 [2]. This is the reason because the head of an axial compressor has blades longer than the final part (the first blades are more loaded).

2.2 Performance of a compressor

The power of the compressor is defined by the mass flow rate and the pressure ratio. The mass flow is a design parameter and the choices in the design process depend on it. The pressure ratio can be a design parameter as well but the achieving of a good level of this variable depends on some factors as the efficiency and the good margin from the surge condition (or stall). The efficiency has already been investigated in the previous paragraph, instead the surge condition will be now explained. Before talking about the surge and chocking conditions it is necessary to introduce the compressor map where it is possible to decide the type of the machine to use under determinate conditions required.

2.2.1 Compressor map

The picture below (fig. 2.5) describes a typical configuration of a generic compressor map derived from a real machine testing. The compressor is considered adiabatic and the fluid is a perfect gas. As it is possible to see, the pressure ratio through the whole compressor is in general in function of the mass flow rate $\dot{m}$ and the rotational velocity of the shaft (N).

The usual method to represent the compressor characteristics in a design practice, is the same reported in that picture, with the corrected values of the shaft speed and the corrected mass flow rate at a specific station. This approach is used because with only one graphic the operation of the compressor can be represented independently on the referenced initial conditions (pressure and temperature). In the same graphic the *constant efficiency contours* is also reported in order to check immediately the performance of the compressor in determinate working conditions. The line passing through the maximum efficiency points (locus of the points), is called *Operating line* and this is very important for the turbocompressor designers because it defines the on-design points for specifics working conditions. This line should be fixed far enough from the surge line because near that zone there is the *Stall Condition*. The last important phenomenon, that could be investigated in that map, is the *Chocking Region*, this is the condition when the mass flow increases too much therefore it remains fixed at the maximum value. Thus the flow is called chocked and it is defined in the graphic by a vertical asymptote of the velocity line.

2.2.2 Surge and Chocking Conditions

The most dangerous phenomenon presents during the work of the compressor, as it has been written in the previous paragraph, is the *Stall Condition*. It has been studied for a long time especially during the second part of the nineteenth century because it was the cause of the failures of a lot of compressors in conditions far from on-design situation. As it is explained more in detail in the next chapters, the stall condition depends on the Mach number and on the incidence angle, both calculated in Inlet of the blade.

Greitzer (1979) [5] found two different types of stall situations in a compressor called:

- Blade Stall: this is the separation condition of the flow started in a generic zone (usually after the maximum height of the Camber line) of the blade in function of

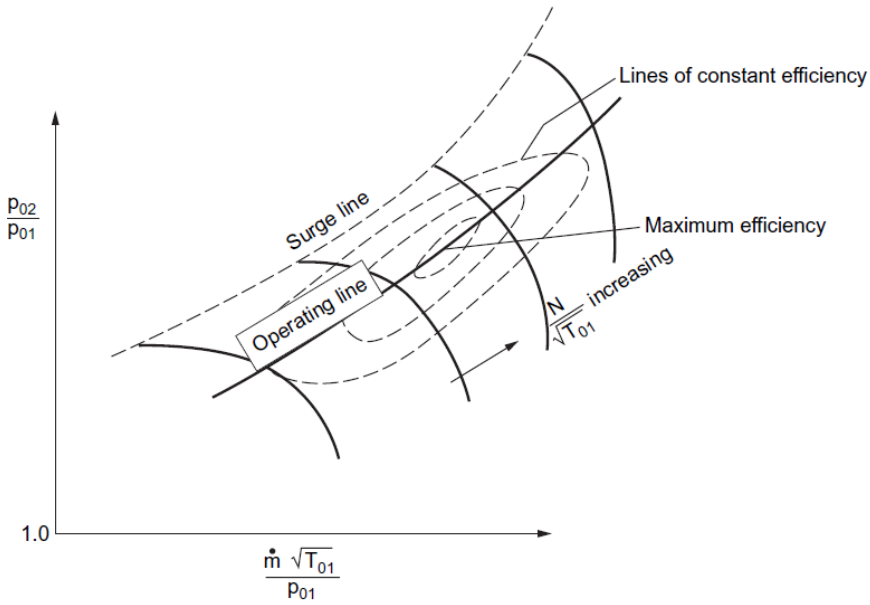

Figure 2.5: Compressor performance map [5]

the mass flow (Mach number as well), and the incidence angle. It could be recognized as a large wake with a lot of dissipative phenomena (high losses).

- Wall Stall: it depends on separation effects as well but near the outer casing.

In this work, for the calculation of the characteristics of blade airfoils, the first type is taken into account because the analysis will be focused only on the profile. Hence, for the Blade Stall it is necessary to introduce the definition of the incidence angle [5] [17] [15] [24]:

$$i = \beta_1 - \beta_{m1} \tag{2.3}$$

where β_1 is the inlet flow angle (average in the spanwise) and β_{m1} is the inlet metal angle (angle tangent of the Camber line of the blade). According to the compressor map (fig. 2.5), if the mass flow is decreased (with constant rotational speed), starting from the design point, the behaviour of the compressor started to be unstable because of the surge condition.

The flow results separated from the suction side and some vibrational effects or pulsation of the flow were born. Due to the separation effects the meridional channel between the blades is partially obstructed and the compressor efficiency drops down.

On the other hand, with the increasing of the mass flow (started from the design condition) the incidence angle decreases, the flow field is changed and it becomes as an convergent-divergent nozzle, and if in the throat area there is the sonic condition (M=1), the mass flow remains fixed at the maximum possible value. In this case there is the second situation of the stall that it is called chocking condition.

The biggest problem for the axial compressor is the surge condition for the resistance of the blades (surge causes flutter phenomena). Thus a good design practice is to fix the design point at the 80% of the mass flow in the chocking condition [5].

2.3 Streamline Curvature

As it is written in the abstract, the focus of the work is to find the loss coefficients and the deflections of the blade profiles in order to implement those results in a new automatic code to analyze the flow and the performances in a two dimensional approach because the problem is easier to handle instead of using the 3D method. The future task is to find a correlation of the results of the different profiles in order to resolve the through-flow problem in the compressors using a computer-aided method. This new code could give a lot of advantages in the thermo-fluid dynamic design of the turbomachinery.

Nowadays, there are a lot of methods focused to resolve the through-flow problem, using more or less the same equations (fluid motion and the energy). The flow through the compressor is considered axial-symmetric [5]. The oldest and the most important technique which implemented those equations is the *Streamline Curvature*, the same method that will be used to elaborate the final results of this work. This is widely used in the gas turbine manufacturing and it can analyze variously shaped boundaries. With one of these approaches it is possible to implement the experimental equations for the 3D losses and so with an iterative method, it is possible to find a new shape of the blades in specific working conditions.

The most important tree-dimensional loss mechanisms are here reported [2]:

- End-wall losses (hub/shroud): it depends on the secondary flow (in particular at tip of the blade), tip clearance, and leakage losses
- Shock losses: this is proportional to the Mach number and it should be studied with the shock waves theory
- Cascade losses: loss coefficient and deflection
- Unsteady flow losses: it depends on the iteration of the rotor and stator blades
- Turbulent mixing: it could happen when two stages are not near or in the last stages of the compressor

At first it is necessary to explain the meaning of a streamline and how to draw it in a generic meridian channel.

In a fluid domain a streamline is the locus of the points where the velocity vector of the fluid particles must be tangential to that line. To draw a streamline it is necessary to define some fixed points, in the fluid domain, and then calculate the velocity. Hence it is possible to divide the passage from hub to shroud with a defined number of streamline in the meridian channel of an axial compressor. The biggest difficulty in a compressor is how to resolve the complex equations of the three dimensional flow, the possible variation of the radius from hub to shroud, the presence of compressible flow and the non-uniform total pressure distribution.

With the streamline the blade can be cut along those lines and its profiles can be analyzed in order to design a new blade concept or only to verify it in a definition condition.

Now a correlation from tree-dimensional to two-dimensional approach must be found, hence translate a meridional flow situation in a blade-to-blade (cascade) flow. As illustrated in the picture (fig. 2.6), a general axial machine is analyzed and the annulus from hub to shroud is ideally cut with a generic number of stream cylindrical surfaces (in a plane the surfaces become a streamline). The surfaces cut the blades in slices in order to define the blade cascade profiles.

The second step is to change the coordinates system in order to study the blade-to-blade view and this is possible with particular equations of transformed coordinates. Now the blade cascade can be analyzed in a plane (not in a cylindrical surface anymore), and all the conditions of the two-dimensional flow can be implemented into the study. In this way a lot of blade slices can be found (depending on the number of the cylindrical surfaces used) and simulated in order to define the characteristics and the behaviours of each profile.

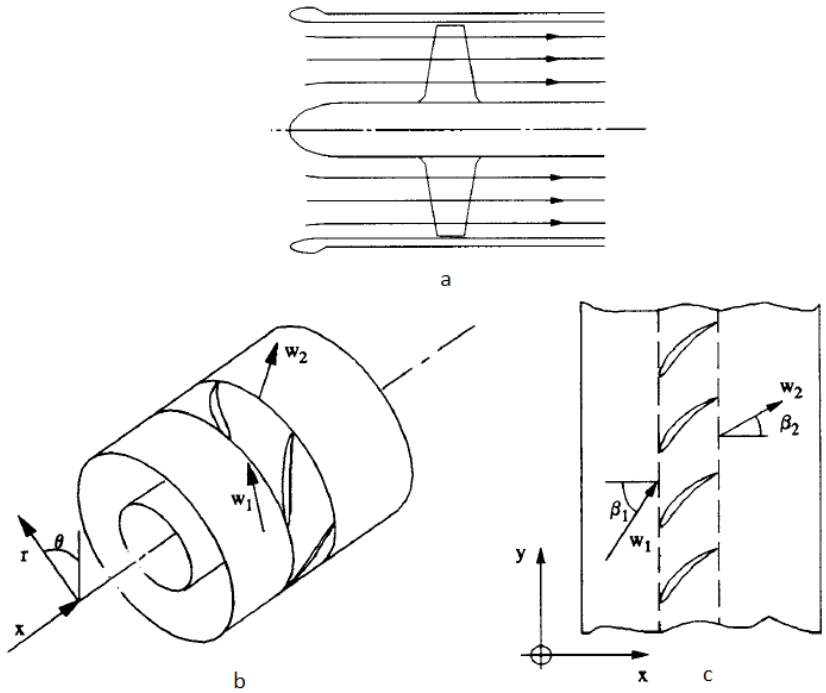

Figure 2.6: Streamline definition: a)the duct is catted with some cylindrical surfaces; b)a generic catted is shown; c)from the cylindrical definition to a blade-to-blade view [17]

The main advantage of this method for the designers is that, they can choose a particular blade definition in a specific slice of the blade in order to satisfy the best conditions required.

Chapter 3

Two-Dimensional Cascade Theory

3.1 Introduction

Several studies and publications have been carried out in the field of compressors, in order to satisfy the new requirements in function of the different uses of the machines. Hence according to the previous chapters, these turbomachines can be employed in a lot of different fields. For example for the heavy-duty gas turbine used in a combined cycle, the compressor should satisfy the requirement of higher power in output, high level of specific work with increasing mass flow rate and also respect the ecological and economical demands. Good final results, in function of these boundaries, can be found implementing the study of the resistance of the material (it depends on the temperatures in the compressor thermodynamic cycle) and also with the analysis of the aerodynamic behaviours. The increasing of the mass flow in inlet, in order to raise the power in output, indirectly means an increase of the frictional losses on the blade's profile and this has an important role in the operating range and thus on the final compressor performances.

As it is written in the brief history of turbomachinery (Chapter 2), the big problem in the past was that the designers had not knowledge and suitable tools to investigate the important phenomena of the iterations of the Mach number and flow condition on the blade airfoils. However after the development of the computer aided methods to draw and analyze the profiles, a lot of families of profile shape have been designed to be used especially in subsonic compressors.

For many years only the profile type NACA (American National Advisory Committee for Aeronautics) series has been used in a lot of heavy-duty gas turbines and in the aviation field for the plane engine. The profile NACA-65 has been deeply studied by many authors [5], by Felix (1957) and then by Horlock (1958), in order to use it also for the profile of the aircraft wings.

The NACA-65 series has a circular or parabolic middle chord and an almost uniform blade loading [20]. In literature (fig. 3.1) it is possible to find a lot of different bending of the profiles in function of the principal parameters of the blade cascade, for example the ratio between thickness against chord and then the Lift coefficient (these two aspects will be described in the next paragraph).

Other types of profiles similar to the NACA are the British C circular-arc blade series and the double circular arc [2] or biconvex blade [20]. The main difference in these profiles is the thickness value in function of the chord, because it can modify the effect and the iteration of the flow on the blade, changing the velocity load on the blade.

How it is possible to see in the figure (fig. 3.1) the NACA-65 series has a stocky shape (in function of the characteristic parameters) and this is the reason why these blade airfoils

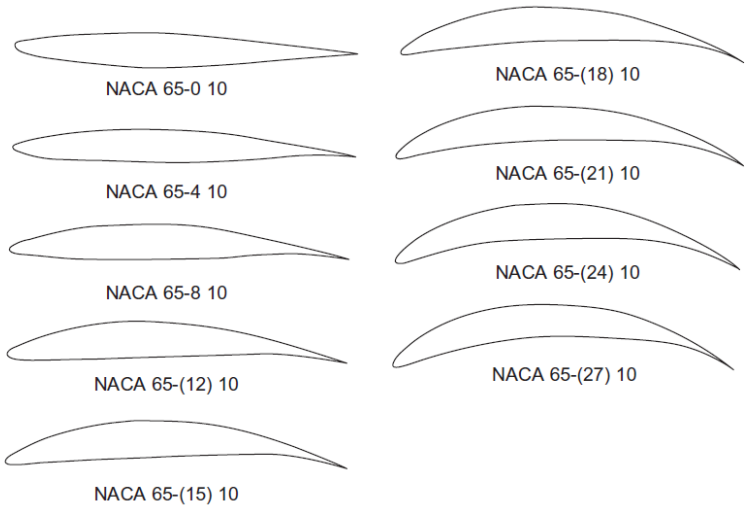

Figure 3.1: Different shape of the profile type NACA-65 [1]

are used especially in a subsonic compressor. Nowadays, because of the high mass flow rate, the compressor behaviours could be transonic (Mach number around 1) or most of the time also supersonic (M>1), in particular in aircraft applications. Hence since the seventies [15] new profiles were researched in order to optimize the compressor operating in critical conditions. One of the first series designed was the controlled-diffusion airfoils (CDA) with experimental and numerical method together.

Two techniques are still today in use to start the design of a new shape definition [15]:

- Direct method: the flow condition in Inlet and Outlet sections and the specifies of the cascade are totally defined, hence the flow field is known. Here it is possible to investigate the compressor in off-design condition and it is also possible to implement an optimization algorithm in order to define automatically (after an iterative loop) the best shape of the profile.

- Inverse approach: the airfoil is studied and optimized starting from the distribution of the velocity on the surfaces of the blade. Hence to define a new profile it is necessary to change manually the velocity distribution in order to study the off-design conditions. After that, a computational method finds automatically the curvature and the thickness of the airfoils in order to satisfy the aerodynamic characteristics required.

The new trend to design blade airfoils is to use optimization methods, that could be automatic and implemented into the direct investigation or in the reverse method. It can be possible to optimize a profile by attempts, it depends on the initial condition or on the type of the data available. The design process start from the experimental data available from a wind tunnel simulations or from old research. The numerical code is represented by the optimization algorithm, and this leads to the CFD (Computational Fluid Dynamic) solver software to extract the final results reevaluated in the optimization process (iterative loop). An example of optimized blade is shown in figure (fig. 3.2), and it represents the profile taken under analysis in this work. In this case the designers started from a profile CDA and with an optimization process (described in the fourth Chapter) they found the new configuration:

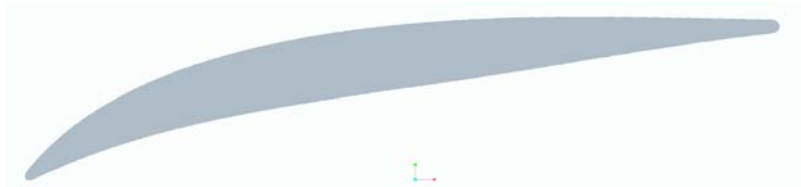

Figure 3.2: Blade rotor hub profile of the axial compressor [profile is not to scale]

Most of the times the available data come from the cascade wind tunnel tests, and this is the real physical approach that is used today for the experimental testing on the blades.

Because the axial compressors can be used in a wide range of Mach number (from 0,2 to more than 1) it is necessary to divide the wing tunnels into two groups:

- low-speed, with M<0,3, thus the compressible effects of the flow are not considered
- high-speed, here the simulations are carried out in supersonic, transonic and high subsonic flow conditions.

The configurations of these two types of wind tunnels are different because the real flow must be recreated but in each case the flow can be considered in two-dimensional configuration in order to study easily the blade cascade. Another reason to study the two-dimensional flow is that the results can be used by the designers in order to provide the performance of the machine with also high precision.

Normally, at the end of the tunnel there are seven or eight blades, and only the central ones are taken into account for the study in order not to consider the three-dimensional effects usually present. In the following picture (fig. 3.3) a high-speed wind tunnel is reported and it is possible to see the position of the blades and the probes for the experimental testing [5].

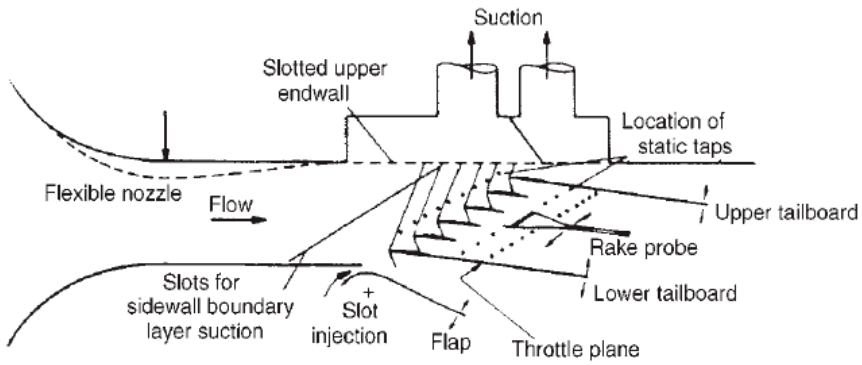

Figure 3.3: High speed wind tunnel for transonic and supersonic investigations [5]

3.2 Profile characteristics and parameters of the cascade

Before starting with the analysis of the blades behaviours it is necessary to introduce some important aspects of the profiles theory, in order to better understand the further discussion presented in this Thesis. The shape of the profile depends on the choice of the type and configuration of the camberline, usually from the design process the angles of the

flow are known and with mathematical correlation, present in literature, it is also possible to draw the final shape of the profile.

3.2.1 General nomenclature

All the angles are defined and measured with respect to the orientation of the axis of rotation of the compressor. How it is possible to see in the figure (fig. 3.4), there are two orientations for the profile; one is the view without the angle of attack, this is the orientation after the drawing of the profile, the second is the view where the blade is set with the orientation with the attack angle. The stagger angle (or attack angle) is the setting of the blade in function of the flow field and this is calculated in the design process to optimize the flow and the operating of the blade.

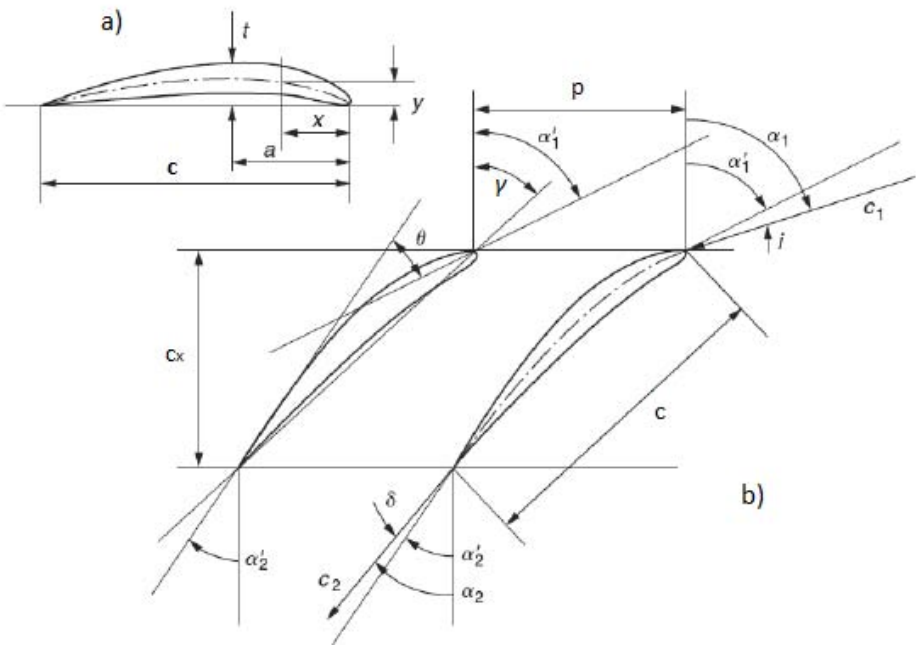

Figure 3.4: Cascade geometry definition for a blade's profile: a) View without stagger angle b) View with attack angle [2]

It is necessary to explain the principal general definitions of the blade from the aerodynamic theory. Indeed, the blade is formed by two surfaces, one of these has convex form, how it is possible to see in the figure (fig. 3.4), and this is called suction side (SS). Instead the other surface, the concave one, is called pressure surface (PS). The curve in the middle of those surfaces is called camberline (or middle line) and this determinate the shape of the profile. From this it is possible to define the thickness of the blade. The trend of the camberline is given in literature and it could be with a circular, parabolic or double circular arc definition.

In the figure it is possible to see the absolute velocity in Inlet and Outlet sections (C_1 and C_2) and all the angles are defined with the stator definition (α), but all the discussion is valid for the rotor as well, but instead of absolute velocity there will be the relative velocities (W_1 and W_2) and the angles are defined with β.

Blade set without angle of attack

- C is the chord of the profile and it is the distance from leading to trailing edge
- t is the thickness of the blade and it is the value measured perpendicularly of the camberline
- a is the distance where the position of the maximum camber high is fixed
- x and y are the necessary coordinates to track the trend of the camberline

Blade set at the angle of attack

- γ is the stagger angle, fixed between the chord direction and the rotational axis orientation
- p (pitch) is the blade spacing or the distance between two blades
- C_x is the axial chord, or the projection of the chord in the axial direction
- α_1 and α_2 are respectively the Inlet and Outlet angles of the flow, these are calculated from the velocity triangles
- $\alpha_1^{'}$ and $\alpha_2^{'}$ are the metal angles of the blades
- θ is the Camber angle and it defines the turning angle of the camberline or the angle of profile bending, and it is calculated with the difference of the Inlet and Outlet metal angles $\theta = \alpha_1^{'} - \alpha_2^{'}$
- i is the incidence angle, and it is the difference between the flow angle and the metal angle in the Inlet section of the profile $i = \alpha_1 - \alpha_1^{'}$, it depends on the flow direction and it could be positive or negative.
- δ is the deviation of the flow at the Outlet section and it is defined as the difference of the value of the flow angle and the metal angle $\delta = \alpha_2 - \alpha_2^{'}$. The value of the deviation is always positive because, for the difference of the pressure between suction and pressure side, the flow is always deflected in direction of the suction side.

3.2.2 Cascade Characteristics

In the performance evaluation or in the design process of a compressor, the important parameters are the initial conditions of the flow field, the shape of the profile with all the parameters described before, and the parameters of the blades cascade, especially important in a two-dimensional study approach. One of the most important parameters to define a blade cascade is the ratio of the profile chord and the distance between two consecutive blades

$$\sigma = \frac{C}{P} \tag{3.1}$$

it is called *Solidity* of the cascade [5]. Considering two different blade cascades with the same value of the chord, lower is the value of the space from two consecutive blades and higher is the value of the solidity, thus the interaction of the blades on the flow field must be considered and it means that the blade cannot be studied with the theory of the isolated profile.

The *Aspect Ratio AR* (or hub-to-tip ratio) is another important parameter and it is the ratio between the height of the blade and the value of the profile chord. This value

should be taken into account when the three-dimensional effects are considered [1], and it can determinate the swirling of the blade and so the loading on it.

The last important parameter is the *Axial Velocity Density Ratio or AVDR* and it considers the contraction of the flow field through the compressor. The contraction of the flow is very important for the two-dimensional condition, hence the value of the AVDR says how far the real condition from the 2-D approach is. There are a lot of papers in literature which explain the effect of the AVDR in the cascade testing [23]. To define the ratio it is necessary to introduce the principle of continuity in a flow duct [2]:

$$\dot{m} = \rho_1 C_1 H_1 p cos(\alpha_1) = \rho_2 C_2 H_2 p cos(\alpha_2) \tag{3.2}$$

where H_1 and H_2 are the heights of the blade in Inlet and Outlet. Usually the values are $H_1 > H_2$ in a compressor. Now it is possible to define the AVDR:

$$\dot{m} = \frac{\rho_2 C_{x2}}{\rho_1 C_{x1}} = \frac{H_1}{H_2} > 1 \; in \; a \; compressor \tag{3.3}$$

3.3 Aerodynamic behaviours

When the airfoil is setting with the stagger angle, the flow field is modified for the presence of the blade and on it, there are some different effects which can determinate the performances of the entire machine.

Experimental tests said that on the suction side and before the maximum height of the camberline of the profile, there is an increase of velocity and a diminution of pressure. Than, in the final part of the profile, there is a decreasing of velocity that leads to a separation flow condition, hence the behaviours at the final part of the blade are very important to define the performance of the profile and thus the loss coefficient. For a good definition of the operating behaviour of a compressor, it is necessary to consider the factors which affect the blade surface boundary layer [5], i.e., velocity distribution on the profile, surface material characteristics, turbulence phenomena, Reynolds number, and Mach Inlet number.

One of the most important factors is the distribution of velocity, and therefore the distribution of pressure on the airfoil surface from Leading to Trailing edge.

The further discussion is based on the correlation of *Lieblein* (1959), NASA (1965) [5], he found that an important increasing of velocity (on the profile), can produce a thick boundary layer and it can also lead to separation conditions. Thus, the increasing of the losses and the wake condition after the trailing edge of the blade are correlated with the amount of the velocity distribution, especially in the suction side. In figure (fig. 3.5) a typical velocity distribution on a general blade airfoil is reported. The velocity distribution is calculated as a ratio of the maximum velocity and the velocity in outlet (C_{max}/C_2) and the value is in function of the percentage of the blade chord. The rate of the velocity in Outlet is an average of the values along of the pitch of the cascade because the flow is not stationary after the Trailing edge of the blade (the same is for the calculation of the flow angles in Inlet and Outlet).

The ratio of the velocities is also called *Diffusion Ratio* and this is an important value in the design process of the blade, in order to limit the losses of Shock and consequentially the stall phenomenon. After that, Lieblein found a correlation between the velocity distribution and the wake momentum thickness which influence the Diffusion Ratio and this gives an idea of the blade loading. For this reason it should be limited and so the wake momentum thickness should be bounded as well.

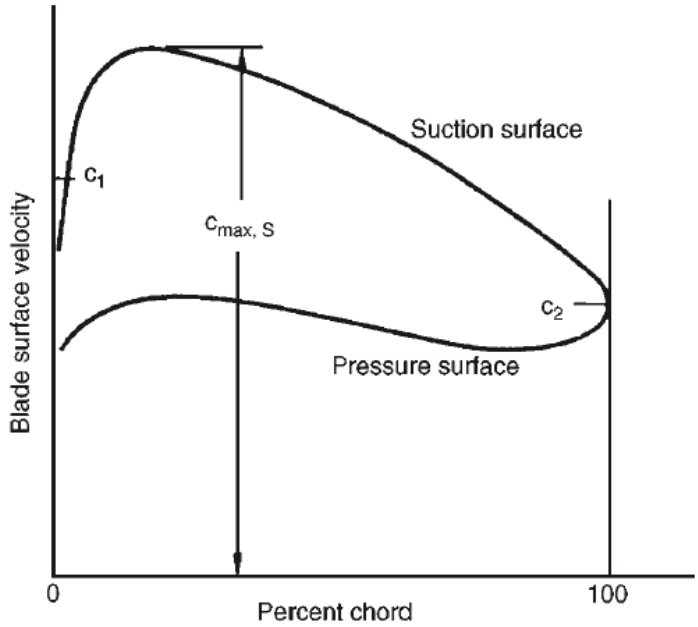

Figure 3.5: Velocity distribution of the velocity on the two sides of the blade [5]

3.3.1 Lift and Drag Coefficient

From the Aerodynamic laws, it is possible to understand that the pressure between suction and pressure side produce some forces on the blade, and i.e., these forces can keep the plane in air. These forces are called:

- Lift (L): this is perpendicular of the flow direction, and on the compressors it is a component of the force given to the fluid:

$$L = \frac{1}{2} C_L A \rho C^2 \tag{3.4}$$

- Drag (D): this is parallel of the flow field and it is the force given from the frictional effects on the blade. This acts in the opposite side of the motion of the fluid:

$$D = \frac{1}{2} C_D A \rho C^2 \tag{3.5}$$

The vectorial sum of these two components gives the total force (R) acts from the blade to the fluid in order to achieve the specific work required.

In the equations for the definition of the Lift and Drag forces the condition of the fluid has been written, like density (ρ) and the square of the velocity of the flow (C^2), and the geometric definition of the flow channel, like the area (A).

In those equations other two coefficients have been reported, like Lift Coefficient (C_L) and Drag Coefficient (C_D), and these can be found from the experimental data from the simulations in a wind tunnel for the single profile. The trend of these coefficients is shown in the figure (fig. 3.6), where it is possible to see the prediction of them in function of the stagger angle (γ), for a particular shape of airfoil [1].

As it is shown in the graphic the choice of the angle of attack should be closer than the low losses conditions, so near the minimum of the Drag coefficient curve, but with the highest Lift Coefficient (so Lift force) as well.

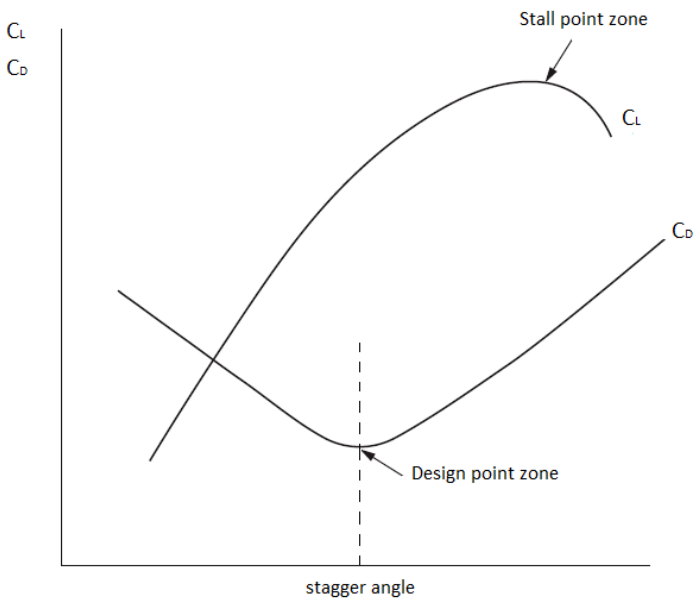

Figure 3.6: Typical distribution of the Lift and Drag coefficients [1]

In literature it is possible to find the correlations to adapt the discussion done for a single profile to a cascade definition and so find the necessary design parameters, like the Lift Coefficient for cascade profiles (C_L^*), that is the discriminant parameter to choose the right shape of the profile. It is in function of the specific work done, meridian velocity and solidity of the cascade. Normally for the compressor the value of C_L^* is between 0,8 and 1,2, because the higher is this value and the more curved is the blade, so it has more load and therefore more losses [2]. If the value is too low, the blade cannot exchange all the specific work required and the efficiency of the compressor drops down.

3.4 Incidence and Deflection

In a design process or in a secondary phase of performance measurements, the most important parameter taken into account is the angle of incidence. In a design that could be hypothesized, at first, and with the values of the corresponding profile losses it is possible to resolve the design problem, hence to define the blade geometry.

Instead in a testing process with the aid of the CFD calculation or with the results from real simulation in wind tunnel, starting from fixed initial condition, it is possible to find the final state of the compressor stage (or only for rotor or stator), and at the end in a post-processing phase the losses can be calculated. The behaviours near the stall zone or the profile losses are in function of the two important independent variables as Inlet Mach number and Incidence angle. With the variation of the first one the velocity changes and the mass flow as well. The second parameter instead, changes the direction of the approaching of the flow in the Leading edge zone, hence the phenomena on the profile must be studied in order to understand where are the stall zone and the starting point of the separation condition of the flow and so trying to define the reasons of the increasing of the entropy value in the compressor thermodynamic cycle.

3.4.1 Loss Coefficient

The most important graphic for a post-processing loss analysis is reported below. The figure (fig. 3.7) shows a typical trend of the loss coefficient in function on the Incidence angle and the inlet Mach number. The picture describes the behaviour of the profile losses for an airfoil taken under exam in this work, and it is simple to understand the dependence of both variables. It is also possible to see as the trend of the loss curves is almost parabolic with the minimum point quite in the same position for all the curves. In the next chapters, when the final results will be discussed, this aspect will be explained with the aid of the CDF analysis.

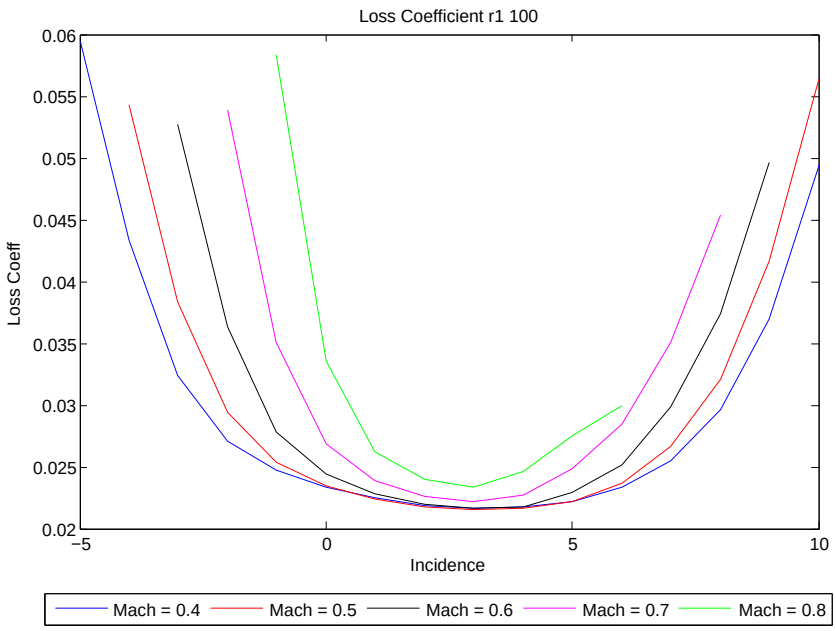

Figure 3.7: Post-processing results of CFD simulations for shroud profile of the first rotor in the axial compressor

When the incidence angle is closer than the design point, where the incidence is around zero degrees (the flow is almost in the same direction as the Inlet metal angle), the values of the losses are the lowest and it means that the compressor is designed well for design condition.

In off-design condition, hence farther than low angles of incidence, losses have a different behaviour in function of the Mach number (and logically of the incidence as well). When the value of the Mach increases the parable gets tight and the variation range of the incidence angle decreases. This also depends on the shape of the blade but generally when velocity increases, frictional losses increase because those are in function of the square of velocity.

In literature, it is possible to find the equations in order to calculate the value of the loss coefficient with a specific incidence angle and Mach number [2]

$$\omega_p = \frac{p_1^0 - p_2^0}{p_1^0 - p_1} \tag{3.6}$$

$$\omega = \frac{p_1^0 - p_2^0}{\rho_1 C_1^2/2} \tag{3.7}$$

The formulation are exactly the same if the Mach number is lower than 0,3 (M<0,3) because the flow is incompressible. When the M>0,3 the flow must be considered compressible and the second equation (3.7) is not valid anymore (see the following sub-paragraph). Those equations are valid for the stator blade but they can be used also for the stator where the absolute velocity is replaced with the relative one. In this Thesis the first definition of the loss coefficient (3.6) will be used because of the high Mach number and in order to compare the final results with the literature one [15] [16].

Compressible flow

With an incompressible flow condition the variations of the fluid state depend only on the expansion or compression process and considering an isentropic transformation, the stagnation enthalpy point can be defined as follows [5]:

$$h^0 = h + \frac{1}{2}C^2 \tag{3.8}$$

with the solution of the enthalpy equations it is possible to define the temperature, because if the gas is perfect $h = C_pT$ and introducing the definition of the Mach number $M = c/a = c/(\sqrt{\gamma RT})$, at the end the ratio of the temperature (total, static) is found:

$$T^0 = T + \frac{1}{2}C^2/C_p \tag{3.9}$$

$$\frac{T^0}{T} = 1 + \frac{1}{2}(\gamma - 1)\frac{C^2}{\gamma RT} = 1 + \frac{1}{2}(\gamma - 1)M^2 \tag{3.10}$$

then introducing the Gibbs law pressure is immediately defined:

$$\frac{p^0}{p} = (\frac{T^0}{T})^{\frac{\gamma}{\gamma-1}} = [1 + (\frac{\gamma - 1}{2})M^2]^{\frac{\gamma}{\gamma-1}} \tag{3.11}$$

the equation of the pressure ratio (total, static) is taken into account for this research because with the compressible flow the Bernoulli principle is not valid anymore, thus the formulation of the stagnation pressure (3.12) must be not considered for this work.

$$p^0 = p + \frac{1}{2}\rho C^2 \tag{3.12}$$

Operation Range

One of the focuses of this work is to declare the operating range of compressor in function of the Mach number and incidence angle. The operating range of a compressor is the field of the variability of the parameters (already described), where the compressor continues to work with a good performance also in off-design condition. The range is defined as twice the minimum value of the loss coefficient $\omega = 2\omega_{min}$ (by Howell and Lieblein) [5] [17], this is only a practical definition that could change considering different authors, i.e., the area of operating is defined as $1,5\omega_{min}$ by Mellor [2]. Hence this range defines the maximum angle possible for the flow at inlet or the maximum level of incidence (positive or negative) before the stall phenomenon. In the figure (fig. 3.8) below a general graphic is reported where the operating field is geometrically described and how it is possible to imagine, if the value of the Mach number increases the range decreases (fig. 3.7).

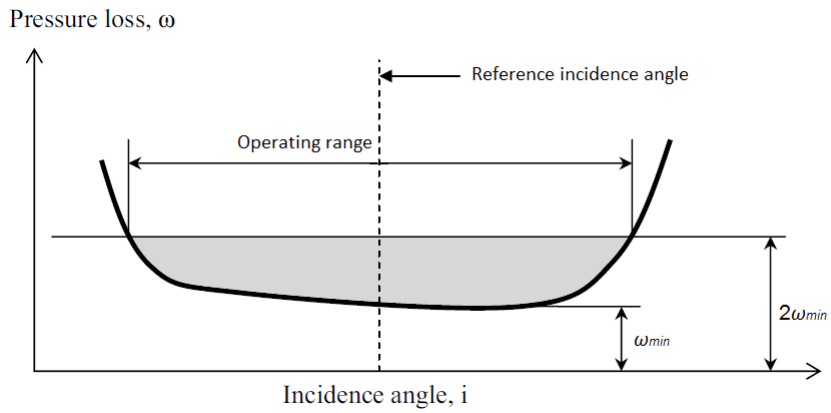

Figure 3.8: Definition of the Operating range of an axial compressor [6]

3.4.2 Incidence and Mach Number effects

Incidence

The variation of the Incidence modifies the pressure (and velocity) distribution on the blade profile from Leading to Trailing edge. Hence the profile should have a wide operation range in order to tolerate variations of the flow direction. The next discussion is based on the picture where the distribution of the velocity on the blade profile (fig. 3.5) is reported.

When the Incidence angle increases, the peak of the velocity on the suction side increases as well and at the same time it starts to move to the Leading Edge. It means that the profile is more exposed to stall effects in a bigger zone on the pressure side.

Otherwise, when the Incidence angle decreases there is an inversion of the role of the blade surfaces, because the peak of velocity in the pressure side increases and it is possible that the maximum value of velocity may be the same or, in the most critical condition, it can happen that the velocity in the pressure surface becomes higher than in the other side. In this last case if the profile has a considerable camber angle (big bending) the bilateral stall phenomenon could happen, it means the flow achieves the separation condition in both sides.

Mach number

It has been already explained that the new concept of compressors is to achieve the highest performances as possible. It is possible to divide the classes of the compressor in function of that variable as it is possible to see below:

- Subsonic compressor: M1<0,7-0,8 (absolute or relative values in function of the reference system)
- Transonic compressor: 0,8<M1<1,4
- Supersonic compressor: M1>1,4

this is not an official classification but it can be useful in a design process in order to check and fix the trend of the mach in the streamwise. In this work the flow has been considered subsonic because the Mach number is below 0,8 (Chapter 4). In the picture (fig. 3.10), where the behaviour of the Mach in a hub rotor profile of the first stage of the compressor analyzed in this work (r1 hub M1=0,7 i=3°) is reported, it is possible to see a

big increasing of velocity in the Suction side of the blade. Hence in that zone the flow will become transonic or supersonic and a sonic ball could form. This is like a wall in the flow field and it can create big losses because the separation condition could occur (fig. 3.9). One of the most important aftermaths is the shock losses because in that bubble a lot of dissipative effects can be born.

Another important phenomenon, in that zone, is the deviation loss, because the flow feels the ball like a real wall (like a surface of the blade) and it attempts to adapt to the new configuration, hence the critical area between two blades is reduced and the chocking condition may occur.

All of these effects lead to a reduction of the operation range of the compressor, and it is not possible to define the operating field anymore from surge to chocking condition.

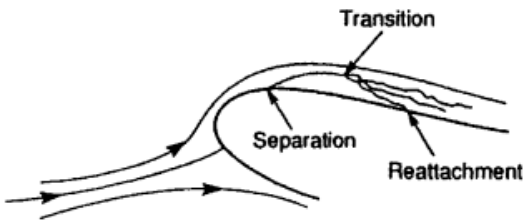

Figure 3.9: Local separation condition [16]

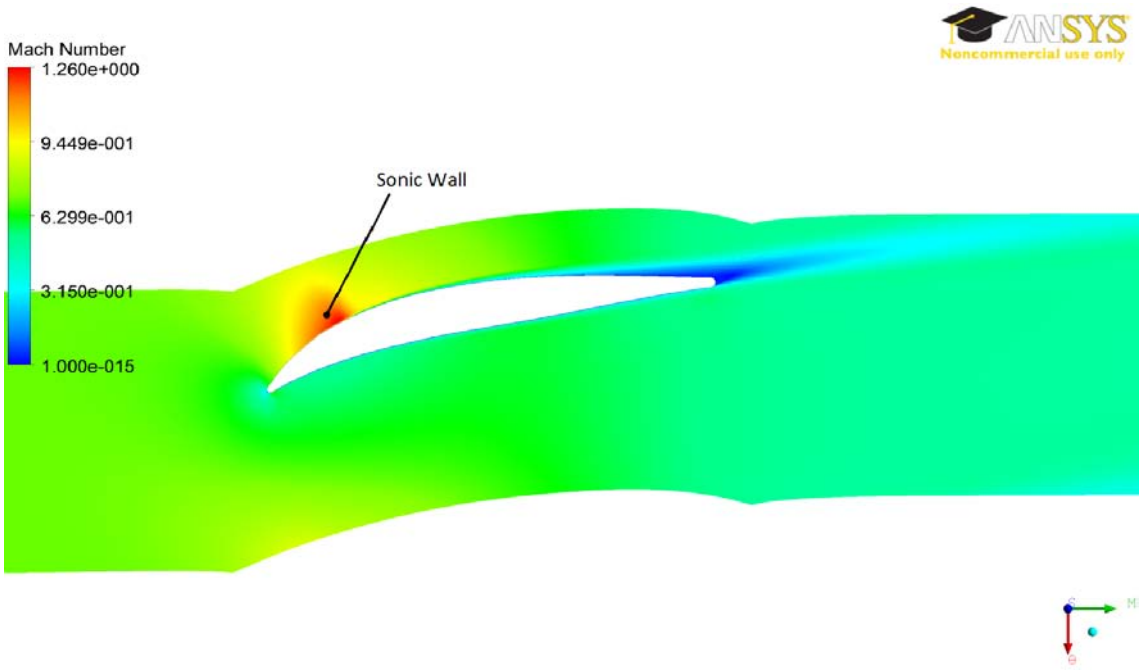

Figure 3.10: Mach effect on the hub rotor profile [profile not in scale]

3.4.3 Deflection

The operation range of the compressors can be found also in another way, it means using Howell's correlation [5] that compares the deflection of the flow with the incidence angle. The fluid deflection angle is the difference between the fluid Inlet and Outlet angles and it

has a trend similar to the Lift coefficient (fig. 3.6) of the profile:

$$\epsilon = \alpha_1 - \alpha_2 \tag{3.13}$$

Hence it is also possible to define the maximum incidence angle in function of the stall region. As it will be reported in the graphic (fig. 3.11) the stall region is where there is the maximum value of the flow deflection, that is called stall deflection (c_s). Howell's correlation said that the nominal operation condition should have an incidence degree such that the deflection will be 80 percent of the stall condition:

$$\epsilon^* = 0,8\epsilon_s = 0,8c_s \tag{3.14}$$

This quantity is very important especially in the post-processing phase in order to check the final results and compare the deflection with the results of the loss coefficient.

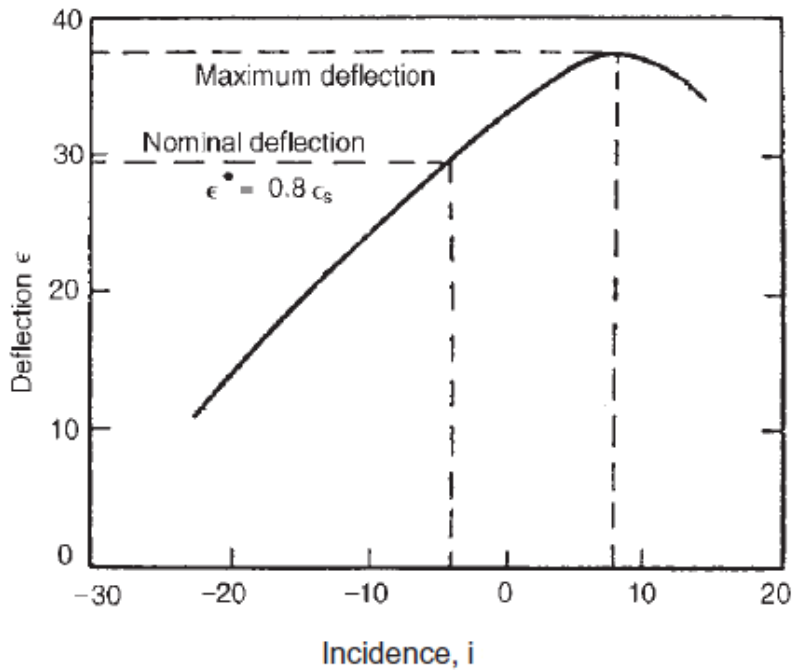

Figure 3.11: Howell's correlation for operating range in function of the deflection [5]

Chapter 4

TurboGrid File Generation

4.1 Heavy Duty Multi-stage Axial Compressor

4.1.1 Introduction

The aim of this work is to analyze the performances, in different operating conditions, of a multi-stage axial compressor, leveraging a two-dimensional approach. The results from each profile simulation will be transferred in a new numerical code, that uses the streamline curvature method in order to predict the performances of a new concept machine.

As mentioned in Chapter 2, the streamline curvature code is useful to analyze the through-flow problem in a compressor duck because it reduces the time needed to simulate the fluid field, compared to a typical three-dimensional simulation. Moreover, the final results with these two different approaches could differ on 10% of the loss coefficient value i.e..

The first part of this work is focused on the behaviours of the compressor in a dry condition (fluid is Air Ideal Gas), and the final results in different operating situations will be used to set the new numerical code.

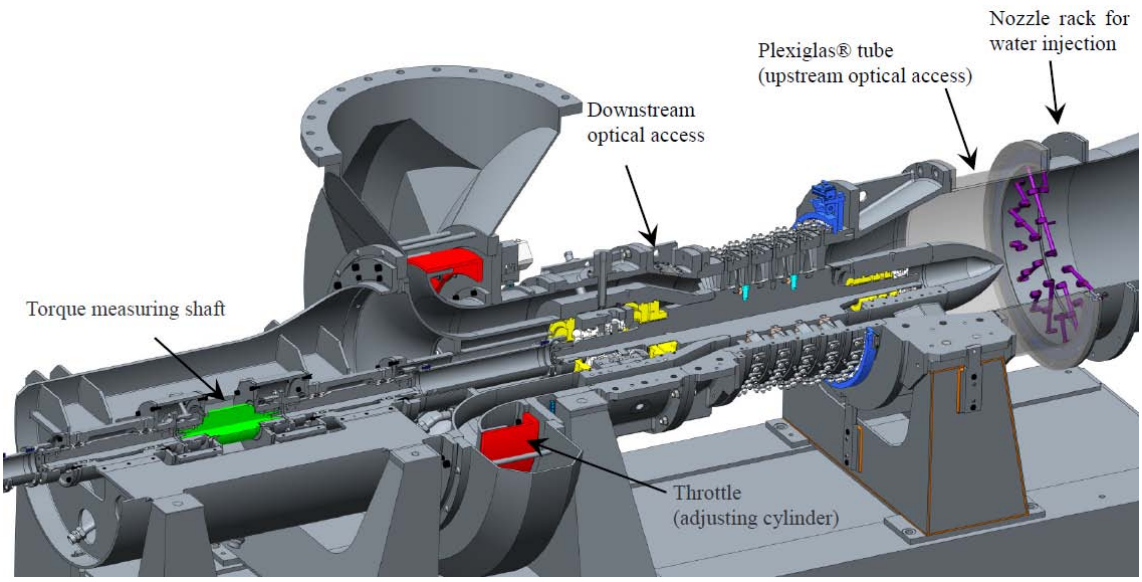

Figure 4.1: Cad Model of the axial compressor and test ring [22]

However the heavy duty multi-stage axial compressor (fig. 4.1), taken under exam in

this Thesis, was tested at the University Duisburg-Essen [22] in a own design testing ring. This machine could work both in a dry and a wet condition, allowing the analysis of the two-phase flow. In the second part of the work, the wet case will be introduced in order to find the right setting for the simulations and to investigated the collision on the blade. However, parameters of loss coefficient and deflection in this condition are not treated for wet case, and left as future achievements.

The two-phase flow is one of the most important working conditions for modern compressors, especially in presence of environments with high temperatures (hot and dry days). In fact, when high power from turbogas is required (the turbine is downstream of the compressor), water is injected upstream to the compressor. By spray action the water arrives to the machine in form of droplets, with a percentage that is function of the air mass flow. The role of the liquid is to decrease the temperature in inlet of the compressor and thus increases the total final power.

Many works on this topic are available in literature, but the main problem is how to choose the right boundaries conditions for the setting of the CFD analysis in order to find the final results (similarly to the study done for the dry condition) and implement the treatment of the droplets evaporation in a streamline curvature program.

4.1.2 Multi-stage Axial Compressor

In the picture (fig. 4 stage [22]) the scheme of the compressor's stage, with the IGV blade is shown. While, in the graphic (fig. 4.3) it is possible to find the map of the machine with a real simulation and the CFD results [22] [4]. In order to drive the compressor there are two DC-motor with a total maximum power of $P_{max} = 980kW$ and a maximum rotational speed $n_{max} = 12000rpm$ [22] [4]. The CFD simulation has been carried out in a steady state condition with the analysis of one blade per row, also the initial parameters like total pressure and total temperature have been fixed [22] [4]:

- $p_{tot} = 1,01325bar$
- $T_{tot} = 15^o$

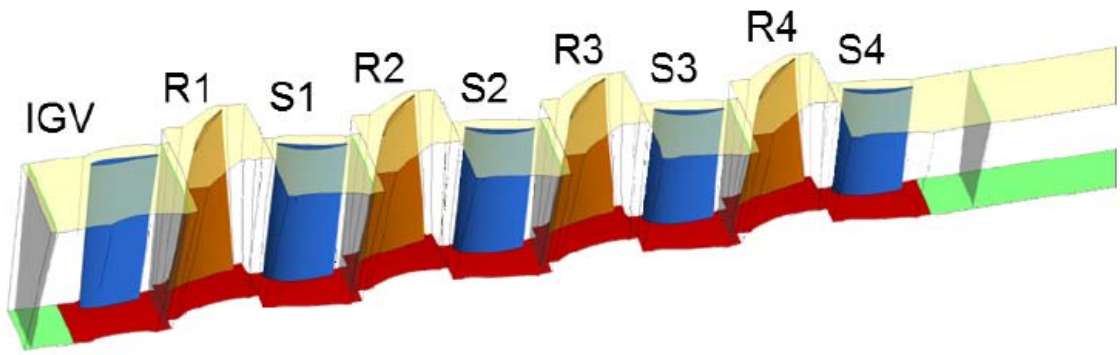

Figure 4.2: Cad Model of the IGV and the four stages of the compressor [22]

Operating Characteristics

In order to provide an easy start-up of the compressor and to allow the control of the mass flow as well, upstream of the first stage there are 29 Inlet Guide Vanes (IGV) blades. They

can be adjusted with a gear motor and so give to the fluid a pre-swirl between $+20^o$ and -20° [22] [4]. The four stages consist of 33 stators and 31 rotors blades, drawn in free vortex design. The shape of the blades is similar to CDA-blades but it consists in a numerically optimized profile (that will be described in the next paragraph). The design relative Mach number in inlet is fixed to $M1 = 0,78$ [22] [4].

The other important parameters to determinate the whole compressor are the following [22]:

- Aspect Ratio: $AR = 0,576$ and the hub radius remains constant from the first stage to the last consequently the shroud one decreases.
- Work input coefficient: $\psi = 0,892$ measured at the first rotor
- Flow coefficient: $\phi = 0,843$ for first rotor at middle span (middle radius)

In order to allow the regulation of the machine, a throttle valve is placed downstream of the blades. This can control the flow field through the compressor. In the inlet section of the compressor water injection system can also be found.

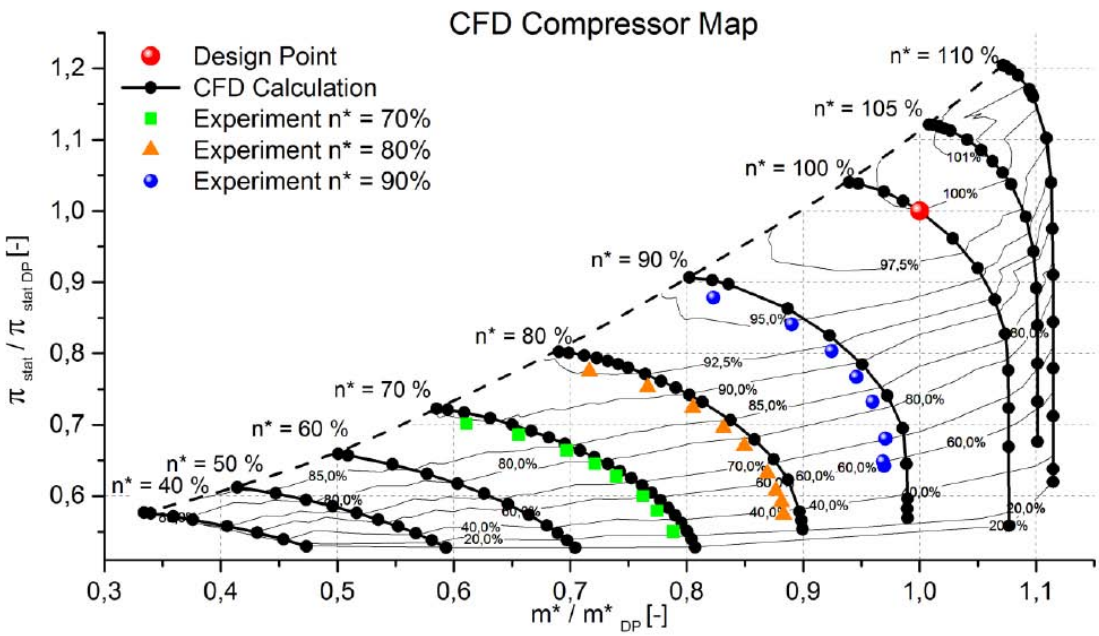

Figure 4.3: Map of the compressor in dry operating condition [22]

4.1.3 Blade shape

The compressor blade profiles have been developed by an optimization process started from the CDA type [4], following two different methodologies. First of all, the design process started from defining all the geometric quantities, such as mass flow, aspect ratio, stage loading etc., in order to achieve the boundaries conditions. All of these quantities were obtained leveraging 1D-Tool or S2-Streamline tools. Then, each blade was cut in 5 slices, in order to optimize each airfoil.

The optimization process is composed of two steps, one focused on the lower profiles (near the hub) and the other, on the airfoils near the shroud in order to optimize the shape

on the pressure side of the blade (in the scientific papers these two approaches are called Method A and Method B [4]).

After the profiles generation, the blade has been formed by the stacking of each profile with the centroid of mass like a reference. Hence, the designers have been meshed and simulated the blade and the final results have been evaluated in order to achieve the objective function of the process, that was to minimize the mechanical stress on the blade [4]. This was possible by changing the twist of the profiles and their position respect of the centroid of mass (iterative loop).

Slice of the blade

In this work, the simulations have been carried out by cutting the blades with five cylindrical surfaces, from hub to shroud, in order to recreate the five imaginary streamlines through the meridian channel. Hence, five profiles have been found at different distance from the rotational axis, and these will be the sketch taken under exam in this analysis. In the picture (fig. 4.4) has been reported the imaginary cut of the blade with the respective nomenclature that will be used in the following study. The profiles are equally spaced from hub (span-000) to shroud (span-100), with a 25% of pitch from each airfoils.

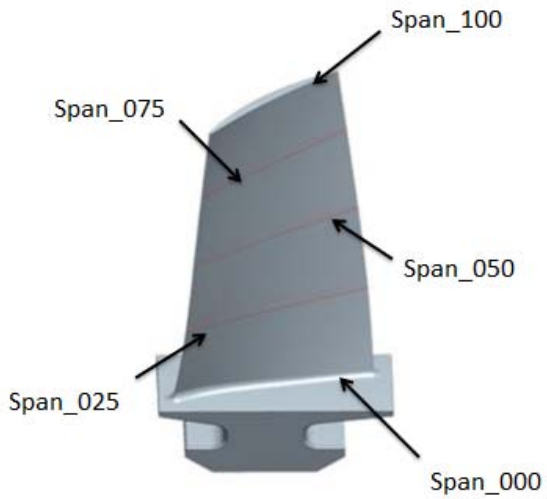

Figure 4.4: 3D blade view and span nomenclature [4]

4.2 Automatic Scripting of Profile

4.2.1 Export profile points

The primary step of this work was to define the points of each profile in order to generate the geometry automatically, via Matlab (v. R2012a) and meshing the domain in TurboGrid (v. 14.0) for the simulations. The reason to find an automatic modality to carry out the process of the geometry construction, was for the high number of profiles analyzed. Indeed, each blade has been cut into five slices, thus 45 profiles have been studied in a lot of different operating conditions as it will be written in the next chapter [Chapter 5].

The blade profile has been derived starting from the three-dimensional model of the entire compressor, and after that a single profile has been saved in specific file (.PART)

in order to export all the points. These results were obtained by leveraging Pro/Engineer tool.

Always with Pro/E, two different approaches have been followed to extract the points, with x y z coordinates, starting from the .PART file:

- .STL format: from the two-dimensional definition of the profile, a small solid model of the blade is created by the extrusion of the profile surface at the thickness value of t=2,3mm (boundary condition). Then, using the STL format to save the profile (fig. 4.5), the solid definition is translated in standard triangular language. As it can be seen in the picture this should be the best method because the spaces definition of the points is automatically fixed by the software, hence near the zone of the Leading or Trailing Edge, a high definition of the profile is given by the high number of divisions. However, in the output file the points are not ordered from Leading to Trailing edge, but they have a a casual definition, and it is a problem for the geometry construction by Matlab.

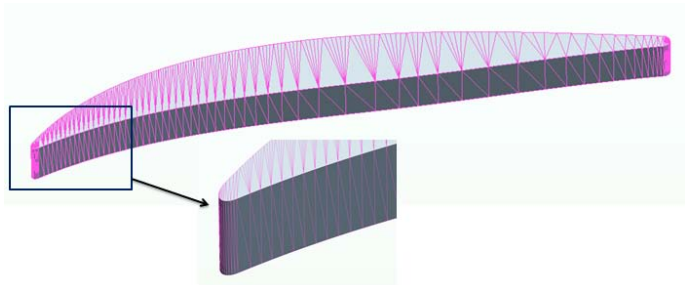

Figure 4.5: .STL format with the particular of the Leading edge definition [profile not in scale]

- .IGS format: differently from the previous approach, here only the 2-D profile has been extracted by the IGS format. The airfoil is divided by equal spaced 2000 points (fig. 4.6) in order to interpolate the coordinates. Then, all these points are saved in a IGS format, written in binary code (for efficiency reasons). This is the main problem of this approach because the text file must be first translated in a normal code, in order to read the coordinates. As it will be written below, a Matlab script has been used to translate the coordinates values and only in a second moment the three-dimensional specification will be created (from Matlab) by coping the coordinates found at the distance of the thickness (t=2,3mm).

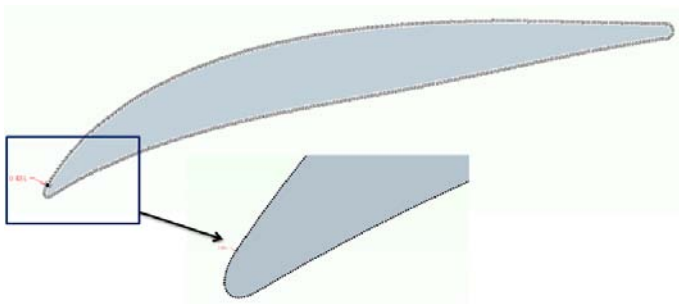

Figure 4.6: .IGS format where it is possible to see the one-dimensional definition of the profile [profile not in scale]

The value of the coordinates are obtained from files structured in both formats, .IGS and .STL, with a Matlab script. Since the ANSYS CFX solver cannot simulate just a profile without thickness, the blade's slice value is set to t=2,3mm, since for a TurboGrid boundary condition this is the lowest possible thickness value. In fact, with a value lower than 2,3mm, TGrid cannot draw the three-dimensional geometry for a cylindrical development problem into the construction process (the hub or shroud profile surfaces are planar, while the hub or shroud machine surfaces are cylindrical).

From each IGS file describing a profile, the coordinates specifications of "hub" and "shroud" are extracted and saved inside a text file. Here, both the coordinates and the position of the Leading and Trailing edge (LE, TE) are represented in x,y, and z specification required by TurboGrid in order to process the information and draw a new profile.

For the purpose of extracting the shape of the blade, the IGS format will be used because, for the order of the points, the Matlab script is faster to create the final text file.

4.2.2 Scale of the blade

In TurboGrid the domain which contains the airfoil as defined above, does not have a planar definition but a cylindrical development. In order to move to a planar definition, the distance from the rotational axis has been increased, obtaining a machine with a greater number of blades, but that maintains the same solidity value. Thus, the cylindrical development can be then ignored. This process was carried out with a simple proportion, correlating the real value of the radius (z component), the real number of the blades (it changes for IGVs, rotor and stator), and the new number of the blades. The result is an increased radius value, while the solidity remains constant; this because the chord value and the pitch between two blades, is always the same. The proportion is here reported:

$$r : Nr = R : Nn \tag{4.1}$$

the two leftmost parameters of the proportion, r and Nr, are respectively the actual radius and the actual number of the blades; the two rightmost parameters of the equation are the values of the new machine. The number of the blades composing the new cascade, represents a TGrid boundary condition, and it is fixed to the maximum possible to 360.

In order to simplify the analysis, the simulations can be considered in a planar section, thus the final reports can be used to define the performances of the blades cascade. The proportion (eq 4.1) is automatically calculated into the same Matlab script used to extract the coordinates. The output of the computation, contained in the final text file profile.curve, is complete and is ready to be processed by TurboGrid.

4.2.3 Control volume definition

In order to define the complete channel flow, TGrid requires the definition of the control volume (domain). The channel between two consecutive blades is automatically defined for the software, but its dimension is a parameter to declare. For this reason, the Inlet hub/shroud points and the Outlet section, has been first defined, as it can be seen in the picture (fig. 4.7). More precisely:

- Inlet (hub and shroud) fixed at a distance more than half axial chord from the LE
- Outlet (hub and shroud) defined at a distance more than two times of the axial chord from the TE

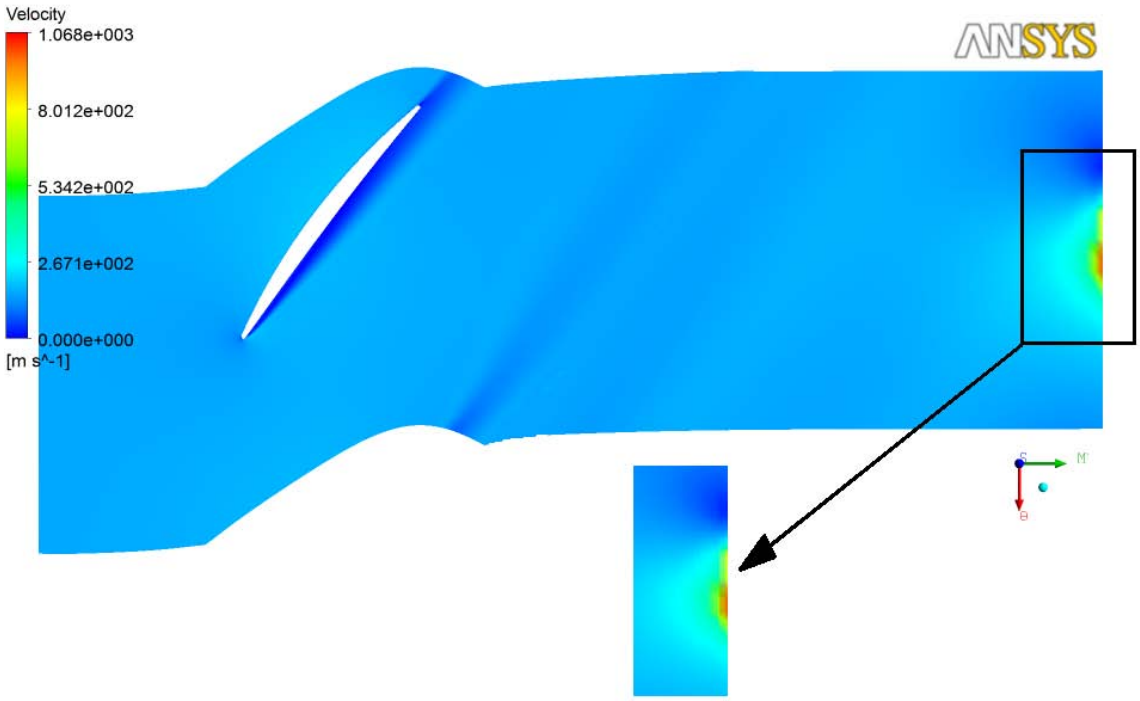

Figure 4.7: Simulation of first rotor shroud profile and a particular of the wall zone

After some trial simulations, the geometric conditions have been changed. The initial definition of the domain, in fact, leads to a bad convergence caused from separation condition at the end of the blade or, more generally, from turbulence effects, so the fluid field cannot develop completely. As a consequence, the solver program fixed an imaginary wall at the Outlet section especially in a conditions far from the design point, i.e., with high Mach number (M>0,7) and incidence far from zero degrees, and the simulation crashed. The solver error shown is reported in the picture (fig. 4.8):

```
****** Notice ******

A wall has been placed at portion(s) of an OUTLET

boundary condition (at   8.8% of the faces,  10.5% of the area)

to prevent fluid from flowing into the domain.

The boundary condition name is: Outlet.

The fluid name is: Air Ideal Gas.

If this situation persists, consider switching

to an Opening type boundary condition instead.
```

Figure 4.8: Part of the Output solver file with the specification of the error

This problem has been resolved increasing the distance of Inlet and Outlet section from the blade. As follows:

- Inlet section positioned at the distance of one axial chord from the LE

- Outlet section fixed at the distance of more than three times from the TE

The specification of the control volume is reported in the picture (fig. 4.9), where the direction of the flow is also reported. Hence, the text file for hub and shroud domain (hub.curve and shroud.curve) are also automatically written in function on the profile coordinates.

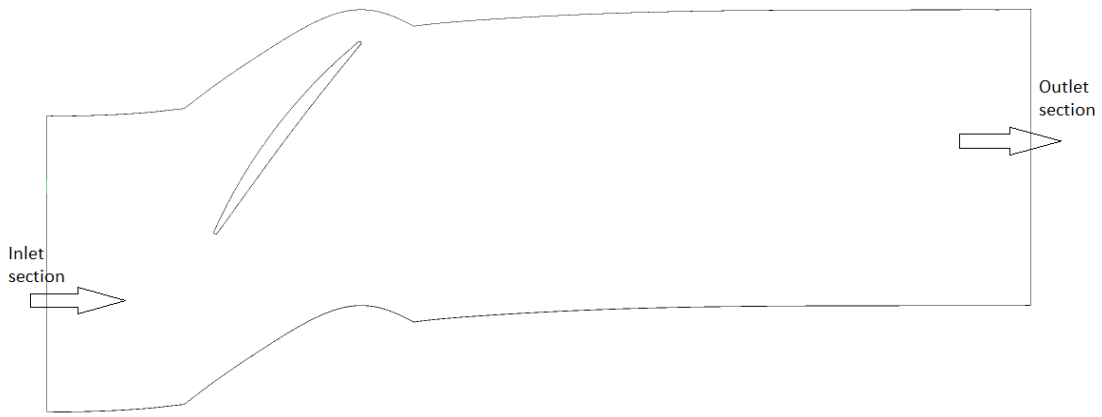

Figure 4.9: Domain definition of the flow field

4.2.4 TurboGrid File Definition

TurboGrid needs the machine data specification in addition of profile and control volume definition. The Matlab script used to process data files, provides all these requirements in a unique text file called information file (.inf), in which TurboGrid can find all the geometric and working descriptions. An example of the information file is here reported (fig. 4.10): At this stage, all the geometric parameters are known and the meshing process can start.

```
!======  ANSYS BladeGen Export  ========
Axis of Rotation: X
Number of Blade Sets:360
Number of Blades Per Set: 1
Blade Loft Direction: Streamwise
Geometry Units: MM
Coordinate System Orientation: Righthanded
Blade 0 LE: EllipseEnd
Blade 0 TE: EllipseEnd
Hub Data File: hub.curve
Shroud Data File: shroud.curve
Profile Data File: file_profile.curve
```

Figure 4.10: Example of file .inf

4.3 Profile Meshing

In order to refine the domain, TurboGrid software requires, in addition to the geometry definitions, the topology specifications, mesh data, eventually some conditions to refine the domain, and at the end the program offers the possibility to check the mesh. In this paragraph the mesh creation process will be discussed in detail, with all the specifications used in this work.

Geometry

As introduced in the above paragraph, the input .inf file is ready to be loaded in TurboGrid. The program needs also, as an input, the specific method to use for the geometric representation. In fact, TurboGrid generates the blades surfaces starting from the profiles, and then by a lofting across the curves. In the simulation preformed in this work, *Flank Milled* method is employed, which uses the follows settings for the Blade Modeler [13]:

- Lofting: *Streamwise*, the corresponding points of two following profiles are connected together and then the surface is created by the lofting of the lines.
- Curve type: *Piece-wise Linear*, the adjacent points between two following curves are connected by straight lines
- Surface type: *Ruled*, this is quite the same of Piece-wise linear approach but in 2 dimensions, so two following lines are connected with a plane.

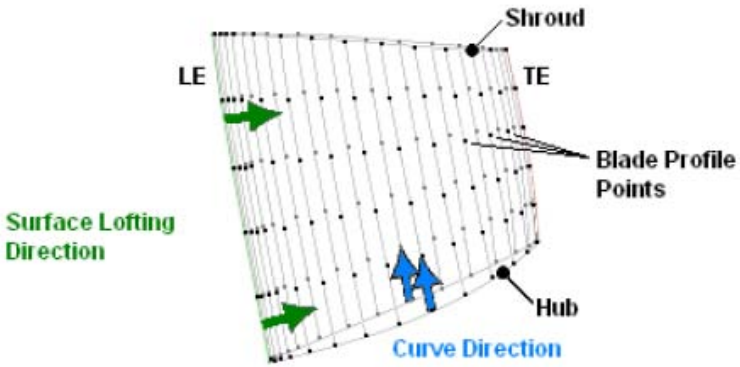

Figure 4.11: Streamwise lofting surface [13]

Topology

The option selected for the mesh of the flow field is *ATM Optimized*, since this method can mesh different types of profiles with the same specifications (for the mesh), as well as optimizing the grid in function on the shape, and it can use a mesh type H or O-Grid with squares elements. In the literature the most used mesh type is the H-Grid [15] [24] and in order to compare the final results with those in the scientific papers the ATM has been chosen (fig. 4.12). This method does not require specific definitions for the mesh just the specifications for the mesh data and eventually for the edge splitting (in order to refine the mesh grid and obtain high precision).

Mesh Data

In order to mesh different shapes of profiles with the same conditions, the general *Global Size Factor (GSF)* has been chosen. This method defines the grid size, and to refine the mesh it is necessary to set a high value of the GSF. Furthermore, in order to control the behavior of the flow near the blade walls (limit the y^+ number), the method *First Element Offset* has been used. This method controls the height of the first element near the blade, and then with a scale factor, increases the size of the grid. As a result, near the profile

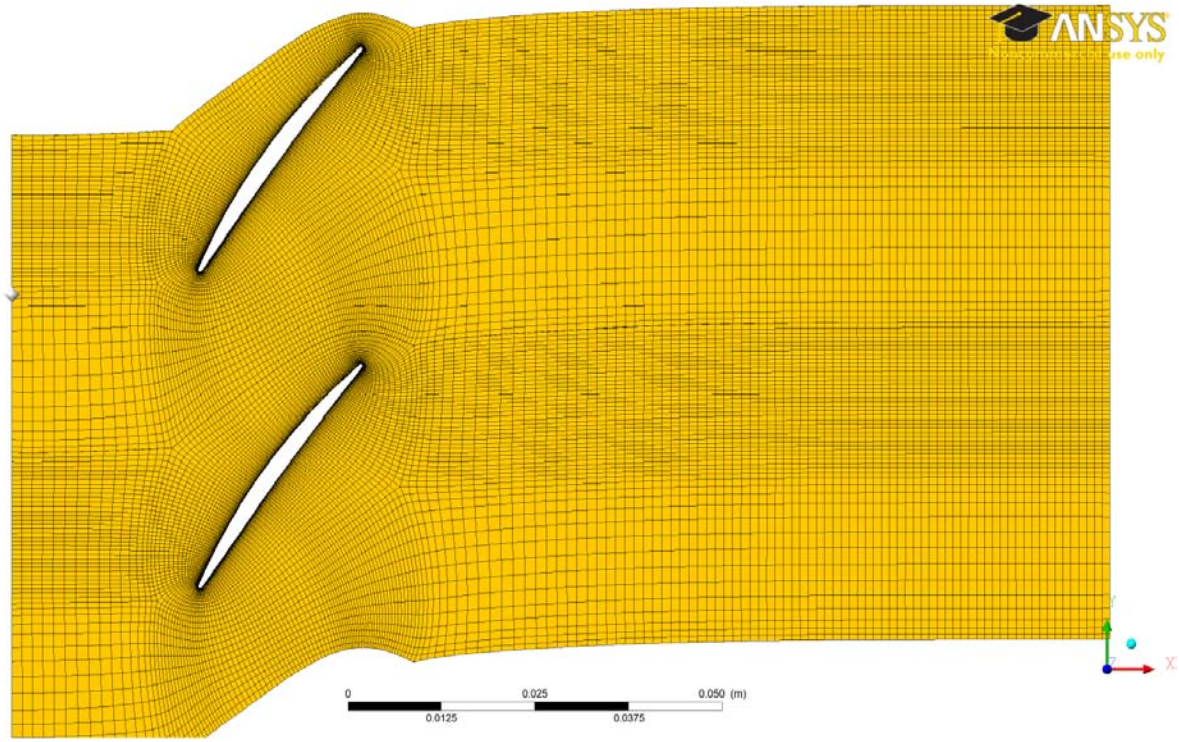

Figure 4.12: H-Grid mesh topology of two consecutive blades (r1 span 100) [profile not in scale]

the grid is very refined and its dimension is highly increased far from the blade walls. It means high precision near the wall and less time to simulate the domain.

The last setting for the whole mesh is the passage definition, in which the distribution of the elements in the spanwise is chosen. In this work, the uniform method has been chosen, thus a number of cells, with the same height in the spanwise, has been fixed.

In this definition phase it is also possible to define the edges splitting, in order to refine the mesh in particular zones. In this case, there are some critical areas near the Leading edge (the presence of the blade interferes the flow field) and near and downstream of the Trailing edge (for the separation conditions). As a consequence, in these zones the obtained mesh has been more refined by the splits of the edges as it is shown in the picture (fig 4.13).

Summarizing, the Global Size Factor has been chosen and then the other values have been fixed. Below a list of the variables is reported with the final values and in the figure (fig 4.13) it is possible to see the mesh specifications:

- Global Size Factor 1,9
- First Element Offset 0,04 (boundary condition fixed $y^+ < 50$ [15] [16]), higher than this value the y^+ increases too much on the blade wall and this is dangerous for the turbulence level
- Number of Elements in the Spanwise 3 because with only two cells there could be an error in the maximum edge length ratio value (>1000) and the simulations can fail (fig 4.14).
- Split Edge at Leading and Trailing edge zones with a refine scale value

Both the number nodes, the number of the total elements and the Mesh analysis errors (the most important value is the Maximum Edge Length Ratio that should be less than 900) depends on the profile. The maximum number nodes is 52096 (first rotor at the shroud profile) and the maximum number of the elements is 38076 (in the same profile). For the setting of the Mesh data parameters, a comparing method has been used, in this work, as a form of a Validation code (which is discussed in the next paragraph).

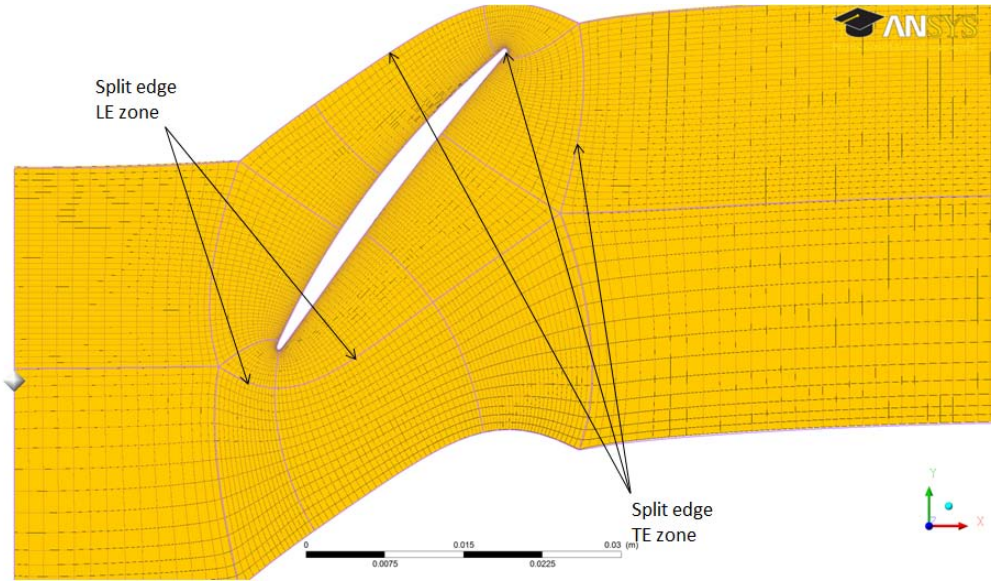

Figure 4.13: Particular of the splitting edge zones (r1 span 100)

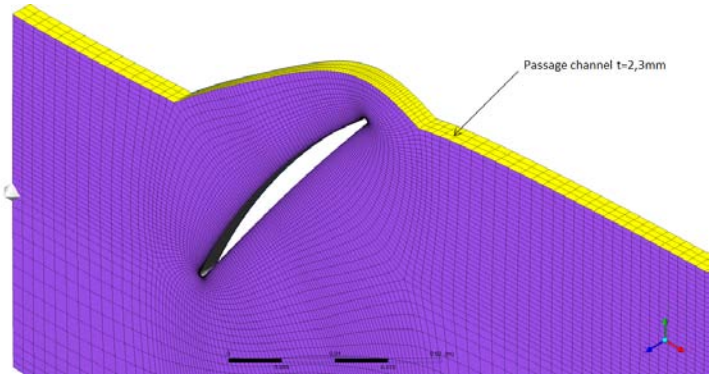

Figure 4.14: Passage channel divided by three cells (r1 span 100)

4.3.1 Validation Code

In order to define the optimal setting for the mesh grid, a "comparing method" has been created and it acts like a Validation code necessary to launch the simulations. This method confronts the final values of the Loss Coefficient (from the post-processing) in different conditions of mesh size. Normally, a validation code starts from some experimental values and with trial initials simulations the designer search the best conditions to minimize the gap between the numerical and experimental data.

In this research, a different approach is used, since no experimental data for the simulations are available. The achievements of the optimization process are to find the best

parameters to minimize the value of the Loss Coefficient, with a high definition and precision of the results, to create a mesh grid not too heavy to simulate (not too many nodes), and try to minimize the simulations time (fig. 4.15). Hence, the process starts fixing the

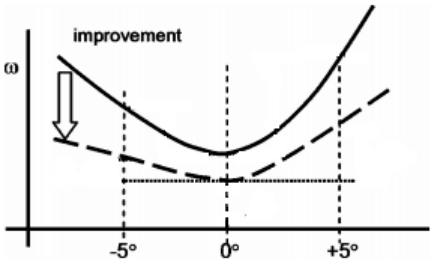

Figure 4.15: Achievement of the comparing method [24]

variation range of the Global Size Factor between 1,5 to 2,1. The Higher is the value of the GSF and the more refined is the grid. If increasing the value of the GSF the rate of the Loss Coefficient does not change anymore, the final setting for the mesh definition is found, and a validation code is successfully done. After that it is possible to define better the mesh specifications with the splitting of the most interesting edges. The picture (fig 4.16) reports the optimization process for the profile of the first rotor at shroud (the most critical one), and as it is possible to see, with a global size factor between 1,9 to 2,1 the results do not change radically, and a value of 1,9 has been chosen to decrease the simulation time and the numbers of the nodes in the domain.

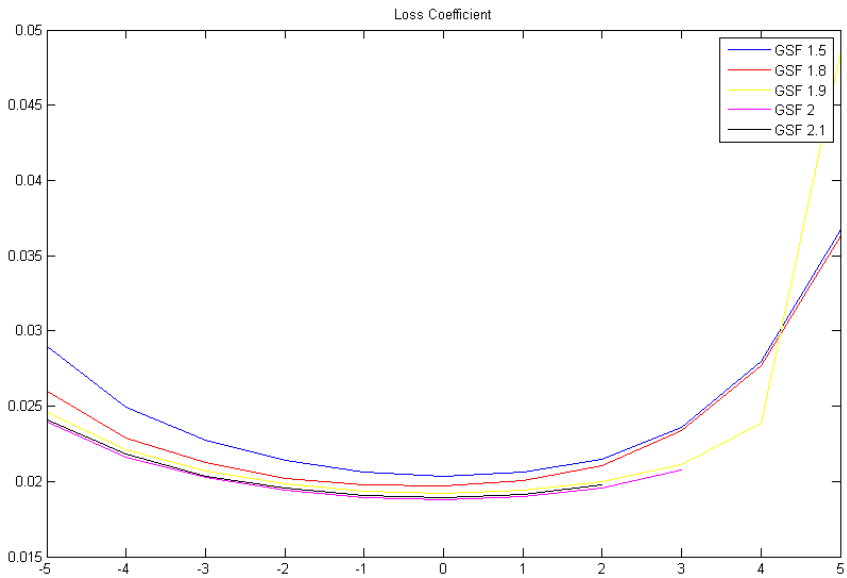

Figure 4.16: Validation code for r1 at shroud

4.3.2 Automatized of meshing process

With TurboGrid it is possible to write a "session file" (text format), where all the steps to create the blade and meshing the domain are written. Hence, with the aim of Matlab the

writing of this session file is automatized for all the profiles studied [Appendix A]. The text file required the path specification for the geometry data, the definition of Leading and Trailing edge (written in the profile point), and the specifications for meshing the domain.

In particular, at the beginning of the Matlab file the following conditions in order to create the session file are required:

- GSF: global size factor
- NESW: number of the elements in the spanwise
- FEO: first element offset
- ESn (where n is the number of the edge to split): Edge Split Factor

After the session file it is necessary to create another one called "state", where the session file is loaded and at the end the final mesh can be saved in a specific format (.GTM), which will be loaded in CFX pre solver software.

For each profile, Matlab researches the right path folder, and different mesh files will be created with all the specifications required. As it is written in the previous paragraph, the mesh topology (ATP Optimized) has been chosen because it can adapt the mesh definition for different geometry conditions. Hence, a general matlab script has been designed with the essential initial conditions:

- mode: type of the blade, r if rotor, s if stator, and igv
- span: position of the profile
- Z: real number of the blade, it must be changed in function on the blade type, if it is rotor Z=31, if stator Z=33, and if igv Z=29

After this, two matlab subscript run, one for the creation of the profile point, the second only for meshing the domain in function of the blade type. In the appendix there will be part of the scripts used in this work, in order to better understand the numerical process.

Chapter 5

Single Phase Simulations

5.1 Operating Range

In the Third Chapter the effects of the variation of the Mach number and the Incidence angle were written and how they can interact with loss coefficient and deflection. The reasons of the different results have been described in a general view. With that knowledge, one of the most important aspects, in order to save time during the simulation loop, is to decide the operating field of research. Thus more details about the work of an axial compressor will be explained, especially about the variation of the Mach number through the stages and some specifications about different velocities to set as well.

In a turbomachine when a rotary duck is studied, the velocity considered is the relative one, while for a stator the absolute is used.

Shape and blade type (rotor/stator) could interact with the distribution of the velocity through the compressor. Normally, the more stressed part is the rotor one, where there are the highest velocities (relatives) than the other zones (stator or IGVs). The compressor experimental data fix the maximum inlet Mach number for the rotor blades around 0,7-0,8 and the maximum value in the stator blades between 0,5-0,6. The three-dimensional developments of the machine were designed by the Free vortex approach [22] [4] and so the velocity can increase very much especially at the shroud regions. Furthermore, as it is possible to see in the previous chapter, the blade (the rotor one) has a high twist angle from hub to tip. All these conditions probably could lead to transonic conditions at the tip of the blade (rotor). In the hub regions instead the mach number cannot increase as from the tip. For all these reasons the choice of the simulation operating range should be fixed reasonably, in order to save time and simulate the process as near as possible to the real working conditions of the machine.

In this work, the steady-state analysis (paragraph 5.2) is studied. Hence there is not difference about the velocity, always the absolute one is considered (the reference system is the absolute), thus the Inlet Mach number is always absolute.

5.1.1 Mach number

According to the previous paragraph, different variation ranges of the Mach number is chosen in function of the real behaviours of the machine. Hence, as it will be explained below, the field of the Mach number depends on the type of the blade and on the position of the profile analyzed as well.

Rotor Blades

Span 000 (hub profile): 0,4<M1<0,7
Span 025 and Span 050 (middle span): 0,4<M1<0,8
Span 075 and Span 100 (Tip profile): 0,4<M1<0,9

As it is possible to see, when the Mach number is lower than 0,4 there are not simulations because only the compressible flow condition is researched, and even when the Mach is higher than 0,9 there are not simulations as well because that value is higher than the real working boundary.

Stator Blades

Span 000 and Span 025: 0,4<M1<0,5
From Span 050 to Span 100: 0,4<M1<0,6

Here, as it has been specified before, the velocities are lower than those in the rotor blades and the variation range is smaller as well.

IGV blade

Span 000: M1=0,4
From Span 025 to span 100: 0,4<M1<0,5

The variation range is smaller than the stator blade because the achievement of this blade is only to introduce the flow correctly (in function of the operation conditions of the compressor), thus the velocities cannot increase too much.

5.1.2 Incidence Angle

The Mach number specification influences the definition of the Incidence Angle range because, as it is reported in the graphic of the loss coefficient (fig. 3.7), the higher is the Mach value and the smaller is the variation space of the Incidence. Hence, the different Inlet flow conditions depend on the velocity and, of course, on the type of the blade.

In a first approach a big range of values has been specified in order to correctly characterize the profile behaviour, because the design point was unknown, indeed the position of the lowest value of the loss coefficient was one of the goals of this study. First of all, the theoretical design point (i=0°) has been fixed without difference between the flow angle and the metal angle of the blade known from the machine design data.

Only in a second phase (after some trial simulations) the results will be evaluated, and the simulations with a high value of the loss coefficient (more than two or three times than the minimum value) will be not considered and the definition of the operating range will be evaluated.

In the picture (fig. 5.1) the meaning of the positive or negative value of the Incidence has been reported.

Rotor and Stator Blades

M1=0,4-0,6: $-20^o<i<+20^o$
M1=0,7: $-10^o<i<+10^o$
M1=0,8: $-6^o<i<+6^o$
M1=0,9: $-4^o<i<+4^o$

Small variation ranges of Incidence for high Mach numbers have been chosen because the operation of the compressor is not assured and the simulations can crash or simply not

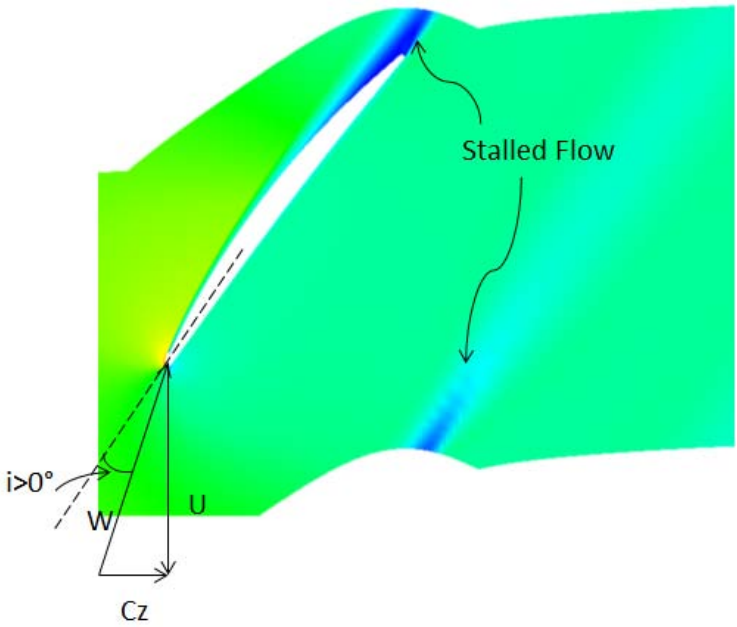

Figure 5.1: Incidence angle specification

converge. Obviously, the values written above are valid for the Stator until Mach 0,6 (no simulations in M>0,6 conditions).

IGV Blades

M1=0,4-0,5: -25°<i<+20°

Here the operation range is bigger than the other profiles because the IGV adjusts and guides the flow into the rotor, hence it should be studied in the whole working range.

5.2 CFX Pre-Solver setting

As it is written before, the CFD simulations have been carried out with ANSYS-CFX (v.14). It is provided with different kinds of specifications in order to investigate a wide typology of machines. This work is focused on a turbomachinery, thus the TURBO MODE has been chosen to start the pre-solver setting definition. In this modality some basic characteristics should be given to the program like: type of machine taken under exam, rotational axis, analysis type (steady-state i.e.), mesh specifications from TurboGrid (.GTM file), and some initial conditions for Inlet and Outlet sections. This option drives the simulations to a possible convergence closer than the real conditions. All the other options, as wall boundaries, flow analysis or solver control settings, can be specified later inside the program.

The analysis has been carried out by steady state method, hence the flow does not change over the time and the simulations do not require information about the development of the flow field through the channel [9]. This is the easiest way to simulate turbomachines because it can save a lot of calculation time, and this method is much more close to the real behaviour after the start up condition. Sometime this type of simulations cannot arrive to a convergence, because there are some problems with the quality of the mesh or with the time step size of the integration [11]. Indeed the residual trend can be oscillatory but this problem could be fixed by changing the value of the time step size (decreasing the value).

Furthermore, in CFX simulations, different conditions of flow field (subsonic, transonic or supersonic) can be studied and the compressible effects can be analyzed by setting the total energy heat transfer model.

Only one profile has been studied for each simulation, hence the interaction between rotor and stator blade has not been taken into account. This condition must be considered in the post processing phase, to extract the final results, especially to fix the position of the reference planes where the measurements make.

5.2.1 Basic Equations

As stated in the previous chapters, the equations of the compressible flow should be considered because the Mach number is higher than 0,3. Hence, the equations of ideal gas and gas dynamic theory have been studied in order to set the initial conditions of the flow field. In the Chapters 2 and 3, the basic theory of gas dynamic analysis and cascade conditions are written, thus here, only the main specifications will be reported in order to better explain the calculation process.

Some parameters at Inlet and Outlet sections should be fixed, according to the literature, in order to define the entire flow field through the domain. ANSYS offers the possibility to specify a lot of different conditions in function of the type of simulations required. In this research the problem is to find how to fix all the initial conditions as a function of only mach number and incidence angle, without considering the Reynolds number because it could be difficult to calculate as initial condition. Hence, in the Pre solver file has been set for the Inlet:

- Total pressure (p=101325 Pa)
- Total temperature (T=288,15 K)
- Cartesian component of the flow direction (Cx, Cy and Cz) (velocity specifications)
- Turbulence level: Medium intensity 5%

Now the Outlet conditions must be specified as well (as a function of the Inlet ones) and to avoid interferences with the physical development of the flow inside the domain, the mass flow rate at Outlet has been chosen as a boundary parameter. With this option, the simulations will take more time than other simulation conditions, but this is the only way to be able to analyze the development of the flow closer than the real operating conditions with those initial specifications. The mass flow at Outlet is known for the principle of continuity, indeed the value at Inlet is the same of that at the Outlet.

The conceptual calculation scheme, stated below, leads to understand the influence of Incidence and Mach number in the evaluation process. The first parameter to study is the ratio of the total and static pressure (5.1) in function of the Mach number

$$\frac{p^0}{p} = [1 + (\frac{\gamma - 1}{2})M^2]^{\frac{\gamma}{\gamma-1}} \tag{5.1}$$

and for the ideal gas condition

$$\rho = \frac{p}{R * T} \tag{5.2}$$

the density value can be found with the inverse equation of the pressure ratio combined between the ideal gas condition:

$$\rho = \frac{p^0}{R * T * ([1 + (\frac{\gamma-1}{2})M^2]^{\frac{\gamma}{\gamma-1}})} \tag{5.3}$$

So, at the end, the mass flow is calculated as:

$$\dot{m} = \rho * C_x * A = \frac{p^0}{R * T * ([1 + (\frac{\gamma-1}{2})M^2]^{\frac{\gamma}{\gamma-1}})} * C_x * A \tag{5.4}$$

As it is possible to see in the final equation (5.4), it depends on the initial condition of the total pressure and static temperature. This last one can be calculated easily with the gas dynamic equations, in function on the fixed total temperature:

$$T_1 = \frac{T^0}{[1 + (\frac{\gamma-1}{2})M^2]} \tag{5.5}$$

then, the mass flow rate depends on the Incidence as well, because of the presence of the axial component of the absolute velocity value (for stator and rotor) calculated from the absolute velocity rate and the flow angle. The last value is a function of the Incidence angle and the Metal angle of the profile, so everything depends only on Mach and Incidence specification.

Inlet Angle specification

The metal angle of the profile has been calculated from the Camber line angle at the leading edge and the angles of suction and pressure side. The metal angle has been defined by the difference between the camber angle and the average of the other two angles:

$$MetalAngle = BetaMetal1 - \frac{LEPS + LESS}{2} \tag{5.6}$$

where Beta Metal1 is the value from the data sheet of the profile and LE PS or LE SS are the rates of the pressure side and suction side angles respectively (always reported in the data sheet).

The reference specification of the Inlet flow angle has been changed, respect to the one implemented in ANSYS, in order to consider the influence of the Incidence:

$$\beta_1 = 180 - \beta_m - i \tag{5.7}$$

as it is shown in the picture (fig. 5.2) with the definition of the incidence angle according to literature (fig. 5.1)

Referring to the figure (fig. 5.2), the meaning of incidence is here reported:

- positive: the inlet flow angle decreases
- negative: the flow angle increases

Now the velocity components can be calculated with the trigonometric laws from the absolute value of the velocity derived from the definition of the mach number:

$$M = \frac{C_{abs}}{\sqrt{KRT}} \tag{5.8}$$

where R and K are the constants of the fluid and thanks to the reverse function the velocity is obtained. Hence, the axial and spanwise components are known as well:

$$C_x = \sin\beta_1 * C_{abs} \tag{5.9}$$

$$C_y = \cos\beta_1 * C_{abs} \tag{5.10}$$

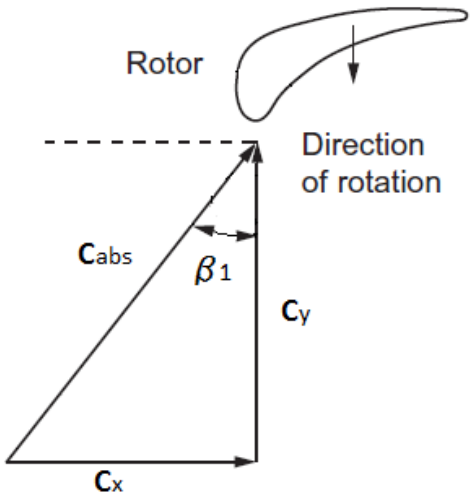

Figure 5.2: Inflow angle specification [1]

5.2.2 Domain analysis

Material

The fluid simulated is Air considered in ideal condition. In order to predict the variation of the temperature and the enthalpy through the meridional channel, the heat transfer model chosen is the *Total Energy* one because the flow is in low-speed condition and the Viscous Work Term for the energy equations is thus possible to study [9]. The Total Energy analysis includes kinetic energy effects and these become very important when the mach number is over than 0,3. Furthermore, this option takes into account the effects of the compressible or incompressible flow and the type of the buoyancy model as well [12].

Another important aspect is the regulation of the turbulence modelling in order to analyze the separation condition as near as possible to the real working conditions. This is a big problem especially because the pressure gradients could be really high in the critical zones. For turbomachines where the stall condition is determinated by the separation of the flow, the prediction of this phenomena is important and it should be done with a high quality and precision. Nowadays, the equations used to regulate this problem are the $K-\omega$ and the $k-\epsilon$, and for these investigations the first one is used.

The $k-\omega$ is based on the *Shear Stress Transport (SST)* model, one of the most important mode to predict the separation condition in zones with different pressures gradients and with inclusion into the eddy-viscosity formulation of the transport effects [12].

General conditions

The domain of each single profile must be ideally connected with the entire machine, hence the passage interfaces should be interconnected with the Rotational Periodicity option, in order to simulate the real annulus of the compressor and not only a single channel. Always for the same reason and for the calculation of the mass and momentum rates, the walls of the domain should be fixed as well in function on the type of the domain interface. The conditions for the blade wall are:

- Mass and Momentum: No Slip Wall, because the surface is considered like a real interface, hence solid and with zero velocity on the blade.

- Wall Roughness: Smooth type because the roughness of the blade is not taken into account.

Instead for the hub and shroud surfaces, other kinds of options have been chosen because the analysis has been occurred with tiny slices of the blade, hence those walls are not the real ones:

- Mass and momentum: Free Slip Wall, hence the flow has a real development in the channel but closer to the surfaces the velocity is considered without friction effects on the domain walls.

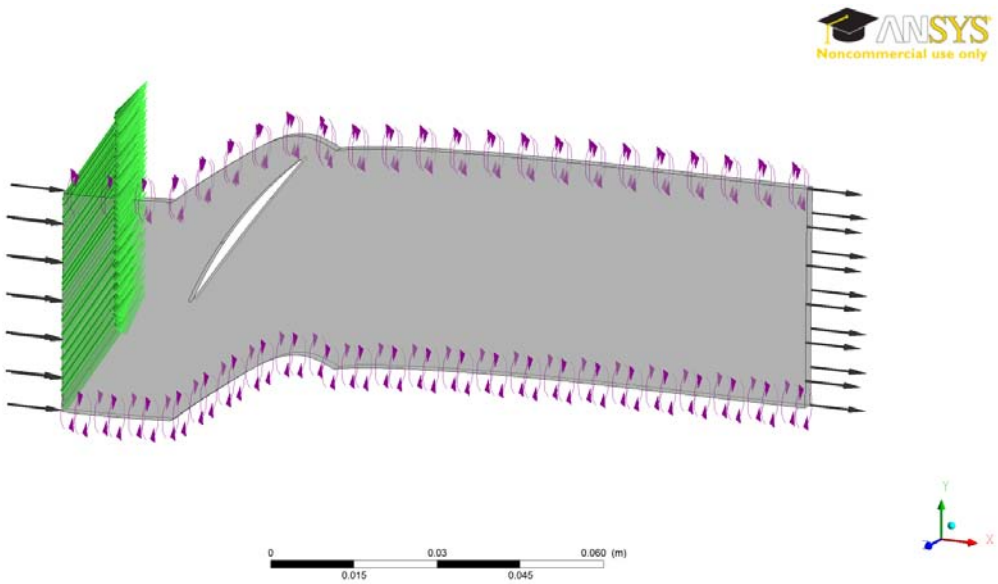

Figure 5.3: Definition of the calculation domain

5.2.3 Solver setting

Solver control

The last step before launching the simulations is to define the solver condition. It can influence the precision of the results and the calculation time, of course both with the mesh size. The first choice is the type of the advection scheme, i.e, the way to calculate the advection terms of the discrete finite volume equations between the first and second order [12]. In ANSYS CFX it is possible to define the blend factor, namely a number between 0 (first order) or 1 (second order) to define the type of the calculation. In this work second order calculation has been fixed because a high precision is required, hence the high resolution option has been chosen also for the turbulence calculation.

In order to control the convergence, a minimum and maximum number of iteration have been defined:

- Min Iterations: 350, high number because most of the time after this iteration the difference between Inlet and Outlet mass flow rate is irrelevant and an interrupt control can be implemented in order to arrest the simulation before achieving the max number of iterations

- Max Iterations: 800, this number has been chosen because after this value the convergence of the Mass,Momentum, Turbulence and Energy is achieved (the residual values are very low)
- Convergence criteria: the iterations are regulated with the control of the RMS (Root Mean Square) values, and the residual target has been set at $1 * 10^{-05}$, hence with residuals values lower than this the convergence is achieved.

In addition, a Local Timescale Factor has been chosen for the convergence criteria, the number is the multiplier of the local element-based time scale [12]. The variation of this value means changing the velocity convergence and in order to stabilize the solution, the number set should be limited (not too high). Indeed there is a maximum boundary after which the solution does not converge. For all of these reasons the time scale number has been fixed to 15.

Interruption control

The particular initial conditions fixed in this work for Inlet and Outlet sections, lead to a low convergence velocity and for the critical situations (it will be explained in the next paragraph) the computational time could be high (15 minutes parallel mode computation). In order to save time an interruption control has been implemented because most of the times the convergence of the general parameters is achieved (RMS residual lower than $1 * 10^{-05}$), but the convergence of the mass flow is not under that level, so the simulation continued until the limit of the maximum number of iterations, and it requires too much time.

Hence, another output control has been monitored in the solver, like the mass flow in inlet and outlet together, in order to check the convergence (fig. 5.4). The interruption condition stops the simulation if the absolute value of the difference of the mass flow rate (inlet/outlet) is lower than $1 * 10^{-09}$ and if the number of iterations is higher than the minimum value (350). With this approach the calculating time has been reduced, sometimes around two or three times.

5.3 Automatic scripting Pre-Solver files

ANSYS CFX Solver required a definition file (.DEF) in order to start the simulations. In that file all the specifics for the calculation are reported, like condition of the mesh file, definition of the Initial condition (Inlet and Outlet), and all the equations valid to start the iteration loop. As for TurboGrid file, also for Solver software an automatic Matlab script has been designed [Appendix B.1.1], in order to write the definition file of each simulation. The only way to automate the scripting of the Pre-Solver file is to write a session running, as for T-Grid, and to launch every time a script with different specifications given by Matlab. Hence, a general script has been written where it is possible to control the overall specifications like: type of the profile (Rotor, Stator or IGV), position of the span taken into account, number of the stage for Rotor and Stator, mach number, and incidence angles given as boundary condition.

The script is defined by a function called `CFX_Pre_xxx` in which the different session files are written. It is specified in a different way for each type of the blade because the definition of the path is different from IGV and Rotor i.e., and the specification of the Inlet angle changes between Rotor and Stator or IGV because the blade has a different definition of the pressure and suction side in function of the shape.

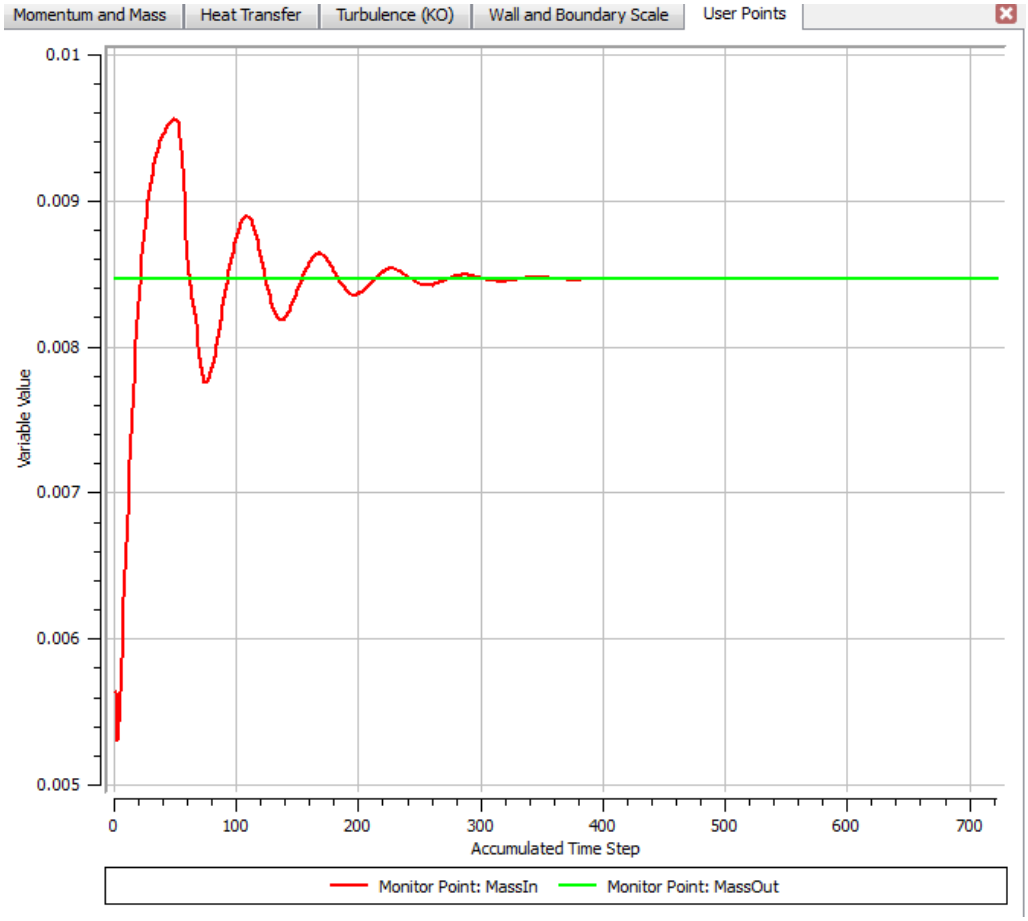

Figure 5.4: Mass Flow Inlet and Outlet monitoring until the convergence

The Matlab function requires also other initial specifications in order to start the iteration loop. They are geometrical conditions (characterization variables) to calculate the value of the metal angle of the profile as it was written in the previous chapter. In particular Matlab reads an external text file where it has been reported the value of the camberline angle and the metal angle of the pressure and suction side in order to subsequently write those into the equations of the session file. The other parameters required for the general definition of the solver condition are:

- LTF, local timescale factor
- MAXIter, maximum number of iterations
- MINIter, minimum number of iterations
- RMS, the residual target for the convergence
- Conv, the value to achieve for the interruption criteria

The script is divided into three big parts, one only for the zero incidence, another for positive values and the last one for negative ones. That has been made in order to save computational time, because the simulations with Incidence value different from zero, starts from the results file of the previous condition, i.e, for i=1 the solver file start the new simulation from the result file of i=0 and so on (the same is for the negative incidence).

Obviously, only the zero condition does not start from initial values because this is the first simulation.

At the end of each session file, a definition file is created to be loaded in the solver program. At the end of each condition a batch file has been created in order to launch the simulations.

5.3.1 Computational details

The simulations have been launched in two computers with the following specifications:

- Processor: Intel(R) Core(TM) i7-2600K CPU @ 3.40GHz 3.40GHz
- Ram: 16 GB
- System: 64 bit

In one of them the simulations for Stator and IGV have been launched with 1824 simulations and it took around 167 hours for the entire calculation process. While on the other computer the Rotor profiles have been simulated with 2164 different investigations and it needed around 200 hours which have been necessary to complete the whole loop. The duration of the simulation depends on the mesh grid size and on the condition of the mach number in function on the shape of the blade. The more bending is the profile the harder is the calculation, especially if the mach number increases.

The conditions for the solver program have been written into the batch file, because if they were written inside the session file the simulation could not start in the future ANSYS releases because the specifications could change. However, the investigations have been launched in parallel mode in order to save computational time, splitting it by each cores available.

5.4 CFX Post Processing

Two different output files have been saved from the Solver for every simulation, one is called Out file in text format, where the entire history of the iteration loop is logged. It is useful to check with an external program (like Matlab) the final results of the iterations. The other one is the real results file necessary to extract the reports in the Post processing phase. First of all, the simulations should be checked: this means reading the output file and checking if the final residual parameters of the iterations can be accepted as good ones (below it will be explained the meaning of good simulation), otherwise the simulation should be not considered. In this work, because of the high number of investigations, the checking phase consists in a big problem because it is impossible to carry it out manually for all the simulations and, as it is written below, an own method has been found in order to accept or not the results.

In the Post solver process (ANSYS CFD-Post) it is possible to calculate and analyze a lot of different characteristics of the blade profiles. Hence, the initial step is to decide which are the most important parameters for the calculation of the loss coefficient and deflection. The following step is to decide where to make the calculation, if near to the blade or far away from it because the results could differ. Therefore it is necessary to define the reference plane for the analysis and this is an important process because the final characterization depends on it.

The other most important specification is how to calculate the results, especially for this kind of simulations where the value of the mach number is quite high (for a subsonic

condition). Thus the effects of the separation flow condition and the high turbulence after the Trailing edge of the blade could create some problems for the calculation of the parameters with the automatic equations provided by the program.

The last task is to decide how to show the results at the end of the evaluation process: it means how to represent the reports, for example in a table view or in a graphical display, like contour plot and charts, or both.

5.4.1 Evaluating of simulations

As it has been written before, a lot of different conditions have been studied in this work (around 4000 simulations), hence in order to check each output file an automatic mode has been found through a Matlab script. It checks the residual results of the iterations of a simulation and estimates if it could be considered or not. One way to evaluate it is to check the global conservation statistic present in the output text file (fig. 5.5).

```
Domain Imbalance :                                        -3.5041E-06

Domain Imbalance, in %:                                      0.0000 %

+-----------------------------------------------------------------+
|                              W-Mom                              |
+-----------------------------------------------------------------+
Boundary         : Inlet                                  -2.0552E-07
Boundary         : Outlet                                  4.3085E-04
Boundary         : r1 Blade                                1.2902E-05
Boundary         : r1 Hub                                  3.0861E+02
Boundary         : r1 Shroud                              -3.0918E+02
Boundary         : Periodic                                5.6414E-01
                                                          -----------
Domain Imbalance :                                         1.4424E-04

Domain Imbalance, in %:                                      0.0000 %

+-----------------------------------------------------------------+
|                              P-Mass                             |
+-----------------------------------------------------------------+
Boundary         : Inlet                                   8.4660E-03
Boundary         : Outlet                                 -8.4660E-03
                                                          -----------
Domain Imbalance :                                        -2.7940E-09

Domain Imbalance, in %:                                      0.0000 %

+-----------------------------------------------------------------+
|                             H-Energy                            |
+-----------------------------------------------------------------+
Boundary         : Inlet                                  -8.5033E+01
Bnd Src/Visc Work: Inlet                                   4.2084E-07
Boundary         : Outlet                                  8.5033E+01
Bnd Src/Visc Work: Outlet                                 -5.9041E-06
Domain Src (Neg) : r1                                     -1.7605E+01
Domain Src (Pos) : r1                                      1.7605E+01
                                                          -----------
Domain Imbalance :                                         5.9128E-05
```

Figure 5.5: Particular of the domain imbalances specification at the and of the output file

In the figure it is reported a small part of the out file where the statistics of the iteration are reported. These are called global conservation statistics and they are calculated for all transient equations [8] like U-Mom, V-Mom, W-Mom, H-Energy, P-Mass and due to these parameters the convergence can be easily defined as good or not. In the output file the total condition is called *Domain Imbalance* and it is the summary of all characteristics present in the convergence results. A small value of this indicates the achievement of the convergence, otherwise the convergence could be not achieved or the results are not satisfactory.

The parameter considered in this work is the percentage of the domain imbalance rate:

$$\%Imbalance = \frac{DomainImbalance}{MaximumOverAllDomain} \tag{5.11}$$

where the Maximum OverAll Domain is the maximum value (absolute) of all the sources and boundaries in a domain [8]. A low absolute value of the percentage means a good convergence achieved, hence it has been chosen like the discriminating parameter to accept or not the simulations.

The automatic checking of the output file accepts the simulations when the percentage of the domain imbalance (DI) respects the following condition:

$$good\ convergence = abs(DI) < 0,1\% \tag{5.12}$$

This value has been chosen mainly for two different reasons:

- The first reason is that considering some simulations the convergence of momentum, turbulence, mass, and heat transfer is most of the time achieved and also the convergence of the mass flow as well, but in some cases, because of the interrupting criteria, it can have a high number of domain imbalance because the Inlet and Outlet mass flow rates are not exactly the same, but the simulations can be accepted because the difference is around $1 * 10^{-08}$ and the imbalance percentage is around 0,1%.
- The second is because the mesh size is not optimized for each profile and it could create a number different from zero in the domain global statistics.

For the reasons written before many simulations could be not considered with a higher value of the percentage despite a good convergence.

5.4.2 Reference planes positions

The turbulence, the effects of viscosity on the cascade and the separation condition usually create many problems for the measurement of the flow angle, velocity and total pressure values across the pitch between two consecutive blades. Thus the reference position and the modality of the measurements can interfere on the final results precision.

In a real testing phase, the different parameters are investigated through seven or eight probes (as it is reported in the picture of cascade high-speed wind tunnel 3.3) positioned downstream of the flow. As it was expected, the effects of the condition written above lead to an instability of the flow field after the Trailing edge of the blade, hence the most important parameters have not constant values in the streamwise (obviously) and spanwise direction. For example, in the picture (fig. 5.6) the trend of the total pressure (outlet) is reported. The pressure has a minimum peak at the Trailing edge zone for the frictional losses on the blades surfaces and then it has a constant value between two consecutive profiles.

A fluctuation of the outlet flow angle occurs as well and it depends on the behaviour of the velocity at the outlet section. In the picture (fig. 5.7) the velocity trend is reported and for the presence of the blade (zero velocity on the walls) a minimum peak of the value is observed at the Trailing edge.

For the reasons written above, it is necessary to make an average of all values between the pitch and to define a reference plane (inlet and outlet) where fixing the measurement position.

The behaviour of the parameters change in the streamwise direction for the propagation of the wake effects after the trailing edge, indeed as it is reported in the picture of a CFD

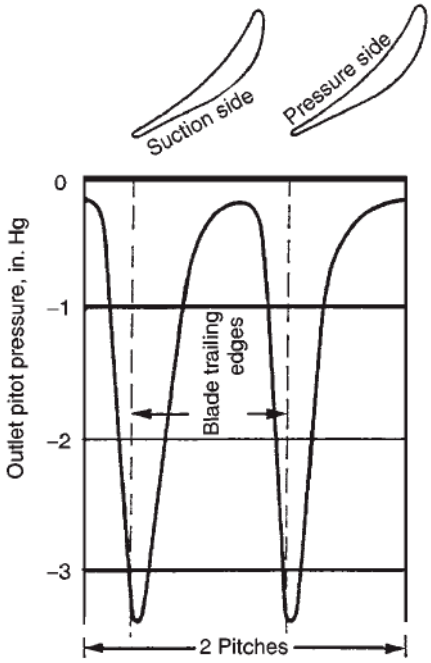

Figure 5.6: Stagnation pressure trend at Outlet section [5]

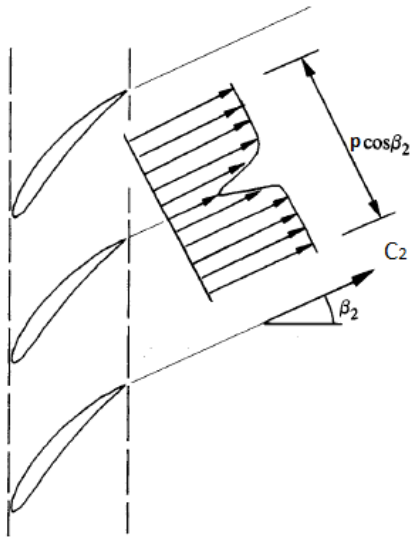

Figure 5.7: Effects of the viscosity on the velocity trend [17]

simulation (fig. 5.8), the dissipative phenomenon leads to increase the wake cone so the dissipative phenomenon is even more important for the variations of the parameters in the streamwise. Thus, the reference plane position is important for the precision of the results and for the reliability of them.

In literature there are many papers that talk about this problem. In this work the calculations have been carried out in these following positions found in the papers [16] [25] [7] [3]:

- Inlet Reference plane=0,5*Chord

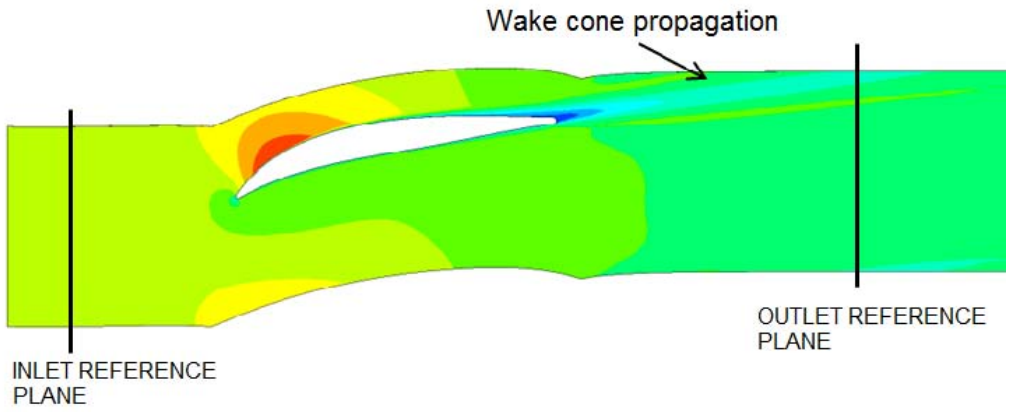

Figure 5.8: CFX simulation post processing results with the development of the wake cone [profile not in scale] and specification of the reference plane position

- Outlet Reference plane=0,9*Chord

In this way the results could be compared for rotor and stator blades always at the same distance from Leading and Trailing edge with the same interactions of the overwrites effects. Now the problem is how to make the averages between the calculations parameters in order to characterize the blade profile as close as possible to the real working conditions.

5.4.3 How to calculate the results

The approach followed in order to calculate the final results is to solve the integers of the calculation process with some total equilibrium models, like the average of the mass flow or the area one. The choice depends on the effects of the flow field conditions (laminar, turbulent etc.) especially at the Trailing edge of the blade.

In the third Chapter the different equations used to calculate the loss coefficient have already been explained. It has also been specified that the loss coefficient will be calculated with the ratio of the pressure, total-total at numerator and total-static at denominator, in order to compare the results in literature [15] [16]:

$$\omega_p = \frac{p_1^0 - p_2^0}{p_1^0 - p_1} \tag{5.13}$$

and for the deflection the following equation will be used:

$$\epsilon = \alpha_1 - \alpha_2 \tag{5.14}$$

ANSYS Post-processing offers many different options to compute the parameters required, in function of the type of the results researched. For these types of calculation the most used approaches in order to specify the pressure and velocity rates are:

- Area-weighted average method [10]
- Mass Flow weighted average method [10]

The first approach, called also areaAve, makes the area-weighted average on a specific surface (or location). The average depends on the mesh size of the domain, indeed without considering the weighted method, the final result could be influenced from the zone with

a small mesh size. Usually the velocity, dependent on the area, is calculated with this approach and in a first part of the work the results have been found in this way. However, after some problems with the pressure values another method has been chosen. Indeed also the pressure rates heve been found, at first, through the calculation of the areaAve. Only in a second moment it has been calculated by the Mass Flow average method (or MassFlowAve), just to make a comparison between the results founded in different approaches.

The MassFlowAve method calculates the average of the variable researched on a two-dimensional surface location in every node of the mesh grid, following the next equation [10]:

$$massFlowAve\ (\phi) = \frac{\sum m\phi}{\sum m} \tag{5.15}$$

where ϕ is a general variable researched and m is the value of the local mass flow. Thus the value of the pressure, i.e., is calculated by the weighted average of the mass flow at each grid nodes of the mesh on the specific location.

As it is possible to see in the graph (fig 5.9), by a comparison of the results from the two different approaches they do not collapse in a same line but there is a difference in the final report (around 5-10%). This effect is explained, looking at the final data, from the high level of turbulence because of the presence of the separation condition at the Trailing edge of the profile (as it is written in the previous paragraph). Thus, when there are some dissipative effects, the two approaches differ especially in off-design conditions for the instability of the flow field.

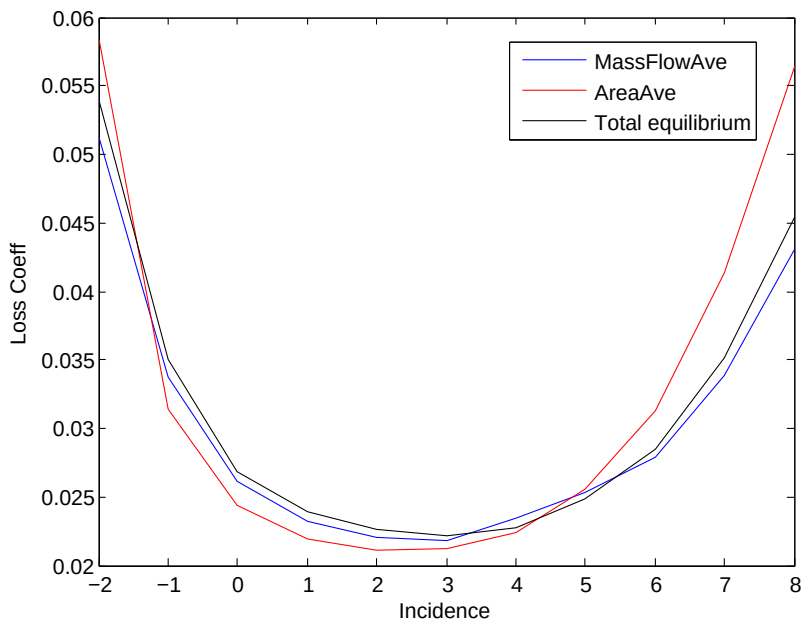

Figure 5.9: Comparison of the approaches (profile r1_100 M1=0,7)

For all these reasons an experimental method based on the total equilibrium approach has been adopted thus, all the parameters like pressure, velocity, angles and so on derive form that kind of calculation. In the graph the final results are quite in the middle of the other two curves as if it were an average of the two methods (fig. 5.9).

5.5 Automatic Scripting of results

The final results of each simulation will be written in an external text file divided by type of profile (stator or rotor, number of stage, span position) and in function on the Mach number. In the text file there will be written the most important data for the further analysis divided by:

- incidence degree
- loss coefficient
- deflection
- inlet flow angle
- outlet flow angle

With an automatic Matlab script all the folders are checked and the file results are searched [Appendix B.1.2]. Thus there are two different possibilities to evaluate the files:

- No convergence (any file results present): in the external file there will be written NaN (not a number) and the specific point is not taken under exam in the evaluation process
- Convergence achieved (file .res present): open the output file in order to check if the simulation is reliable or not (simulation good or not), in function on the domain imbalances (previous paragraph).

At this point all the percentage values of the domain imbalance are checked and the acceptance condition should be achieved in order to evaluate the results of a simulation:

$$good\ convergence = abs(DI) < 0,1\% \tag{5.16}$$

and as it has been done in the previous phase, two different possibilities have been defined to evaluate the process:

- No good convergence (DI>0,1%): In the external text file there will be written NaN in the specific incidence condition and the parameters will not be calculated
- Good convergence (DI<0,1%): The parameters can be evaluated

Now only the reliable simulations are considered as ready to be evaluated. Thus in the same Matlab script, after the checking phase, there are the specifications for an ANSYS Post-processing session file where it is possible to define the following conditions:

1. specify the position of the reference surfaces in function on the chord value (calculating of the chord) and thus defining the evaluation position
2. write the equations in order to evaluate the parameters (areaAve and MassFlowAve methods at first) and then writing the experimental equations used in this work
3. create a table where the most important results maybe summarized. As it is reported in the picture (fig. 5.10), in the table there is the calculation of the loss coefficient in the three different ways in order to find the most reliable results by a comparison between them.

```
M1          0.70
Incidence   0.00

Mass Flow Ave                          Area Ave
Pt1 Ref    101325.00 [Pa]              Pt1 Ref Area      101325.00 [Pa]      %total pressure Inlet
Pt2 Ref    100587.00 [Pa]              Pt2 Ref Area      100635.00 [Pa]      %total pressure Outlet

Rho1 Ref  0.97 [kg m^-3]                                                     %density
Cabs1 Ref          227.38 [m s^-1]                                           %absolute velocity value Inlet

P1 Ref     73036.20 [Pa]               P1 Ref Area       73038.90 [Pa]       %static pressure Inlet

Beta1 Ref          55.50 [degree]                                            %Inlet Flow angle
Beta2 Ref          51.12 [degree]                                            %Outlet Flow angle

Loss Coeff1         0.0261             Loss Coeff3        0.0244             %loss coefficient

Delta Beta          4.39 [degree]                                            %deflection

New Approach
Pt1 Ref    101327.00 [Pa]
Pt2 Ref    100566.00 [Pa]

Rho1 Ref  0.97 [kg m^-3]
Cabs1 Ref          227.37 [m s^-1]

P1 Ref     73043.80 [Pa]

Loss Coeff5         0.0269
```

Figure 5.10: Particular of the external text file at the end of the evaluation process (profile r1_100)

4. save the table as an external text file which it will be analyzed by the Matlab script and only the required results will be extracted from its.

The final task of the automatic script is to summarize all the externals text files in a definitive one, as it has been written at the beginning of the paragraph.

All the points described are reported in a unique script and it will be launched as a Matlab function from the general script where the principal parameters should be specify in order to start the checking and evaluating loop (it is written in the same form as it has been done for the definition of the Pre-solver file).

5.5.1 Cleaning results

As stated in the third Chapter, the operating range is defined where the maximum value of the loss coefficient is twice of the minimum one (Howell and Lieblein correlation [5] [17]). Obviously at the beginning of the work the operating range can not be known and for this reason a lot of conditions have been evaluated. After the Post-processing phase the design condition will be found and thus the working range will be specified as well.

With the help of another Matlab script the results will be cleaned, it means considering only the reliable results under the Howell or Lieblein boundary. However, in the Matlab script all the results under three times the minimum value of the loss coefficient are taken into account only to have a good static distribution for future interpolations of the reports:

$$\omega < 3 * \omega_{min} \tag{5.17}$$

This approach has been adopted because far away from the design condition, and far from Howell or Lieblein correlations, the results are not reliable anymore because the compressor is not working far from the normal operating range.

Chapter 6

Two-Phase Flow

6.1 Introduction

Two-phase or generally multiphase flow is a condition where two (or more) fluids are present together in a flow domain. They can be mixed (in macroscopic or microscopic scale) or have their particular flow field [12]. In this situation, the simulations must consider the development of the principal flow and the injection condition of the other flow. In compressor field, where the main fluid through the channel is Air, it is possible to find some configurations with injection of water at the beginning of the compressor. This practice is used a lot, especially for a turbogas, where the increasing of air temperature (at the head of the compressor) leads to a reduction of density at the beginning and thus at the output of the turbine [26]. This phenomena could lead to a reduction of the power produced by the turbogas and an unstable working condition for the compressor, because the initial conditions change and this leads to an off-design situation.

To avoid this, a method of droplet injection by water spraying action at the beginning of the compressor has been found in the past. This method can increase the efficiency of the entire machine and the output power as well. The research filed has even more focused in this direction, indeed in literature there are many scientific papers that discuss about this topic but knowledge is not so much because there could be problems caused by the difficulty to describe the two-phase flow condition [22].

6.1.1 Overview of spray action

As mentioned in the introduction the water is sprayed into the compressor (at the beginning) in form of droplets. This process is also called overspray fog cooling used in hot or dry days to cool the suction air and this is the most economic method to increase the output power and decrease the compressor work [14]. Droplets injected upstream of the compressor evaporate in the hot air (through the stages) and this leads to a reduction of the heat of it. The reduction of temperature leads to an increasing of the density of the suction air and due to this effect the thermodynamic cycle is much closer to an isothermal compression. Thus less compressor work is required and the thermal efficiency therefore increases [26].

This method may be studied well because some consequences of the droplet evaporation can lead to a worse working of the turbomachine. Thus the design process must take under exam some critical conditions that are present. Indeed, when the droplets are injected into the flow field, the stage load changes because of the evaporation. Therefore the first stages, where water particles are not totally evaporated, have a higher loading, while the last ones

(rear of the compressor) reduce it. The blade loading is important because with a high value of it the separation condition can increase the dissipative effect on the flow field, especially in a zone between the casing and the rotor blades for the presence of the shock wave. Thus it is essential, in a design phase, to count an increasing loading on the blade for the first stage of the compressor in order to optimize the working condition for the two-phase flow [26].

The droplets mass flow is normally a parameter in function of the suction air mass flow. According to the literature, the water mass flow is fixed between 1 or 2% of the air mass in function of the inlet air conditions. Also the diameter of the water particles is in function of the quantity injected into the compressor, and the size could be smaller or bigger in function of the inlet air conditions as well. The behaviours and the performances depend on the diameter size of the droplets for the interaction with the air flow field and the collisions on the blade walls.

For large size ($d > 20-30\mu m$) the evaporation takes more time with respect to droplets with smaller diameter ($d < 10-10\mu m$), and this leads to a reduction of the pressure ratio and a decreasing of the performances of the machine [14]. This is because the fine droplets follow the flow field and adapt their direction better than the bigger ones. Indeed, the particles with a large diameter size can collide the rotor blades surfaces, and because of the centrifugal effect, given by the rotation of the rotor, they reach the outer case of the compressor. This can create a film of liquid that can block the normal air flow, and in long time operations, this can lead to erosion phenomena for the presence of the water impurity. All these effects can increase the problem of the stall on the rotor blades [26].

Other associated problems in the spraying action for cooling the flow are here reported in order to better understand the main problems of the application of this process [14]:

- erosion of the blades caused by the passage of the water droplets
- integrity problem of the compressor for the application of the fogging devices
- troubles for the manufacturers because the performances could be lower

However, as it has been mentioned above, this application is becoming even more important for the high potential in efficiency augmentation, and many studies and researches are now focused on this field in order to improve the method. Furthermore, in some previous research it has been found that the water droplet injection interacts with the compression process [19] and in particular the main effects are here reported:

- the evaporation condition leads to increase the risk of stall for off design situation
- the distribution of the droplet size can interfere with the irreversible entropy generation
- droplet size interacts with the evaporation and thus with the final output power
- the evaporation can reduce the necessary compression work

6.2 Axial Compressor wet condition

As stated in Chapter 4, where the compressor has been described in all its parts, the machine can work both in dry and wet (droplet injection) conditions. Moreover some research has been carried out at the University of Duisburg-Essen, where an own test ring

has been designed and manufactured in order to test the real behaviours of the compressor in different operating conditions [22] [4].

In the picture (fig. 6.1) a particular section is reported, of the three-dimensional model of the compressor, where it is possible to see the position of the nozzle rack for water injection [22] and the position for the flow field investigations. These are carried out by laser technique called Phase Droplet Particle Analyzer (PDPA), thus the evaporation process has been studied without interfering with the flow field.

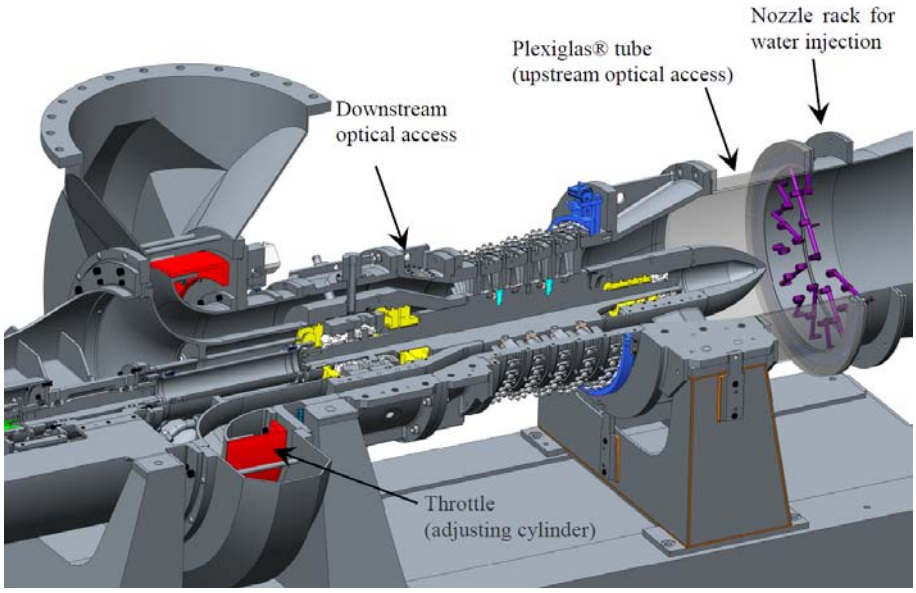

Figure 6.1: Particular of multistage axial compressor with the nozzle rack for water injection at the beginning [22]

Looking at the picture, it is possible to see the 25 possible injection positions of the nozzle rack and the two different positions for the evaluations. The first point to make the measurements is fixed upstream of the compressor, and through a Plexiglass®tube it is possible to investigate the behaviours or the characteristics of the droplets. The second optical access for the measurements is fixed downstream of the compressor and this is useful to compare the two-phase flow condition between inlet and outlet of the machine [22].

Some result extracts from previous simulations on this machine and present in literature [22] focused the attention on the behaviours of the particles and in particular on the size of them. Indeed there is a difference of directions for big and small droplets because the first ones collide to the blade and they change the direction with respect to the main flow. This phenomena can increase the separation condition effects and the compressor is more exposed to the stall situations [22].

For these reasons the investigations of the droplet size is one of the most important aspects to be investigated in order to set the wet working conditions of the real compressor to increase the performances of it. Indeed the diameter size can be optimized to decrease the temperature of the flow without interfering too much with the main air flow.

6.2.1 Achievements of the work

As stated in the previous paragraphs, the behaviours of droplets in a generic flow field through a compressor is one of the most important phenomena to evaluate the wet operating condition of the machine. Furthermore the particle size should be analyzed because,

as it has been reported in the introduction, this parameter influences the performances of the overspray application and thus of the entire compressor. The machine has already been investigated in a three-dimensional approach, hence some results of the investigations are presented and reported in scientific papers [22] [4]. However in order to implement the evaluation of the wet condition in the streamline curvature software, mentioned in Chapter 2, other simulations adopting the two-dimensional method should be carried out, following the same methodology of dry condition. Hence each profile should be studied in a steady-state analysis investigating the performances of them in function on Mach number and incidence angle.

However the main purpose of this work is to find the right setting for the simulations in a wet condition and thus investigate the behaviour of the water particles through the compressor passage. In other words the simulations will be focused only on one profile (first rotor at hub) in different operation conditions in order to describe the following phenomena:

- Streamline particles tracking through the compressor in order to define which ones can reach the outlet section without colliding the blade

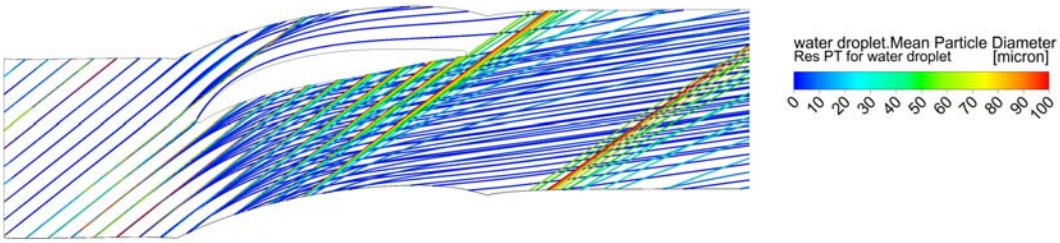

- comparing inlet and outlet condition, leveraging on the distribution of the discrete particle mass in function of the droplet size. With this kind of graphic it is possible to define the best condition of the diameter to introduce in the compressor in order to prolong the cooling action of the water as long as possible.

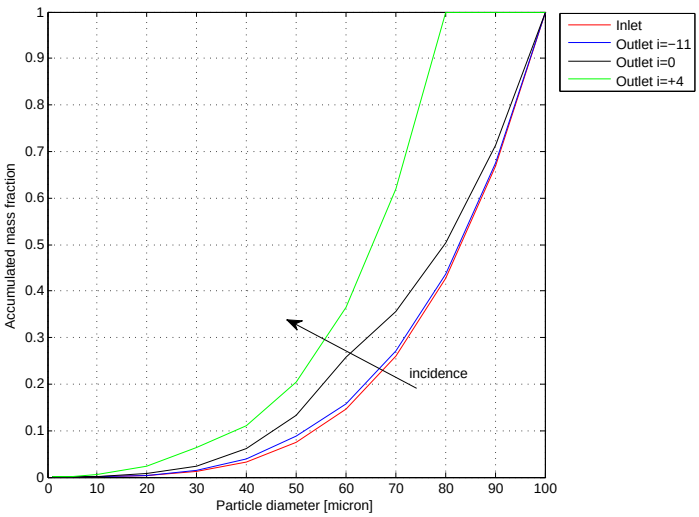

This second task is the most important one to set further simulations of the blades after the first rotor. Without this type of investigation it is impossible to say how many

particles achieve the outlet section of the first rotor, thus how many enter in the first stator and so on.

6.3 Two-Phase Simulation

The already mentioned three-dimensional investigation carried out at the University Duisburg-Essen [4] followed the state of the art for these types of simulations. Thus the water particles were represented with a nonuniform distribution at Inlet surface and in order to easily evaluate the behaviours, a specific diameter distribution method has been imposed for all the droplet injected. The main initial conditions used in that research for the setting of the numerical code are here reported:

- Air temperature: 288,15 K
- Air pressure: 1,01325 bar
- Water temperature: 288,15 K
- Iteration method: between Eulerian and Lagrange phases

The CFD investigation has been carried out by ANSYS CFX commercial software, which is able to take into account many different simulation conditions. As it is possible to see in the list above, the software can investigate the two-phase flow condition in two different ways, Eulerian-Eulerian or Lagrangian Particle Tracking. These are two different methodologies for a qualitatively and quantitatively investigation of the droplet dispersion during the simulations. These respect two different governing equations of motion (and reference system), which are reported in many scientific papers in literature, for the dispersed liquid-phase [21]. A brief of these two different methods is reported below, without theoretical description because this is not the task of the present work.

Eulerian-Eulerian Multiphase model

Eulerian-Eulerian is one of the ways to evaluate the two-phase flow condition and in this method it is possible to calculate the important terms (momentum, heat, interphase transfer model) using the different modeling for the droplet specifications [12]. By ANSYS CFX software it is possible to investigate the droplet behaviours with Eulerian approach, and in particular some advantages by leveraging this method are here reported:

- global and complete information of the particle phase
- wide range of volume fraction can be considered
- turbulence is automatically calculated

But the setting conditions are not so easy to find especially for the investigations that are purposed for this work, in particular it is not possible to fix an injection point in a defined position hence it is possible to have different locations and the comparison in different operating conditions is not reliable.

Lagrangian Particle Tracking

The other method applied in ANSYS is the Particle Transport model (or Lagrangian Particle Tracking), able to model a discrete distribution of dispersed phase content in a continuous phase. The model can calculate the source terms generated in each phase in order to evaluate the effects of the droplets injected. Thus the model proceeds to calculate the continuous phase with the Eulerian model and for the dispersed one the Lagrangian transport model is used instead of the Eulerian one. In a multiphase flow case the particles are considered like a dispersed phase and in order to define the interactions between particles and blades the method tracks the particle paths through the flow field. This represents a streamline of a droplet and in this way it is possible to evaluate their behaviours [12].

Tracking of the particles flow field is one of the tasks of the present work so this method will also be used for the simulations, as it has been written in the next paragraph. As it was for the Eulerian-Eulerian method some advantages are here reported [12]:

- large range of variation for particle size
- more flexible than the Eulerian one when there is a wide size distribution of droplets
- all the information of residence time and behaviours of the particles

6.3.1 Analysis Conditions

In order to define the right setting of the simulations in wet conditions leveraging an almost two-dimensional approach, only one profile has been studied in different operating condition both for the main flow field (Air as ideal Gas) and for the injection of the particles. The profile taken under exam for this analysis is the one at hub of the first rotor (r1_000), because this is the most critical one for the shape of it comparing with the other profiles of the same blade (high velocity at hub the velocity for the blocking of the blades). A rotor profile has been chosen also for the possibility to evaluate the behaviours of the droplets injected with a wide range of Mach number and incidence angle. Indeed as it was stated in Chapter 4, the variation ranges of both those parameters are quite big:

- M1=0.4/0.8
- i_{max}=-20°/+15° [this is the maximum because the variation depends on the mach condition]

All the investigations will be evaluated starting from file.res (result file) of the dry condition analysis in order not to resolve again the flow field. ANSYS Solver can solve the problem of the particles tracking without iteration to find the final result. Hence it is possible to add an injection region (as it will be specified in the next paragraph) and specify the discrete distribution of the droplet diameter.

In this first analysis the evaporation process is not taken under exam because this will be focused only on the study of the particle paths. In other words evaluating how many droplets injected at Inlet region reach the Outlet of domain without colliding the blade and it is then possible to draw the graphical distribution of the particle mass.

Because the evaporation is not considered, the coupling between Fluid and Gas is defined only in one way direction, the one of the main flow field (from Inlet to Outlet and not backwards).

According with the simulations done in a three-dimensional approach of the entire compressor in wet condition, the same initial set-up will be used in this work as well. The

most important initial conditions (for the dispersed phase) have already been written in the previous paragraph, where Temperature, Pressure and Velocity were the same for both phases. In this first analysis indeed the variations of Pressure and particle density will be not considered.

This first step investigation will include a wide range of discrete particle diameters, all injected at the Inlet section of the flow domain (in the middle of it between upper and lower domain surfaces fig. 6.2) with 10 different equally spaced injection positions. The discrete diameter distribution taken under exam for this task is here reported:

$$1,\ 2,\ 3,\ 4,\ 5,\ 10,\ 20,\ 30,\ 40,\ 50,\ 60,\ 70,\ 80,\ 90,\ 100\ [\mu m] \tag{6.1}$$

Thus at the end the total number of particles in the blade domain will be 150 (10 injection points with 15 particles each).

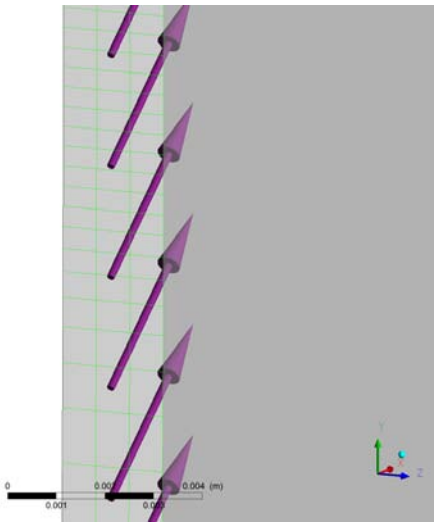

Figure 6.2: Particular of Injection regions in the middle of Inlet surface

6.4 Simulation setting

As it has been written before, the wet condition has been studied started from the result file of the dry condition and the iteration loop of the new investigation takes less time than the other (dry condition). Indeed the file.res contains all the information necessary for the post-processing and for the pre-solver phase because it has the information from the definition file (Chapter 5) and the flow field has already been resolved. Leveraging on this property offered by the software, for this work it is only necessary to add the injection particle points, setting the disperse phases and running the solver. The iterations in this case will be very fast (few seconds) and in the post-processing it is possible to track the particle paths and extract the discrete distribution of the droplets diameter.

For the main flow of the continuous phase (Air ideal Gas) the initial settings found for the dry condition are not changed for this evaluation, thus a brief description of them is here reported. For Inlet section:

- Total pressure=101325 Pa
- Total temperature=288,15 K

- Cartesian components of flow direction (Cx,Cy,Cz) in function of mach number and incidence

- Turbulence=5%

And for Outlet section the value of the Outlet mass flow rate has been fixed (calculated by the principles of continuity between Inlet and Outlet).

All the equations to describe the calculation process are the same (Chapter 5) and no others are implemented for this evaluation.

6.4.1 Pre-Solver Setting

Basic Setting

After loading the result file in ANSYS CFX Pre-Solver, in order to investigate the behaviours of water droplets in the flow domain it is necessary to add a new fluid in the Basic setting of the domain option. Here there is the possibility to choose different kinds of materials, as it is for Air ideal Gas, and in this case normal water is chosen in order to describe the properties of the droplets. In ANSYS, water is refereed at 25^oC of temperature and 1 atm of pressure (the software has a complete database of many kinds of materials with all the properties that are necessary to a thermodynamic investigation). Furthermore, as a final definition of the droplets, a choice of their morphology is required and the numeric model that is followed to evaluate the particle behaviour depends on it (Eulerian-Eulerian or Lagrangian Particle Tracking).

As stated in the previous paragraph, an equally spaced definition of the injection point is required in a particular position (in the middle of the Inlet surface). It has already been known that with the Eulerian-Eulerian method is not possible to fix a determinate position of the injection point and this approach requires droplet specifications that are not necessary for this investigation. Thus in order to simplify the calculation and define the own position of injection, the Lagrangian Particle Tracking is chosen hence the Particle Transport Fluid option is set [12].

As a fluid model, the option "Fluid dependent" is set for the heat transfer and the turbulence modeling is analyzed by the $k - \omega$ based on the Shear Stress Transport (SST) model as it was for dry condition (Chapter 5). The heat transfer model for Gas remains the Total Energy one, while for the dispersed phase this is not considered for the reasons already described. As stated in the previous paragraph the one way option is set for the fluid coupling (for more details consult ANSYS CFX User's Guide [9]).

In order to track the fluid paths of the droplets and to evaluate their impact on the profile, it is necessary to define the typology of the blade walls (suction and pressure side). Thus if the particles collide the blade these are not reflected but absorbed in the blade, it means that when a collision happens the droplet stops its way on the blade surface. With this consideration only the particles that do not collide the profile walls can reach the Outlet section and it is thus possible to make a valuation of the collision. In ANSYS CFX Pre-Solver when a particle is injected for a wet condition investigation, in the blade domain (Blade definition) it is possible to change the boundary condition for water droplet. The specification for the typology of the blade remains the same that was for dry condition (No Slip Wall as it is reported in Chapter 5) and a wall iteration is now possible to be specified: parallel and perpendicular coefficients of velocity component are fixed at 0. It means no reflection of the droplet that reaches the blade as reported in the picture (fig. 6.3):

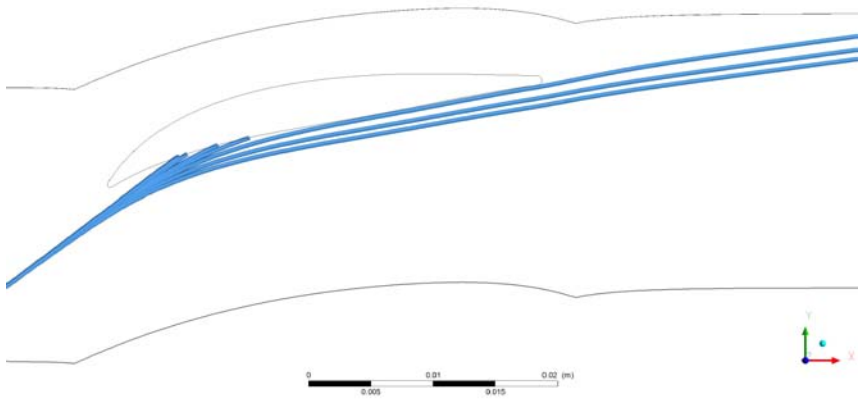

Figure 6.3: Particular of the collision on the blade wall for the first Injection flow path

Particle Injection Region

ANSYS offers the possibility to define the injection region where water is introduced in form of droplet. Every region corresponds to one point where the particles are introduced and in this evaluation the injection positions are fixed on the Inlet surface. The particles should have the same direction of the main flow (Gas) because the investigation should be done near the real working condition (air and droplet come from a duck before the IGV blades). Thus, 10 equally spaced points are fixed on the Inlet surface where water sprayed inside the domain. In ANSYS CFX this could be done by choosing a cone modality injection but without an opening angle of it. Hence the cone positioned in one specific point of injection collapses in a line. This is the only and the easiest way to simulate a two-phase flow domain for the analysis condition fixed.

On using the cone modality it is necessary to specify some further options, which are reported below:

- Specify position of injection point using x,y, and z coordinates (treated more in detail below)
- Specify the injection direction leveraging on the vectorial component of the velocity given for the air mass flow as well (Cx,Cy,Cz)
- Specify the velocity in Inlet, and in this case the two-phase flow is considered without slip condition, it means no velocity difference between water and air, so the absolute velocity component is considered (the same calculated for the main flow Cabs)
- Number of positions that is the total representative number of particles (equal or bigger than the number of diameter specified before [12], thus there will be 1 particle per specified diameter)
- Particle diameter distribution (treated more in detail below)
- Particle Mass Flow rate that is fixed at 2% of the air mass flow for these simulations. This value is considered for all injection points, hence for one of them the particle mass flow is fixed as a tenth of that value (because there are 10 injection positions).

As stated in the list above, an important specification for these investigations is the definition of the injection point positions. It has already been known that they should be fixed in the middle of the Inlet surface of domain (between the upper and lower surfaces

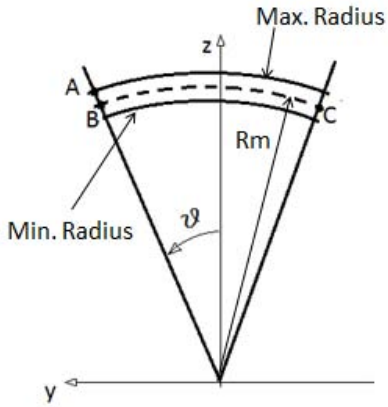

Figure 6.4: Geometrical definition for injection position

which define the height of the small blade) and equally spaced in tangential direction. In order to better understand the procedure designed to fix them, it is necessary to look at the picture (fig. 6.4) where a scheme of the process is reported.

From a post-processing investigation of dry condition file result, it is possible to determinate (automatically or manually): y coordinate of the point A (Y_a), distance of the upper surface from the axis in z coordinate definition (Max Radius), calculate the distance from the axis of lower surface by considering the thickness of the domain (t=2,3mm) (Min Radius), hence it is also possible to calculate the value of the Middle Radius, where the injection points lie:

$$R_m = \frac{MaxRadius + (MaxRadius - 2,3)}{2} \tag{6.2}$$

In this way it is also possible to calculate the opening angle of the point A, which is the same of the point B (defined on the middle radius):

$$\theta = \arcsin \frac{Y_a}{R_m} \tag{6.3}$$

because the radial distance of the point A from the rotational axis is always the same for the upper surface for the cylindrical development. Thus now it is possible to define the Cartesian coordinates of point B:

$$y = R_m \sin(\theta) \tag{6.4}$$

$$z = R_m \cos(\theta) \tag{6.5}$$

and the x component is also calculated from the post-processing because it is the distance of Inlet surface from the origin (always the same for every injection point).

Because the whole opening angle, between point B and C, is 1° (360 blades in 360°), the 10 points will be spaced to 0.1^o (1/10). Thus it is possible to determinate the coordinates of each injection position by decreasing the value of the θ angle of 0.1^o every time:

$$x = Inlet\ Surface \tag{6.6}$$

$$y = R_m \sin(\theta - 0.1) \tag{6.7}$$

$$z = R_m \cos(\theta - 0.1) \tag{6.8}$$

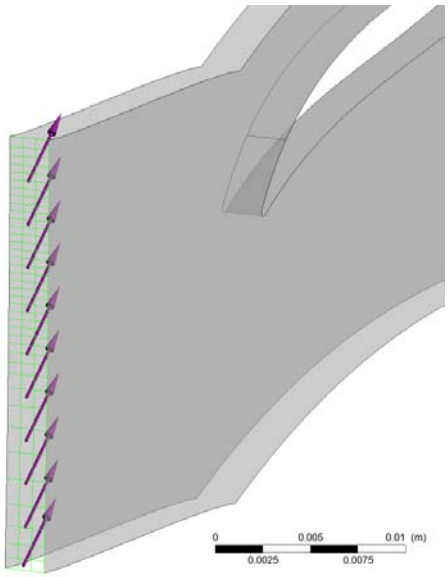

Figure 6.5: Particular of the 10 injection points

Thus 10 Injection regions should be created where only y and z coordinates change for each of them and at the end it is possible to define the Inlet region as it is reported in the picture (fig. 6.5):

Another important specification is the Particle Diameter Distribution, as mentioned in the list above, where the particle sizes are defined (form 1 to 100 μm) with the number fraction list that is the probable distribution of the particles in function of the representative generated number (the sum of them must be equal at unity and in this case 1/15 for each diameter). The last option to set in order to totally describe the diameter distribution is the Mass Fraction List where the values of the physical particle mass are reported and normalized to their total value. In order words the physical mass of a particle is calculated as follows:

$$m_{di} = \frac{4}{3} * \pi * (\frac{d_i}{2})^3 * \rho \tag{6.9}$$

where d is the diameter of the droplet (considered spherical), ρ is the density of water [from ANSYS $\rho = 997.0 kg/m^3$] and i is the index for the number of diameter ($i = 1 \rightarrow 15$). This physical mass is calculated for every diameter specified before (15 values) and multiplied by the number of particles injected (with the same size). In this case there are 10 injection points, thus 10 particles with the same diameter definition are injected. After calculating of the m_d the total value can be found with a sum of those values:

$$m = m_{d1} + m_{d2} + ... + m_{d15} \tag{6.10}$$

thus the values required in the mass fraction list option are defined as:

$$m_{fi} = \frac{m_{di}}{m} \tag{6.11}$$

this is the mass fraction normalized distribution at Inlet region and the normalized values are found as follows:

$$m_{f1tot} = m_{f1} \tag{6.12}$$

$$m_{fitot} = m_{fi} + m_{fi-1tot} \tag{6.13}$$

$$m_{f15tot} = 1 \tag{6.14}$$

and this is the distribution that will be used in order to evaluate the impact on profile characteristics by a comparison with the values calculated at Outlet.

With the specifications written above the software can calculate the number of particles to inject inside the domain for each value of diameter.

6.4.2 Solver Setting

The Solver setting used for dry condition is the same as the one of the evaluations in wet conditions. Thus, the way to calculate the advection scheme terms of the discrete finite volume equations is fixed of second order, high resolution level for the calculation of the turbulence, Local Timescale Factor (LTF=15) for the convergence criteria and the control specification number for the RMS (Root Mean Square) values always set at $1 * 10^{-05}$ [Chapter 5].

The number of Iterations min and max should be changed because the flow field is not resolved again, hence the calculation is focused on the tracking of the particles path trough the domain and it takes few seconds for 1 or 2 iterations. Thus the minimum number of them is set at 1 and the maximum at 10. For the same reason the interrupting condition is not considered anymore.

In order not to solve the flow field again with ANSYS it is possible to set some Expert Parameters where, i.e, the options in the Model Over-ride specification are disabled. In this case the attention is focused on the behaviours of the droplet in function of the diameter (and also of the Mach and incidence specification) thus all the options are disabled.

As it was for the other condition, the new specification file is saved as definition file for wet analysis and the simulations process can start. Since the flow field is not resolved the iterations will start from the dry condition file result, where the history of the old convergence is reported. Also the same mesh is taken under exam for this investigation because the geometric definition is always the same in both cases. The main difference between these two conditions is the modality of the calculations. In order to investigate the dry condition, the simulation has been launched in parallel mode, splitting on the four cores of the computer. While only for the Tracking of the particle paths the parallel mode can not be set anymore, because ANSYS cannot split the evaluation in more cores, hence the simulations are launched in serial mode.

6.4.3 Post-Processing

In this typology of investigations it is not necessary to check the good convergence of the simulations, because only the good ones of dry condition are investigated (read the post-processing phase of Chapter 5 in order to understand the meaning of good simulation). Furthermore the calculation convergence of the wet condition is certainly achieved because the flow field is not resolved again.

If the Pre-solver phase is conducted in a right way, in ANSYS CFD-Post the results of Particles Tracking (res PT) for water droplet are automatically shown by the software. Thanks to the Lagrangian calculation modality the fluid paths have been calculated in the Solver and with the option *res PT* it is possible to see the behaviours of the particles in the flow field. ANSYS Post processing offers various opportunities to evaluate the water droplet behaviours but a manual way has been chosen in order to compare the distribution of the water mass fraction Inlet against Outlet (the achievement of this work). This is because the software can calculate the total number of the water particles inside the whole domain and not only at Outlet section, as it is required in this investigation.

With ANSYS-CFD Post it is also possible to filter the Particle Tracking by setting the researched diameter and fixing where to make the investigation (Outlet region). Thus in this way diameter by diameter it is possible to evaluate the number of the droplet the reach the Outlet region. Because of the collision on the blade the number at Outlet should be less than at Inlet, in other words if 150 particles were injected from the Inlet (15 different droplets in 10 injection points) at Outlet a minor value is expected.

With the number of the droplet at Outlet for all the simulations extracted manually it is possible to make the same valuation of the mass fraction distribution that has been made for the Inlet definition (Pre-Solver setting), obviously considering the different number of the particles present:

$$m_{di} = \frac{4}{3} * \pi * (\frac{d_i}{2})^3 * \rho * (n) \tag{6.15}$$

where n is the number of the droplet investigated for each diameter. Thus the same calculation way is followed in order to find the discrete and normalized distribution of the mass, so the same equations are now considered. At the end the final graphic (fig. 6.2.1) where the Inlet and Outlet droplet behaviours will be drawn in function of the different condition of the Incidence angle.

6.5 Automatic Scripting of the Simulations

As stated in Chapter 5 ANSYS CFX-Solver requires a definition file (.DEF) in order to start the simulations. Hence, as it was for the dry condition, another general Matlab script has been designed [Appendix C] where it is possible to control the overall specifications like type of profile (in this investigation it is always the same: r1_000 first rotor at hub), Mach number and incidence angle given as boundary conditions. In order to write the different session files for ANSYS, a general Matlab script calls for every iteration the own made function called CFX_Pre_wet where the session file is written by changing every time the initial specifications. The Matlab function requires other initial definitions as well in order to start the iteration loop. These conditions are:

- radius (R_m fig. 6.4): mean radius value comes from dry post-processing conditions. This is the average of the distance from the rotational axis of the upper surface of the flow domain and the lower one
- θ (fig. 6.4): value of the opening angle of the points A and B. This is necessary in order to fix the first injection point and then with a subdivision of 0.1^o it is possible to define all the other injection positions.

The session file consists of loading the dry condition file result and add the specifications for water droplet:

- Setting new domain conditions by adding the second fluid (Particle Transport fluid)
- Definition of the liquid phase flow and the interaction with Air Ideal Gas
- Fixing the Particle Injection Region (for each region Matlab calculating automatically the new coordinate values)
- Blade wall interaction specification and new Solver setting definition
- Definition of Expert Parameter options
- Creation of the Definition file by saving the new setting condition

After this for each condition a batch file has been created in order to launch the whole simulation loop.

Then a second Matlab script has been designed to write a Post-processing session file in order to check and count the number of the Droplet which can reach the Outlet surface (without collide the blade) for each injection point. Inside the session file there is the possibility to saving a .CSV file for each injection position where the paths of the droplet inside the domain are reported. By the counting of only those ones that can reach the Outlet surface for all the injection positions, it is possible to investigate the total number of droplet at Outlet for each diameter group.

At the end a text file has been extracted in order to investigate the difference of Inlet and Outlet mass fraction value for each incidence condition with different mach number specification.

Chapter 7

Results of Simulations

7.1 Single Phase Flow Results

According to the literature two types of graphics have been extracted from the final file results and one shows the total pressure losses, while the other reports the deflection rates. These two typologies lead to understand the performances of the compressor blade cascade, thus it is possible to define the best working conditions of the machine and the maximum regulation range before the stall (positive and negative one [Chapter 2]). The final graphics will be reported together in one page for each profile, in order to directly compare them in different working conditions. On the left side of the page there will the loss coefficient graphs, while on the right there will be the deflection ones.

Total pressure loss coefficient

The graphs of Loss Coefficient will be reported for each span, from hub to shroud (five profiles), with the all values of the good simulations. In each graph it is possible to see the different condition of the Inlet Mach number and thus the behaviours of the airfoils. As stated in Chapter 5, the total pressure loss coefficient has been calculated with the equation here reported:

$$\omega_p = \frac{p_1^0 - p_2^0}{p_1^0 - p_1} \tag{7.1}$$

The achievement of this investigation is to determinate immediately the characteristics of the profile by a comparison of the results for each span of one blade. Furthermore, from each graphic it is possible to extract the follows conditions:

- Determinate the real design condition: because of the interaction of dissipative effects on the flow field, the condition of zero degrees Incidence is not the real design point but it could be a little different (positive or negative), in function of the initial condition and behaviour of the profile, thus the real Inlet flow angle can be calculated.

- Define the minimum loss coefficient value: the design condition discussed in the point above is the area where the loss coefficient is the lowest one. It can differ from hub to shroud for the bending of the profile and for the working function of it (if rotor, stator or IGVs).

- Operating range: With Howell's or Mellor's [Chapter 3] correlations it is possible to investigate the working range of the compressor, thus to define the on and off design conditions.

Deflection

Further investigation of the results will be carried out with the deflection graphics. As stated in the Chapter 2 and 5, this is the difference between Inlet and Outlet flow angle:

$$\epsilon = \alpha_1 - \alpha_2 = \beta_1 - \beta_2 \tag{7.2}$$

in the graphics ϵ will be called $\Delta\beta$ (α for stator and β for rotor but here the definitions are the same because always the absolute velocity is considered).

This typology of graphs is important to aid to better understand the reason of the loss coefficient trend. This because the higher is the deflection and the higher will be the value of the loss coefficient because the blade, in that profile, will be more bending and thus more loaded.

In each graph the behaviours of one profile will be reported (always from hub to shroud) in different conditions of Inlet Mach number and incidence angle. Thus it is possible to define the stall region as well (positive and negative).

Another task of those types of graphics is to declare the design condition, leveraging the Howell's correlation. According to that definition a nominal operation condition (design point) is fixed at the 80% of the stall deflection value.

7.1.1 IGV Results

Total pressure loss coefficient

The graphics of the loss coefficient (left side fig. 7.6), report a particular specular parabolic trend of the losses in function of the Mach number, respect the zero incidence condition. It means a specular behaviour in off-design condition (positive and negative) for each profile in different operation conditions. This could be expected before the simulations as well for the shape of the profiles, indeed as it is shown in the picture below (fig. 7.1), the chord is a straight line. In other words the middle line of the profile (chord) has the same y coordinate from Leading to Trailing edge, so suction and pressure side are specular respect the chord.

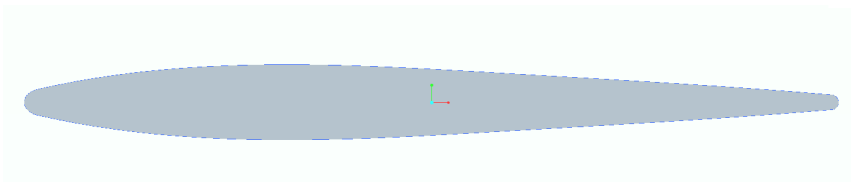

Figure 7.1: Hub profile of IGV blade [profile not in scale]

This specular trend characterized each graph from hub to shroud, because those profiles have the same shape and the IGV blade is not twisted. Thus the two surfaces are only translated in radial direction, but the y coordinate of each profile is always the same (if the blade is not adjusted in other direction).

The imaginary symmetry axis of the "parable" (it is not exactly a parable but the trend is quite parabolic), lying in a range (from hub to shroud) between -1° and +1° of the incidence angle. Thus it is possible to fix the design condition in that range because, as reported in the graph, the value of the loss coefficient is the lowest (left side fig. 7.6).

This value changes from root to tip (IGV is a stator blade so it is fixed at the outer case of the machine) of the blade and in particular it decreases, indeed as an example the

values of Loss Coefficient for Inlet Mach number M=0.4 (the lowest value, thus the lowest loss coefficient) are here reported:

- Hub (tip) (igv_000): $\omega_{min} = 0.0199$ (-3°<i<4°)
- Mid span (igv_050): $\omega_{min} = 0.0152$ (-3°<i<3°)
- Shroud (root) (igv_100): $\omega_{min} = 0.012$ (-1°<i<1°)

As it is possible to notice from the graphics and the description above, the operating range decreases from hub to shroud as well. Thus for the profile at the root of the blade the value of the loss coefficient increases very slowly in off-design condition (wide opening of the parable), while at tip of the blade the value increases quickly. These effects mentioned will now be taken under exam deeply with the aid of the post-processing images.

The main important aspect to explain is the difference of the minimum value of the loss coefficient from hub to shroud. Indeed, as reported in the list above and in the graphics, there is a difference around 6-7% of the loss values by comparing only these two profiles. This effect can be explained by studying the development of velocity through the passage channel (between two consecutive blades).

As it is easy to imagine, the pitch between two blades is less at hub than at the shroud, for the cylindrical development of the machine. Thus the solidity of the cascade is totally different from these two sections because the pitch value changes.

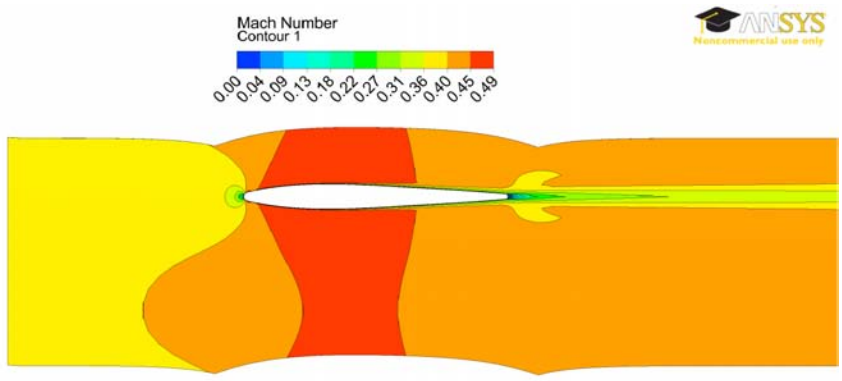

(a) Hub Profile

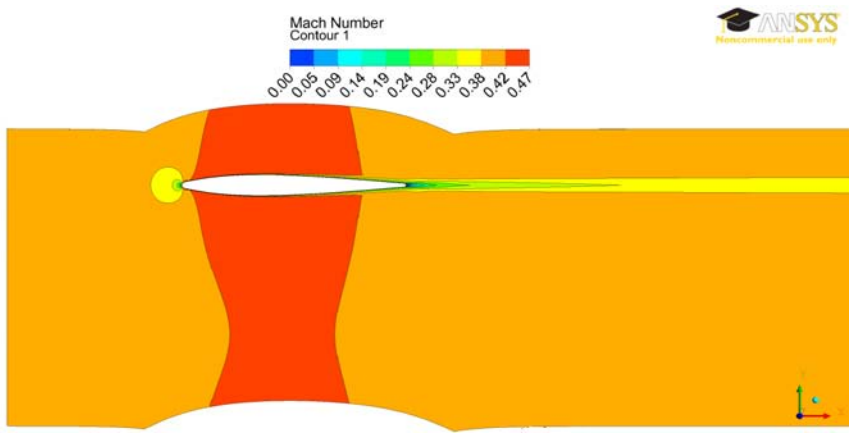

(b) Shroud Profile

Figure 7.2: Comparison of the velocity distribution between hub and shroud through the passage channel [profile not in scale]

For this reason when the fluid with a defined mass flow rate reaches the blades, the behaviour of the velocity changes near the inner casing respect to outer casing of the machine. This because of the blocking of the blades. Indeed the radius is minor at hub so the pitch between two blades is minor as well and the mass flow must enter in a surface smaller than at the shroud where the radius value is bigger. The consequence of the blades blocking is that the velocity into the channel increases more at hub respect to the shroud, and as it is already reported in the Chapter 3, the losses increase because they are related with the square of the velocity. As it is possible to see in the picture (fig. 7.2), where hub and shroud profiles are compared, the maximum velocity in the case igv_000 is bigger than the other. The difference is not so big, but the losses take into account the square of those values.

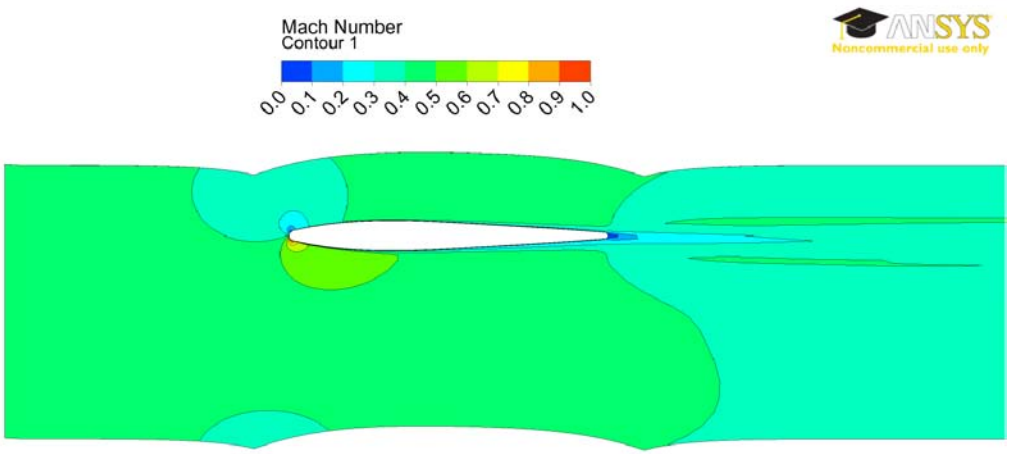

(a) Hub Profile

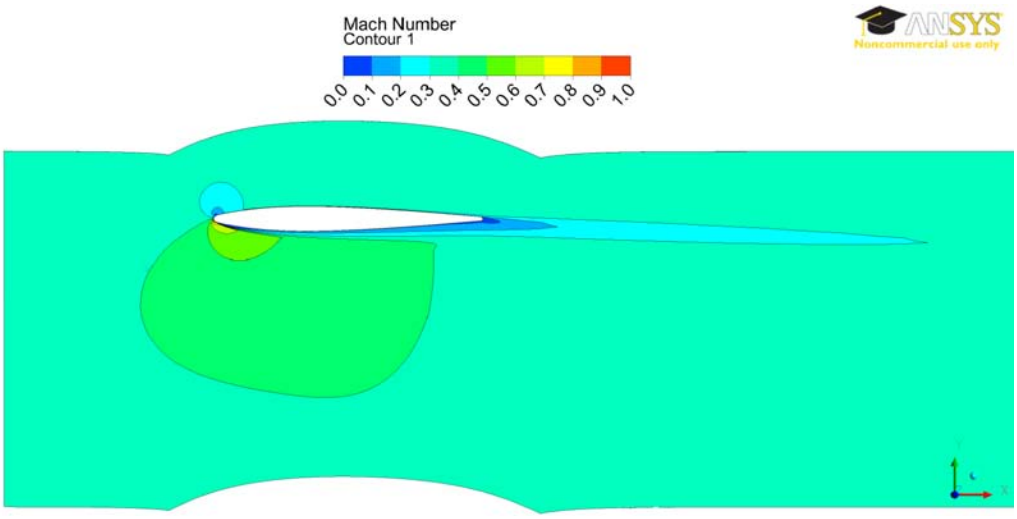

(b) Shroud Profile

Figure 7.3: Comparison of two off-design situations for hub and shroud. Inlet mach number M1=0.4 and the incidence angle for each picture is i=+15° [profile not in scale]

A secondary consequence of the velocity development through the passage channel, is that the operating range of the machine decreases from inner to outer casing of the machine (as it is possible to see in the graphics). This because of the high velocity which is present in the channel of hub profiles and which aids the fluid to slide on the surfaces, keeping away

the separation conditions especially in off design situations. It means that the separation conditions (that appear in each case especially near the Trailing edge) happen for shroud profile not so far from the design condition, thus the loss coefficient value increases faster and the parable becomes closer than the other one for hub profile. In the picture (fig. 7.3) the comparison of the two types of the profiles is reported, in off design condition, so it is possible to investigate the starting point of the separation flow on the blade.

Thus a high velocity value is desired to keep as away as possible the separation condition in off design, but it means high level of losses on the blade walls.

As last observation the trend of the curves, in the same graphic in different condition of Inlet Mach number, is the same that is possible to find in literature. Also the minimum value ($\omega_{min} = 0.02$ for NACA-65 [2]) is near that one in scientific papers so the simulations can be considered reliable and closer to values present today at the state of the art.

Deflection

The Deflection graphs, reported in figure (right side fig. 7.6), do not have the typical trend as stated at the end of Chapter 3, but they have quite straight trend from negative to positive incidence values. This can be explained again for the symmetry of the profile, indeed the behaviour of the two sides of it is not so different when the flow arrives to the blade with positive or negative angle.

High values of the deflection are observed because when the flow arrives at the end of the profile (Trailing edge) this is directed to the suction side because of the depression present in that zone. Thus, as it is reported in the picture (fig. 7.4) the flow is deflected and the amount of this depends on the velocity which is present in the channel and of course on the pressures on both sides.

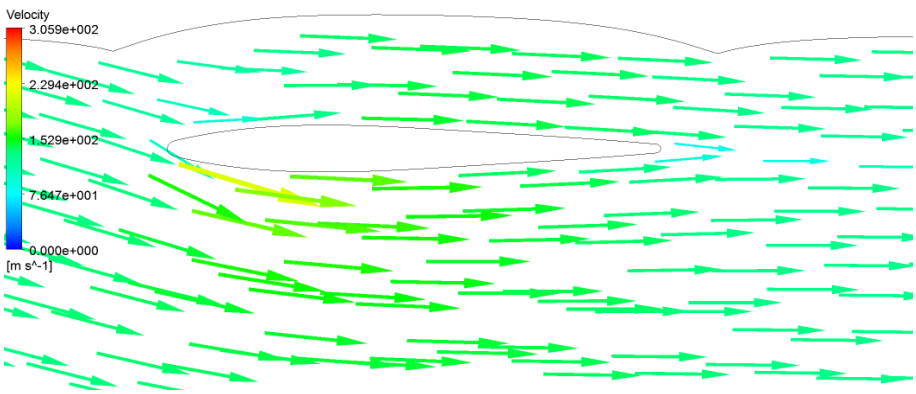

Figure 7.4: Particular of flow field direction in off-design condition on hub profile at M1=0.4 at i=+15° [profile not in scale]

Positive or negative stall condition happens at the same degree of deflection (for igv_000 M=0.4):

- i=-20° $\Delta\beta$=-18.13^o
- i=20° $\Delta\beta$=+18.11^o

As it is possible to see in the picture (fig. 7.5) in off design working the profile does not change very much the behaviour, because of the symmetric definition.

The interaction of the Mach number on the deflection is not so important as it was for the loss coefficient, indeed most of the times the different curves collapse in one. Only the

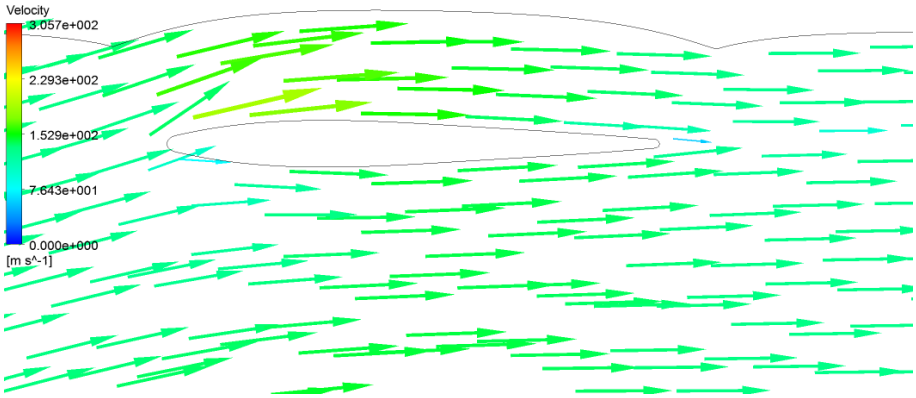

Figure 7.5: Particular of flow field direction in off-design condition on hub profile at M1=0.4 at i=-15° [profile not in scale]

stall region position depends on the Inlet mach number, thus the IGV profiles are not in function of it far from the stall regions.

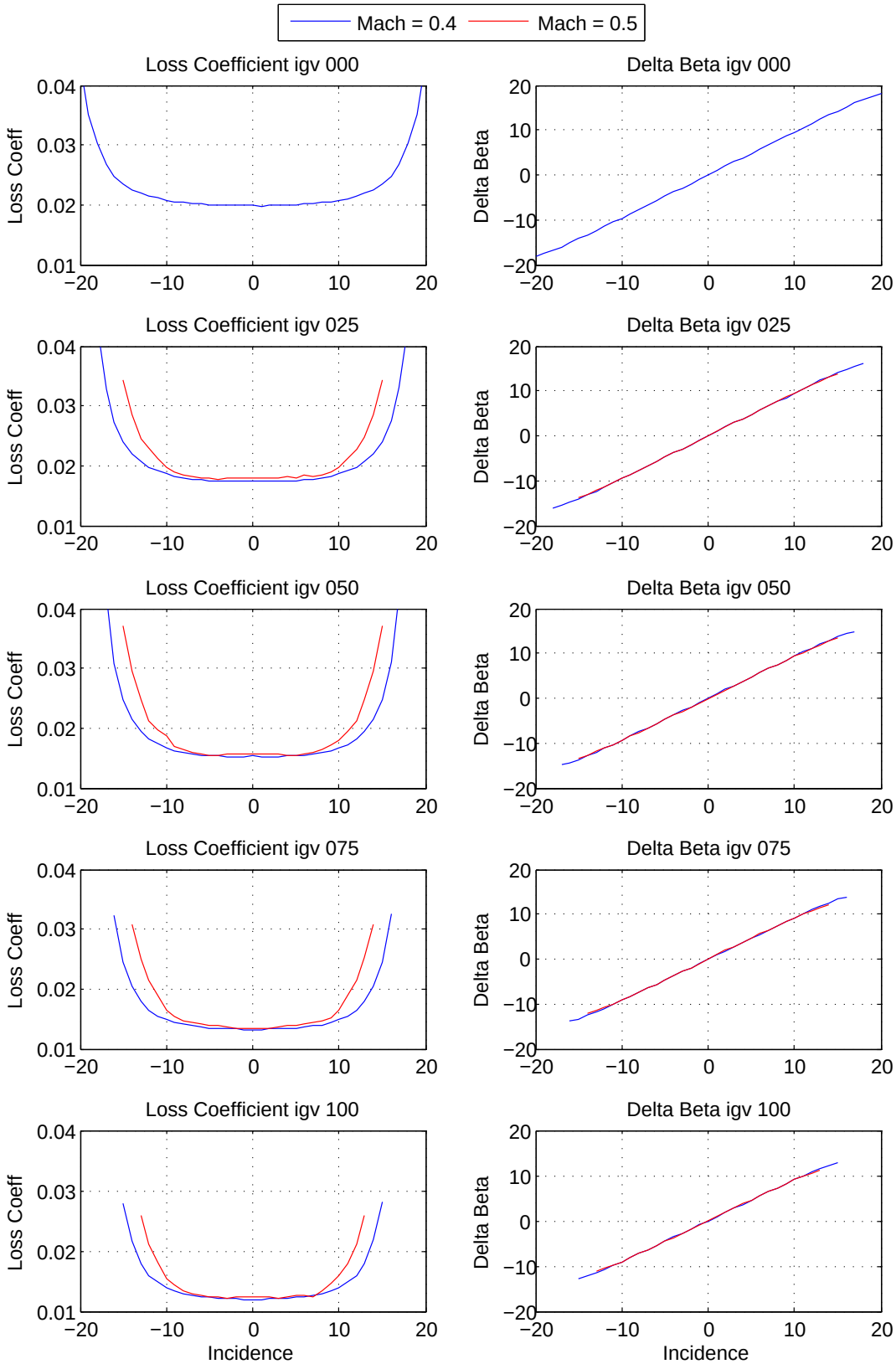

Figure 7.6: Summary of the results for Inlet Guide Vanes (IGV) Blade. From up to down, the profile are neatly reported from hub to shroud. In the right side there are the graphics for the total pressure loss coefficient, while on the left one there are the deflection trends

7.1.2 Rotor Results

As for IGV blade also for Rotor blades all the graphics of the loss coefficient and deflection will be reported for each profile from hub to shroud. As it is already known (Chapter 4) there are 4 stages, thus the results for every conditions will be examined in detail for each blade position. In these simulations a wide range of Mach number has been considered, because in real working conditions, on the rotor the relative value of the Mach number should be analyzed. As mentioned in the theoretical description (Chapter 2-3) the velocities through the rotor are higher than those through IGV or stator blades, thus the range of investigation of the Mach number is bigger.

As reported in Chapter 4, the three-dimensional development of the compressor stages has been designed by the free vortex method [22]. In this approach the product of tangential velocity and radius remains constant, and the axial velocity value remains the same before and after the blade [5]. As a consequence of this approach the following effects are present on the blade [5]:

- High value of mach number near the shroud zones because the tangential component of the absolute velocity decreases from shroud to hub, so the relative Mach number (in this case the absolute one) is very high
- High deflection of the flow near the inner zones of the blade because the profile is more bending than that one near the outer zones
- High value of twist angle from root to tip of the blade (this can explain the difference on the deflection values in those zones)

The maximum tolerable value of the Inlet Mach number depends on the position of the profile, and as it is shown in the result investigation (fig. 7.12) the variation ranges are:

- hub profiles: $0.4 < M1 < 0.6$
- span 025 (middle span): $0.4 < M1 < 0.7$
- from middle span to shroud: $0.4 < M1 < 0.8$

In the following picture (fig. 7.7) the two typologies of profiles are reported (only hub and shroud). There it is possible to see the big bending of the profile at root of the blade and the big value of the twist angle for the tip profile. The picture is referred to the first rotor, but the shape of the other profiles is almost the same (in function of the span position). It should be considered that the radius for the hub of the compressor never changes, only that one at the outer wall decreases from the first rotor to the fourth. This last specification is important to understand why the results of two different blades change in the same span position.

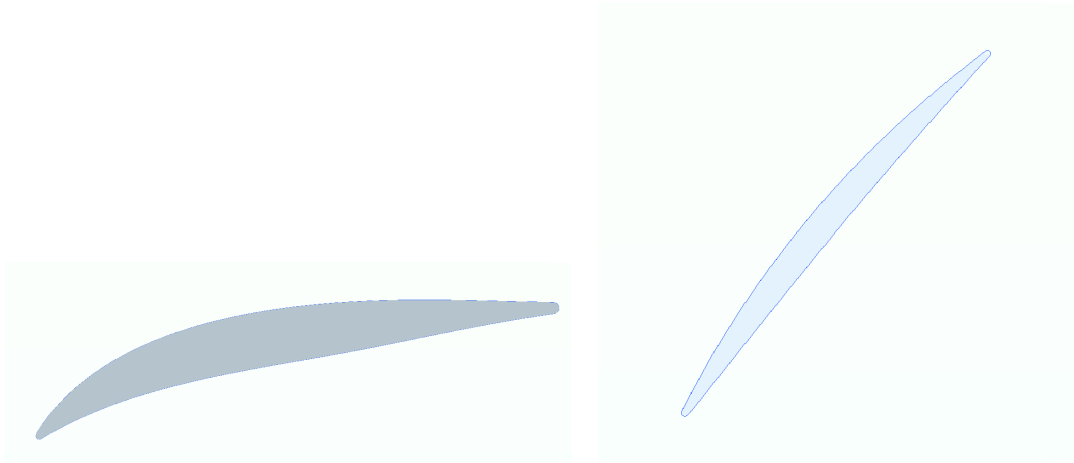

(a) Hub Profile (b) Shroud Profile

Figure 7.7: Hub and Shroud profile of the first rotor of the axial multistage compressor [profiles not in scale]

Total pressure Loss Coefficient

Only the reliable results will be reported because the bad simulations will not be taken under exam. It means that if the loss coefficient trend is not "parabolic" or the minimum value in the design condition differs a lot with the other, so if one curve has a higher origin point, the simulation will be ruled out in order not to affect the future investigations with errors.

As it is possible to see in the result graphics (left side fig. 7.12), the loss trend is in accordance with the literature with a "parabolic" behaviour, where the minimum of the parable (design point) is near zero incidence condition. Furthermore, the higher is the value of the Mach and the closer is the operating range of the compressor. Moreover for this typology of profiles, the minimum value of loss coefficient differs from root to tip, as the same that has been investigated for the IGV. The reasons are almost the same reported in the previous analysis, so velocity has an important role on the loss evaluation. Indeed, also here velocity is higher at the inner zones of the machine and lower at the outer ones. Thus the higher is velocity and the bigger will be the losses, but in off design condition it limits the separation flow effect from the blade walls. That means a bigger operating range for sections near the hub and even smaller for the others.

However, the loss coefficient is higher than in the IGV profiles and the operating range is smaller as well, in the same condition of Mach number. Thus here the problem, in addition to the velocity behaviour, is the shape of the profile. Indeed, as it is reported in the picture above (fig. 7.7) the profile, especially at the root of the blade, has a big bending and both hub and shroud have not a symmetric definition of suction with respect to the pressure side. These characteristics lead to an increased value of the loss coefficient and of a smaller operating range for these profiles.

More in detail, at the root of the blade the velocity is higher than near the other zone and if the profile has a big bending, for the flow it is much harder to follow the blade shape thus the separation condition could happen even in a design condition, at least on the suction side where the pressure is lower (fig. 7.8)

As it is possible to see in the picture (fig. 7.8), in off design if the incidence increases ($i>0^o$) the problem of the stall is even bigger because on the suction side the interaction

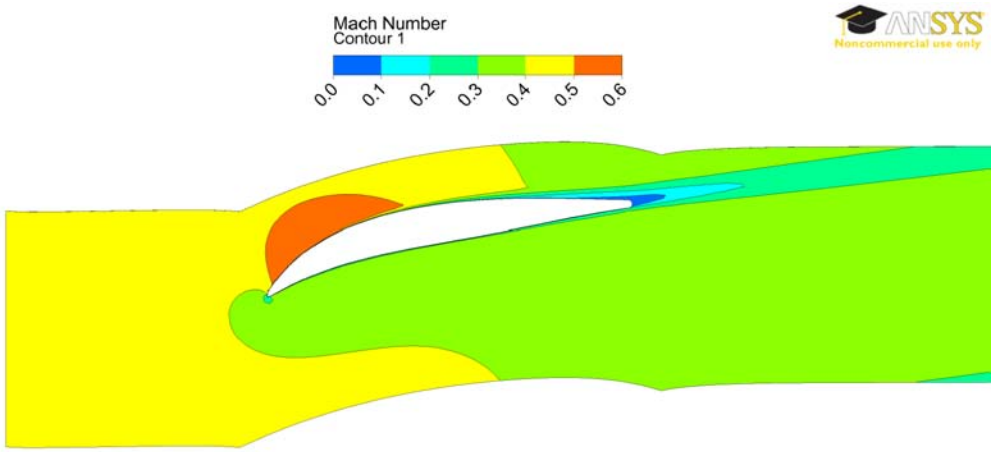

(a) Design condition (i=1°)

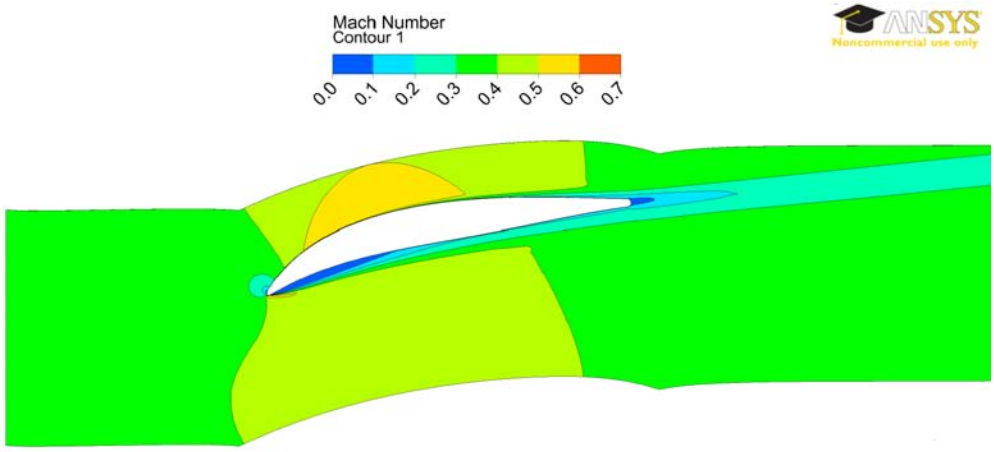

(b) Off design condition (i=−15°)

Figure 7.8: Comparison of the flow separation for an on and off design condition for hub profile at M1=0.4 and different incidence angles [profiles not in scale]

of the separation increases. Otherwise, if the incidence decreases (i<0°) the flow is even more directed to the suction side, and the result is that losses are limited. These are the main reasons why the trend of the loss coefficient is not specular to the design condition fixed for the first rotor at (hub):

- M1=0.4 $\omega_{min} = 0.0281$ (0°<i<2°)

The parable starts to become even more closer, especially for the negative values of incidence, where the profile bending decreases, thus when the attention is focused on the outer zones. Indeed, for the shape of the profile at shroud (almost with a straight chord), the value of the loss coefficient decreases because velocity is smaller and generally the air particles can follow the direction imprinted from the profile (there is not a big obstruction). However, the range is smaller because the off design behaviour becomes unstable in condition not so far from the design point.

The profile continues to have a good working in positive incidence value, so the separation condition is limited and it could happen only on the suction side. Otherwise with negative incidence conditions the separation effects can happen on both sides (fig. 7.9).

These could be the reasons why the loss coefficient decreases at the tip of the blade

(a) Off design condition (i=-4°)

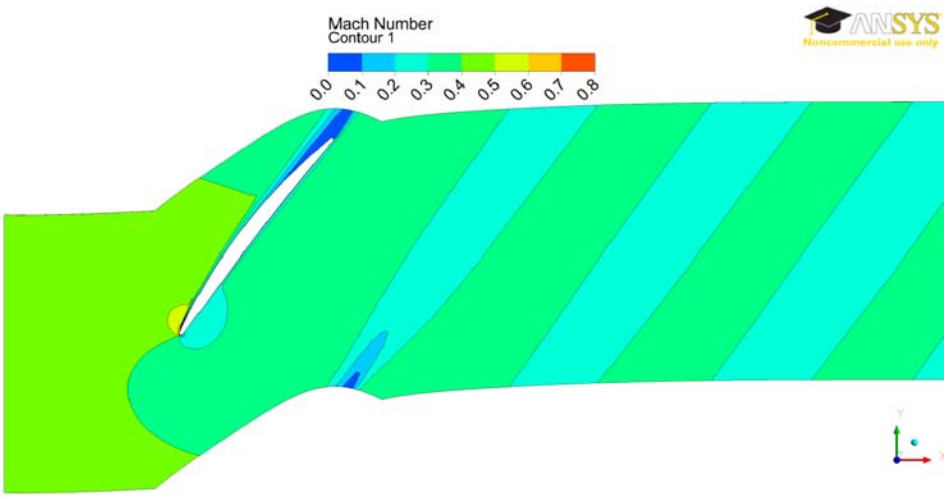

(b) Off design condition (i=9°)

Figure 7.9: Comparison of the flow separation in two opposite off design conditions on shroud profile at M1=0.4 and different incidence angles [profiles not in scale]

and the operating range decreases as it is here reported:

- M1=0.4 $\omega_{min} = 0.0217$ (i=3°)

The previous discussion has been focused on the first rotor of the multi-stage axial compressor, but it can be extended to the other stages as well. Indeed looking at the graphics of the second (fig. 7.13), third (fig. 7.14) and fourth rotor (fig. 7.15), there are not substantial differences. Obviously not for the profiles to the root of the blade because they have always the same geometric definition and the same distance from the rotational axis. Thus the interaction fluid-blade in those zones is almost equal for all stages.

The main differences are noticed for the zone far from hub because the height of the blade decreases even more, but the geometric definition and the twist angle decreases (the last blade is less loaded so less twisted). Indeed the loss coefficient is even smaller from the first to the last rotor and this thanks to the high value of velocity (it increases because the inlet area of the channel decreases for the blocking of the blade), but the shape of the profile is not bending too much so the fluid can follow its direction (in design point).

However, as it is possible to see from those graphics, the operating range decreases from the first to the last rotor because of the shape of the profile that in off design condition can create easily the separation flow worse than that one present at the first rotor because of the high velocity present in those positions. As examples the values of the loss coefficient for the shroud profiles are reported (M1=0.4):

- r2 ω_{min} = 0.0190 (0°<i<1°)
- r3 ω_{min} = 0.0191 (0°<i<1°)
- r4 ω_{min} = 0.0192 (i=1°)

Deflection

The trend of the deflections in the graphics (right side fig. 7.12), respects the discussion already done for the loss coefficient. The trend is not as symmetric as it was for the IGV because the shape of the profile is not symmetric. More in detail the deflection is very high for the hub profile and this is because of the bending of it. It has already been explained that for the particular approach adopted to design the blade (free-vortex method), big deflections are a normally consequence. The deflection rate decreases from hub to shroud for the shape of the profile and for the distribution of the pressure on both pressure and suction sides. As examples the values of deflection are here reported only for hub and shroud (M1=0.4):

- r1_000: $\Delta\beta$=37.65^o (i=11°)
- r1_100: $\Delta\beta$=10.06^o (i=8°)

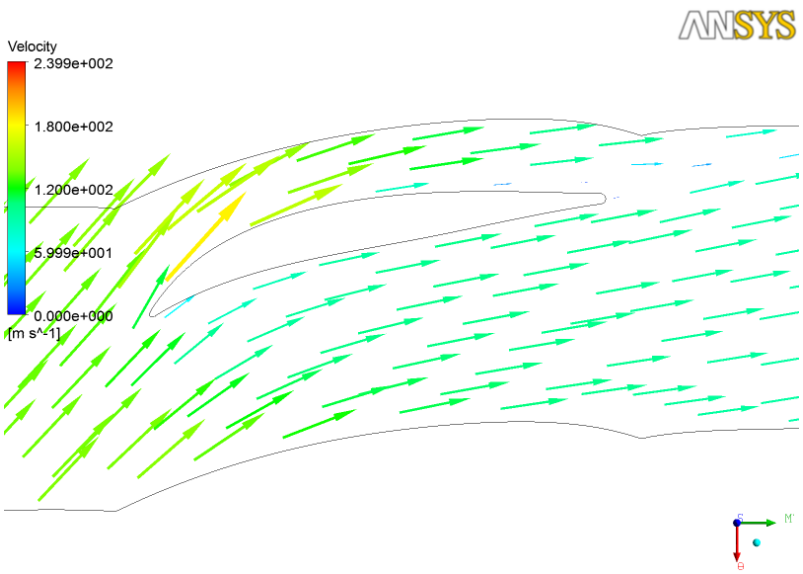

Figure 7.10: Flow deflection in Hub profile in off design condition M1=0.4 at i=9° [profile not in scale]

Thus the high value of the loss coefficient for hub profile is explained for the big value of the deflection as well. It means that the profile has a big bending, and it is much harder for the flow following the shape. In the pictures (fig. 7.10 and 7.11) two different profile

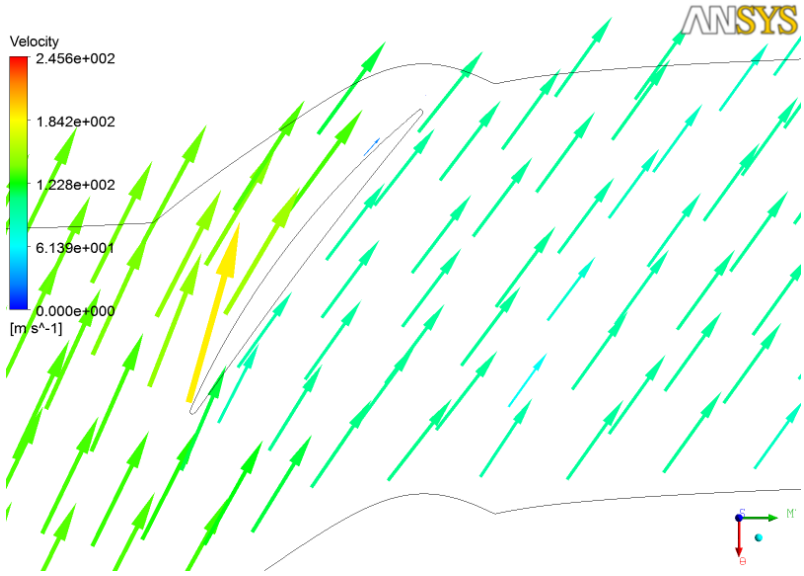

Figure 7.11: Flow deflection in Shroud profile in off design condition M1=0.4 at i=9° [profile not in scale]

are reported (root and tip of the blade) in order to explain the problem with the aid of the post-processing evaluations.

As for the loss coefficient analysis, the treatment of the deflection is valid for the other stages as well, and looking at the deflection results for them there are not big differences also comparing with the reports for the first rotor. Again obviously for hub there are no differences for the reasons stated above, and only for the shroud profile something changes. Indeed the maximum deflection values slowly increase from the beginning to the end of the compressor, but it can be explained by analyzing the stagger angle that is not always the same, as it decreases because the fourth blade has a smaller twist angle than the first (less loading). As an example the maximum values are here reported for all the rotors at shroud (M1=0.4):

- r2_100: $\Delta\beta$=11.56^o (i=7°)
- r3_100: $\Delta\beta$=12.50^o (i=6°)
- r4_100: $\Delta\beta$=12.97^o (i=7°)

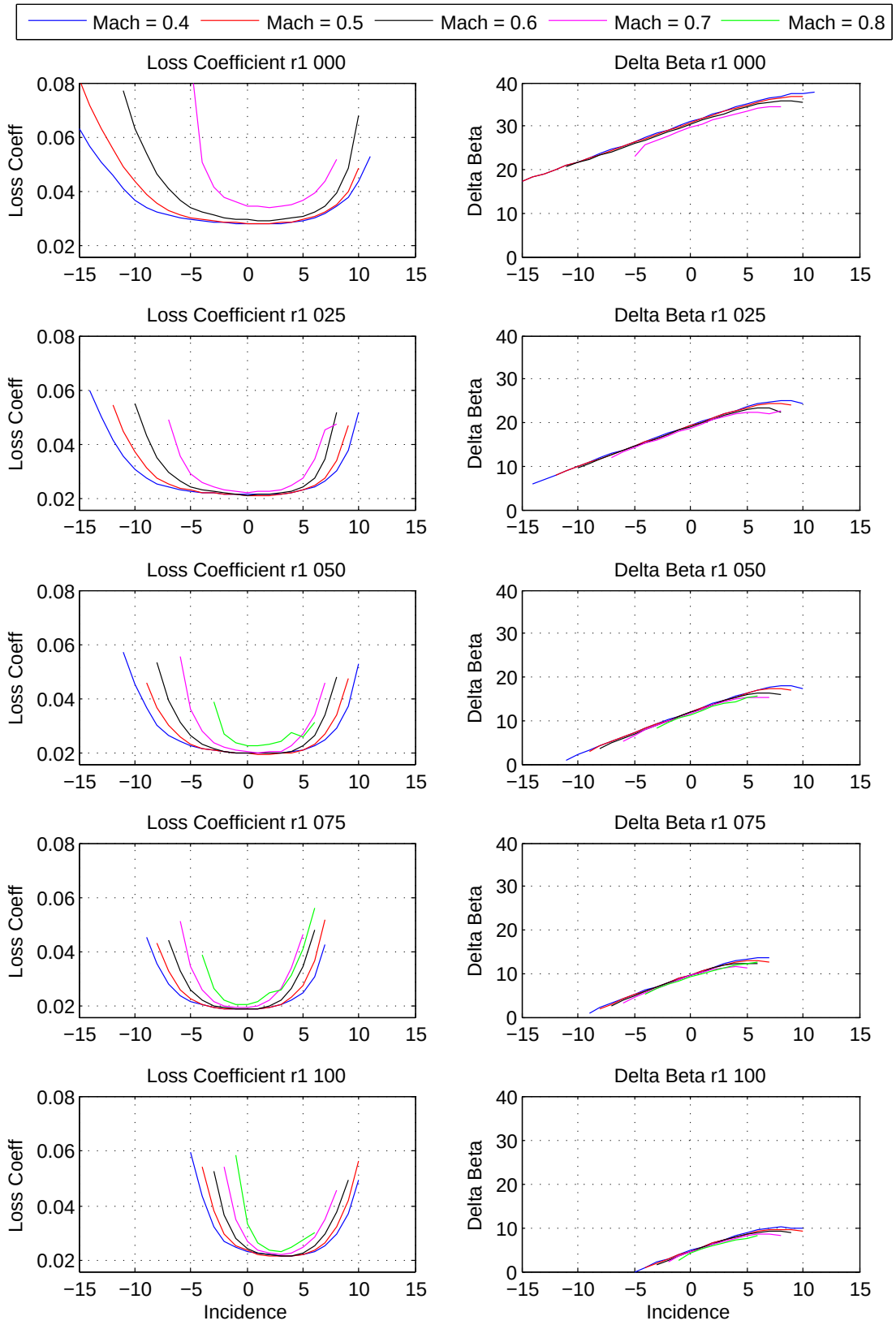

Figure 7.12: Summary of the results for the first rotor blade (r1). From up to down, the profiles are neatly reported from hub to shroud. On the right side there are the graphics for the total pressure loss coefficient, while on the left there are the deflection trends.

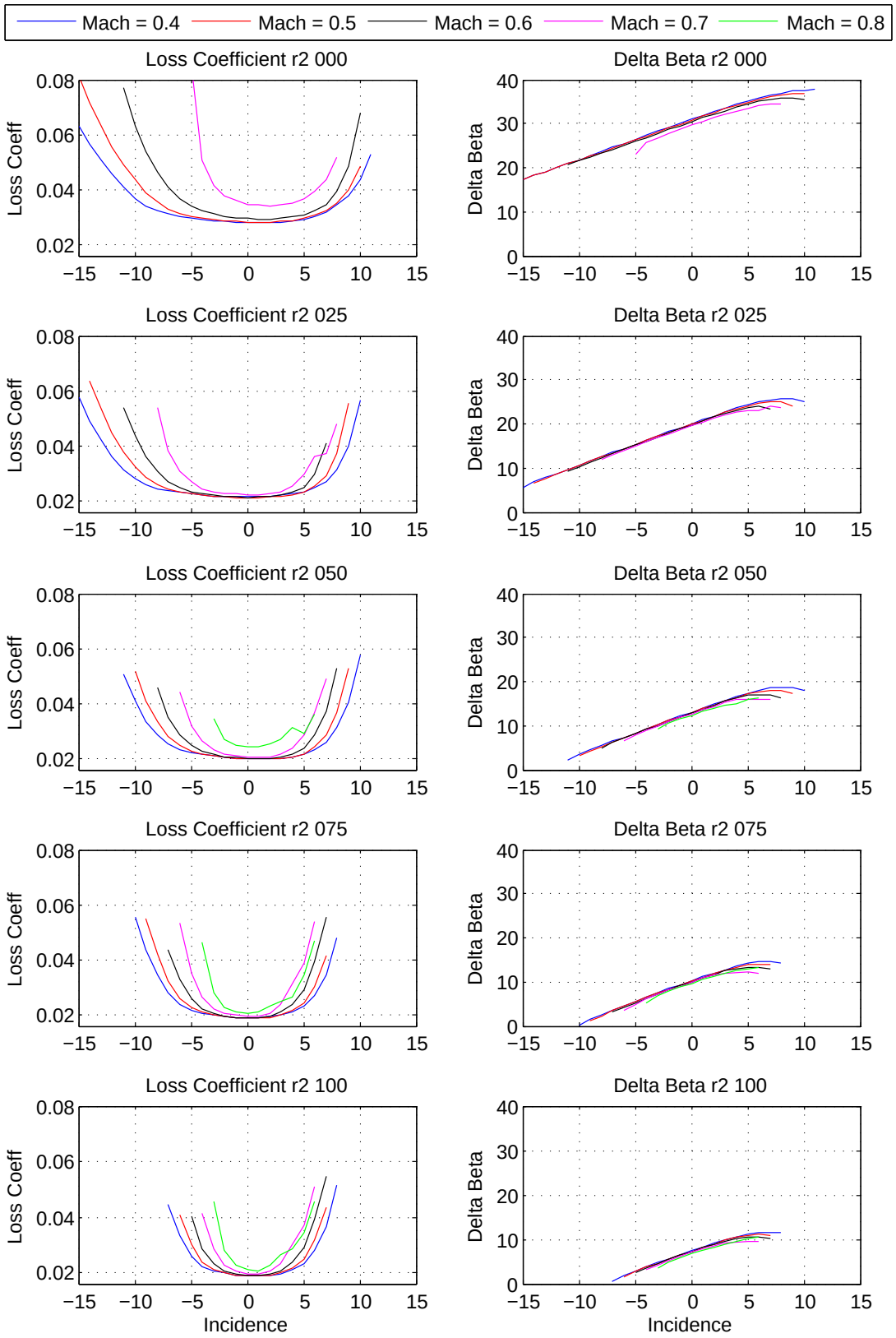

Figure 7.13: Summary of the results for the second rotor blade (r2). From up to down, the profiles are neatly reported from hub to shroud. On the right side there are the graphics for the total pressure loss coefficient, while on the left there are the deflection trends.

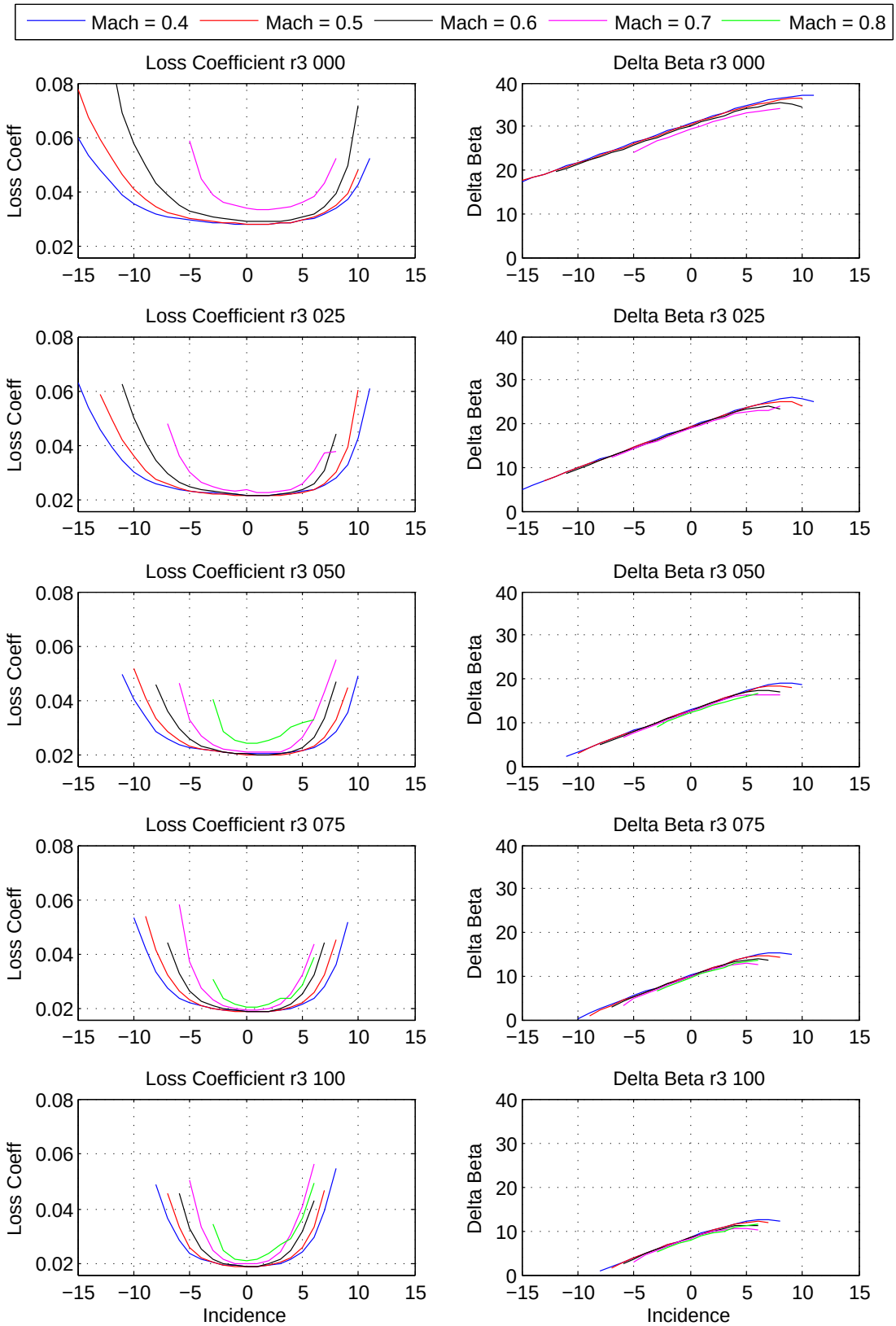

Figure 7.14: Summary of the results for the third rotor blade (r3). From up to down, the profiles are neatly reported from hub to shroud. On the right side there are the graphics for the total pressure loss coefficient, while on the left there are the deflection trends.

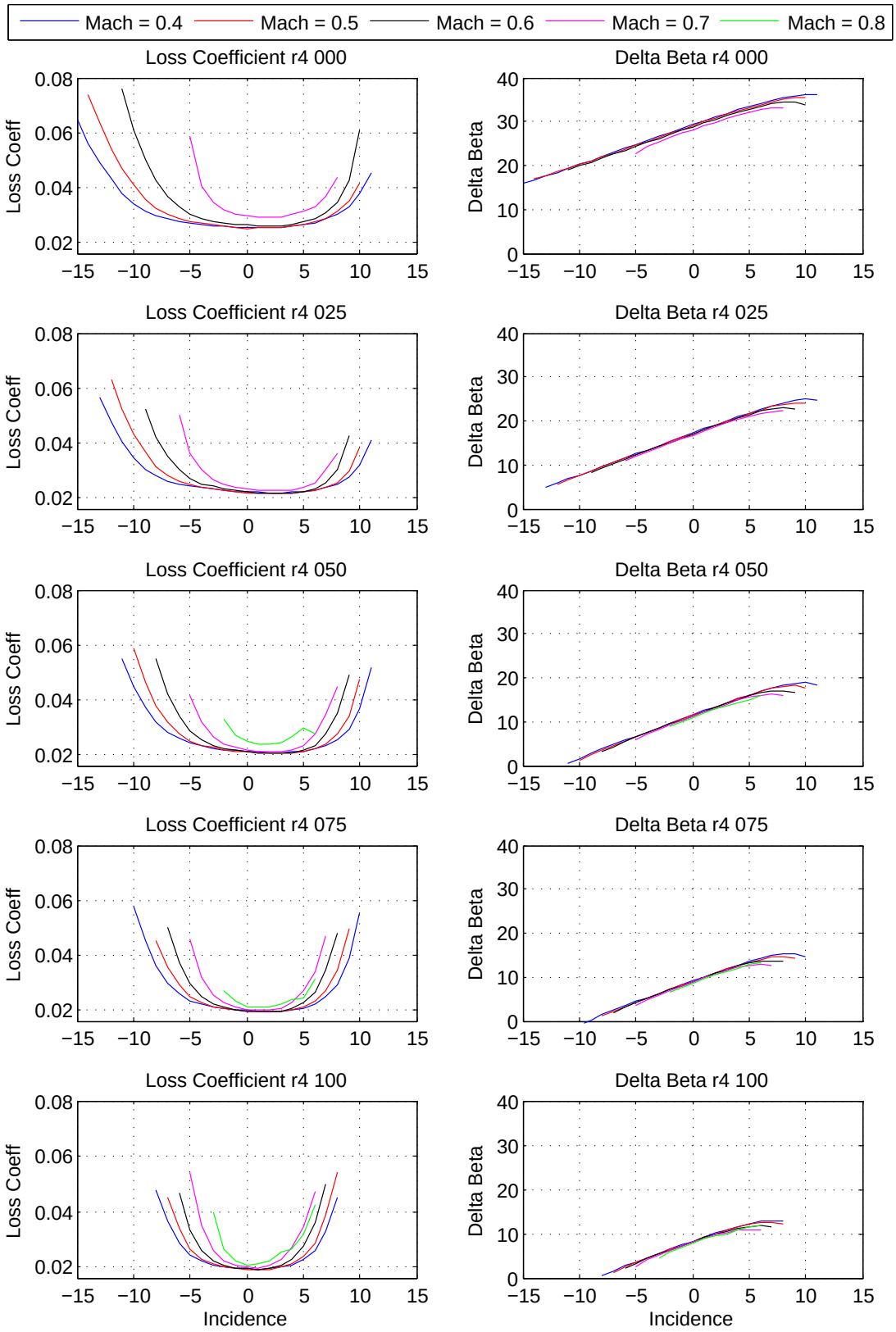

Figure 7.15: Summary of the results for the fourth rotor blade (r4). From up to down, the profiles are neatly reported from hub to shroud. On the right side there are the graphics for the total pressure loss coefficient, while on the left there are the deflection trends.

7.1.3 Stator Results

In order to investigate the stator blade profiles all the final graphs will be reported together for each profile at the end of the discussion, from the first stage to the last one (as it was for rotor and IGV). As for the previous evaluations, the future considerations will be explained taking under exam the first stator, but everything will be valid for the others as well.

According to Chapter 4, the range of Mach number is smaller than that one analyzed for the rotor profiles, because here the absolute velocities are lower. As it is possible to see in the graphics (fig. 7.19), the maximum value of the Inlet Mach number is M=0.5 because the simulations for M=0.6 do not have good definitions. It happens perhaps because the velocities increase too much through the channel leading to a chocking condition of the flow. Thus the simulations do not converge because the mass flow remains fixed at the maximum value given in function of the dimension of the throttle area and Inlet/Outlet conditions.

The last consideration before starting to evaluate the results is that now the definitions of root and tip of the blade are opposed with respect to the rotor (but the same respect the IGV). Indeed the stator blades are fixed on the outer case of the machine, so at the shroud (of the machine) there is the root of the blade, while at hub there is the tip of the blade. In the picture below (fig. 7.16) the two shapes of the profile for hub and shroud are reported.

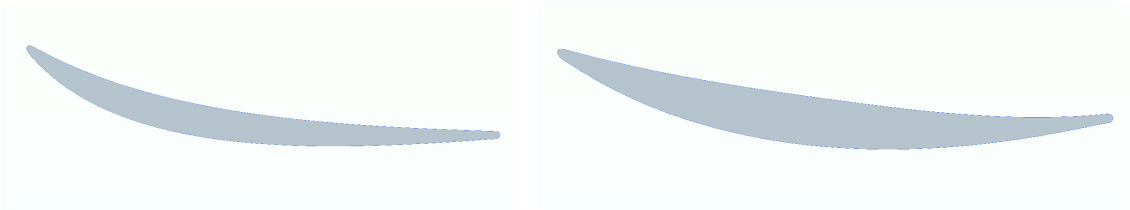

(a) Hub Profile (b) Shroud Profile

Figure 7.16: Hub and Shroud profile of the first stator of the axial multistage compressor [profiles not in scale]

Total pressure Loss Coefficient

The considerations written for the Rotor and IGV of the Loss coefficient evaluation are still valid for the stator profiles as well. Thus, according to the literature, the trend of the losses is almost like a parable (left side fig. 7.19) with the design condition near the zero Incidence definition. As it is for rotor and IGV, for the cylindrical development of the machine, the velocities near the inner zones are higher than those at the outer zones for the blocking of the blades.

The loss values are lower than those evaluated for the rotor because of the completely different shape of the profiles (as it is possible to see in the picture fig. 7.16). Indeed the stator blade is less bending respect to the rotor one, thus the lower is the bending of the Camber line and the more easily the fluid can follow the profile delaying the separation condition as near as possible to the Trailing edge. As for the other profiles, there is a gap or a difference from the minimum value of the loss coefficient from hub to shroud and the possible causes have already been explained in the previous treatment (the values of the velocities). As examples the values of hub and shroud for M1=0.4 condition are here reported:

- hub $\omega_{min} = 0.023$ (-1°<i<1°)
- shroud $\omega_{min} = 0.0157$ (-5°<i<2°)

Always looking at the results, the first important consideration regards the variation of the operating range of each profile. Contrarily to the rotor, in the stator profiles it does not change substantially from root to the tip of the blade. This effect could be explained by differentiating two cases:

- hub profile: it has a considerable curvature but the high values of the velocities maintain the flow field closer to the blade and the separation condition happens near the Trailing edge of the profile.
- shroud profile: low values of velocity and the shape of it leads to a separation condition not so far from the Trailing edge and in off design situations as well.

Another important observation is that both hub and shroud profiles have a good behaviour in off design condition especially for negative incidence, because for a positive value of it the separation of the flow happens obviously on the suction side, while with negative angle this is more limited (fig. 7.17 7.18)

As it is possible to see in the final graphs or also in the short list written above, the design point (minimum value of loss coefficient) moves the zero incidence condition for the hub profile to a negative incidence situation. The reason for this is that the profiles have a better working with negative incidence angles caused by the shape of the profile.

As for the previous investigations, a short comparison of the results for the other stages is reported, looking at the other final graphics of s2 (fig. 7.20), s3 (fig. 7.21), and s4 (fig. 7.22). For this kind of profiles there are no appreciable differences, only a small increasing of the operating range for the shroud profiles is noticed (especially for the last rotor). This is because those profiles have not a big curvature and if velocity increases this aids the off design situations to have a good performance.

In order to better understand the behaviours of the other stages the final results are here reported near the design condition only for the shroud profiles and for Mach=0.4:

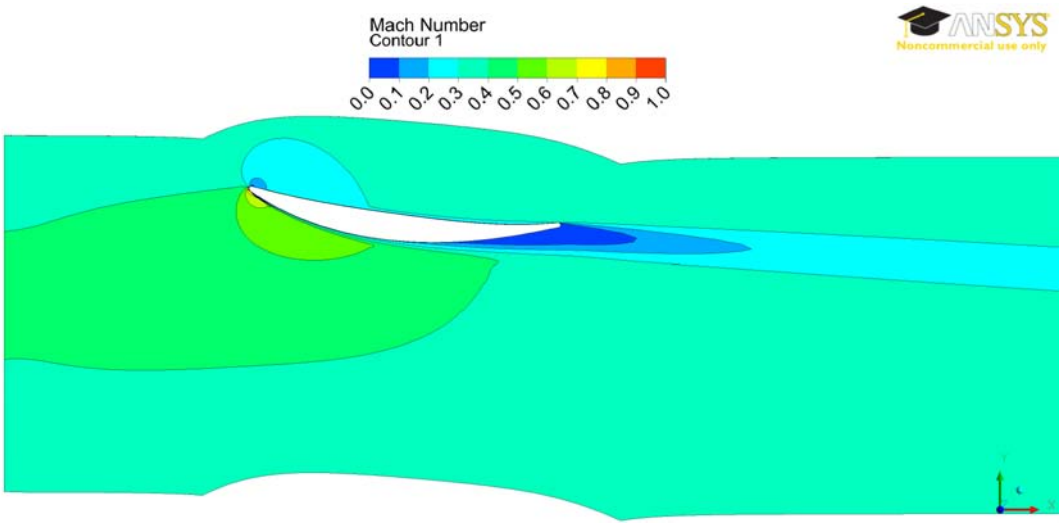

Figure 7.17: Comparison of the flow separation in two opposite off design conditions. Shroud profile at M1=0.4 and i=10° [profile not in scale]

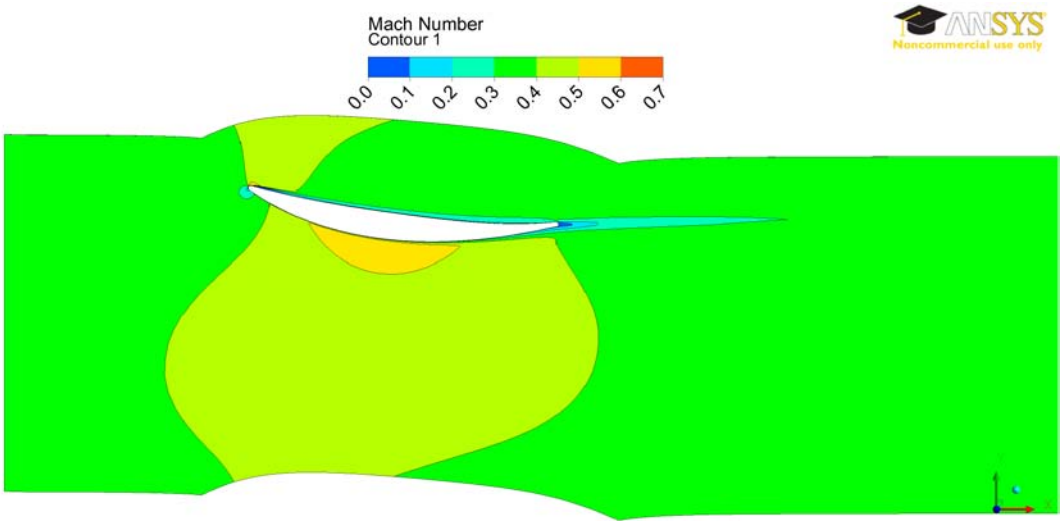

Figure 7.18: Comparison of the flow separation in two opposite off design conditions. Shroud profile at M1=0.4 and i=-10° [profile not in scale]

- s2 ω_{min} = 0.0163 (-5°<i<4°)
- s3 ω_{min} = 0.0166 (-5°<i<2°)
- s4 ω_{min} = 0.0230 (-1°<i<1°)

Deflection

According to the graphs of the loss coefficient, deflections are lower than those present for the rotor blades (so the losses are lower), as reported in the defection graphics (right side fig. 7.19). This is because the blade has not a big curvature and the maximum values are more reasonable with respect to those for rotor. However the differences are not big from hub to shroud and this is because the curvature of the blade is not so different from these two profiles. Below some values are reported in order to understand the variation of the parameters:

- s1_000: $\Delta\beta$=41.03^o (i=10°)
- s1_100: $\Delta\beta$=27.86^o (i=9°)

These conditions can better explain the reason why there is not a big difference in the minimum value of the loss coefficient from hub to shroud as well.

By comparing the results of the other stages it is possible to see that the deflection behaviour is almost the same for all of them. In the graphics an appreciable difference is that the maximum value of the deflection increases, especially for the shroud profiles, because the blade changes the twist (it decreases) from the first stage to the last. As an example of this factor, the reports for each shroud profile for all stators is here reported (M1=0.4):

- s2_100: $\Delta\beta$=29.27^o (i=9°)
- s3_100: $\Delta\beta$=29.48^o (i=9°)
- s4_100: $\Delta\beta$=28.96^o (i=9°)

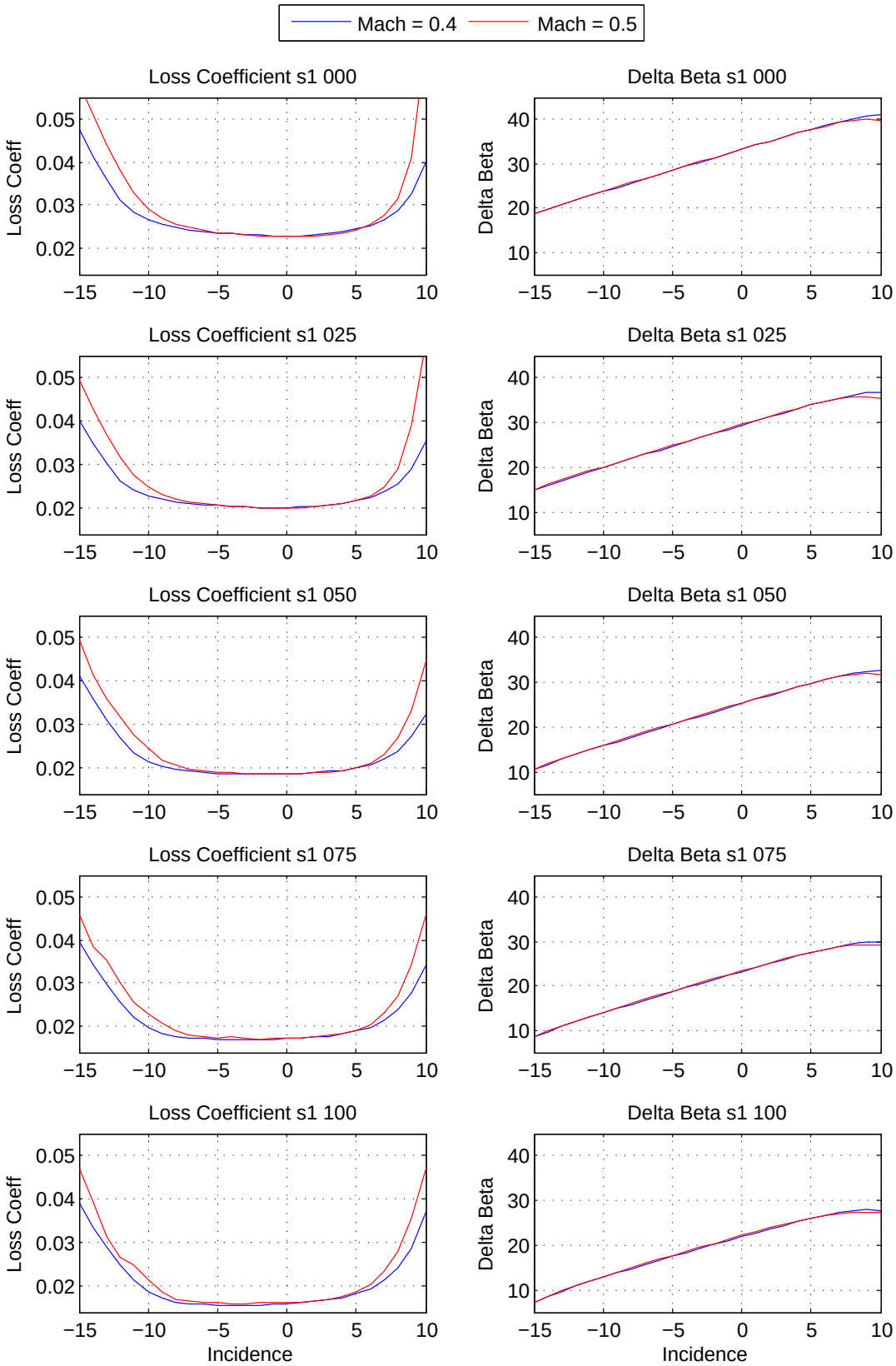

Figure 7.19: Summary of the results for the first stator blade (s1). From up to down, the profiles are neatly reported from hub to shroud. On the right side there are the graphics for the total pressure loss coefficient, while on the left there are the deflection trends.

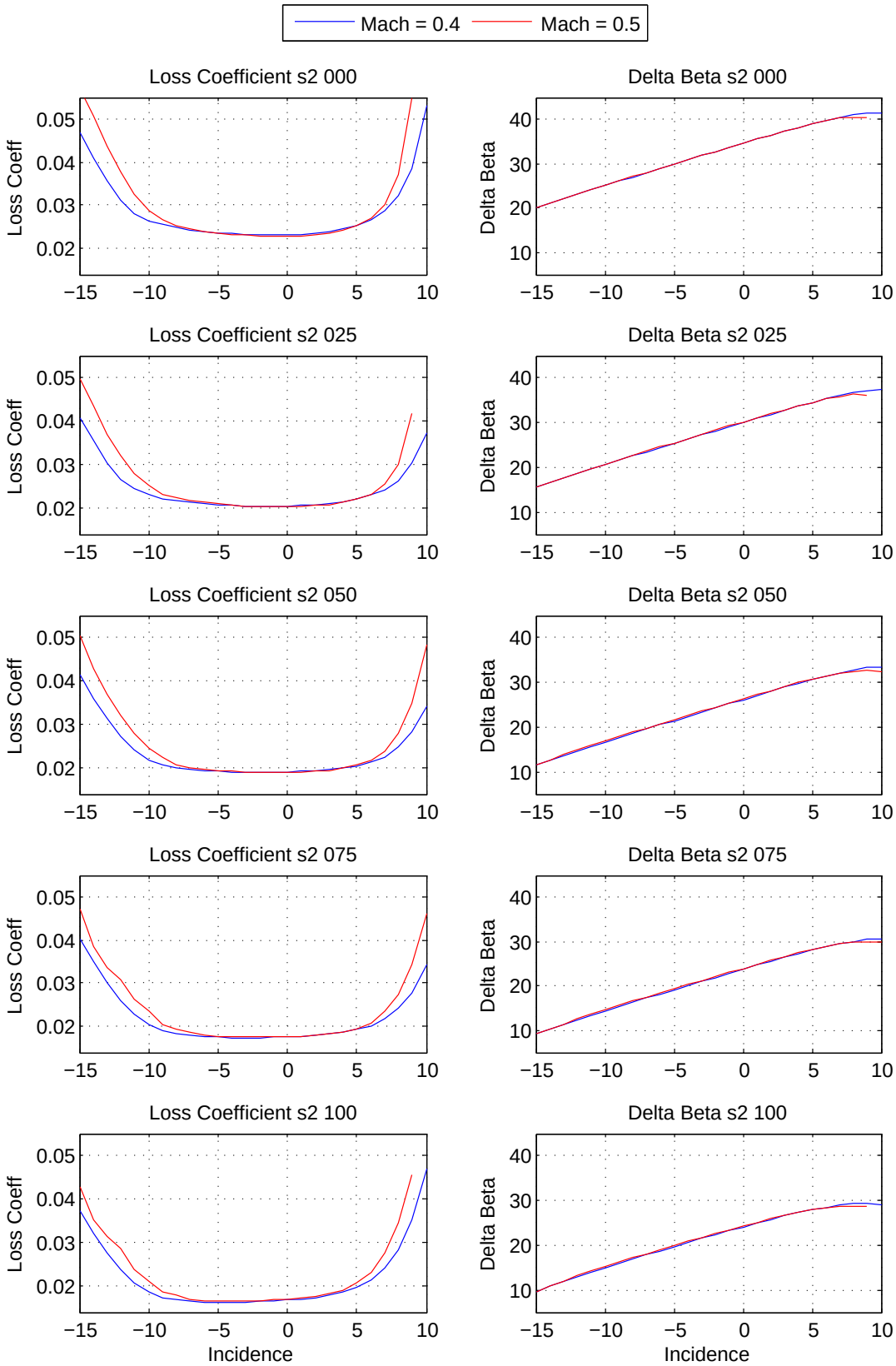

Figure 7.20: Summary of the results for the second stator blade (s2). From up to down, the profiles are neatly reported from hub to shroud. On the right side there are the graphics for the total pressure loss coefficient, while on the left there are the deflection trends.

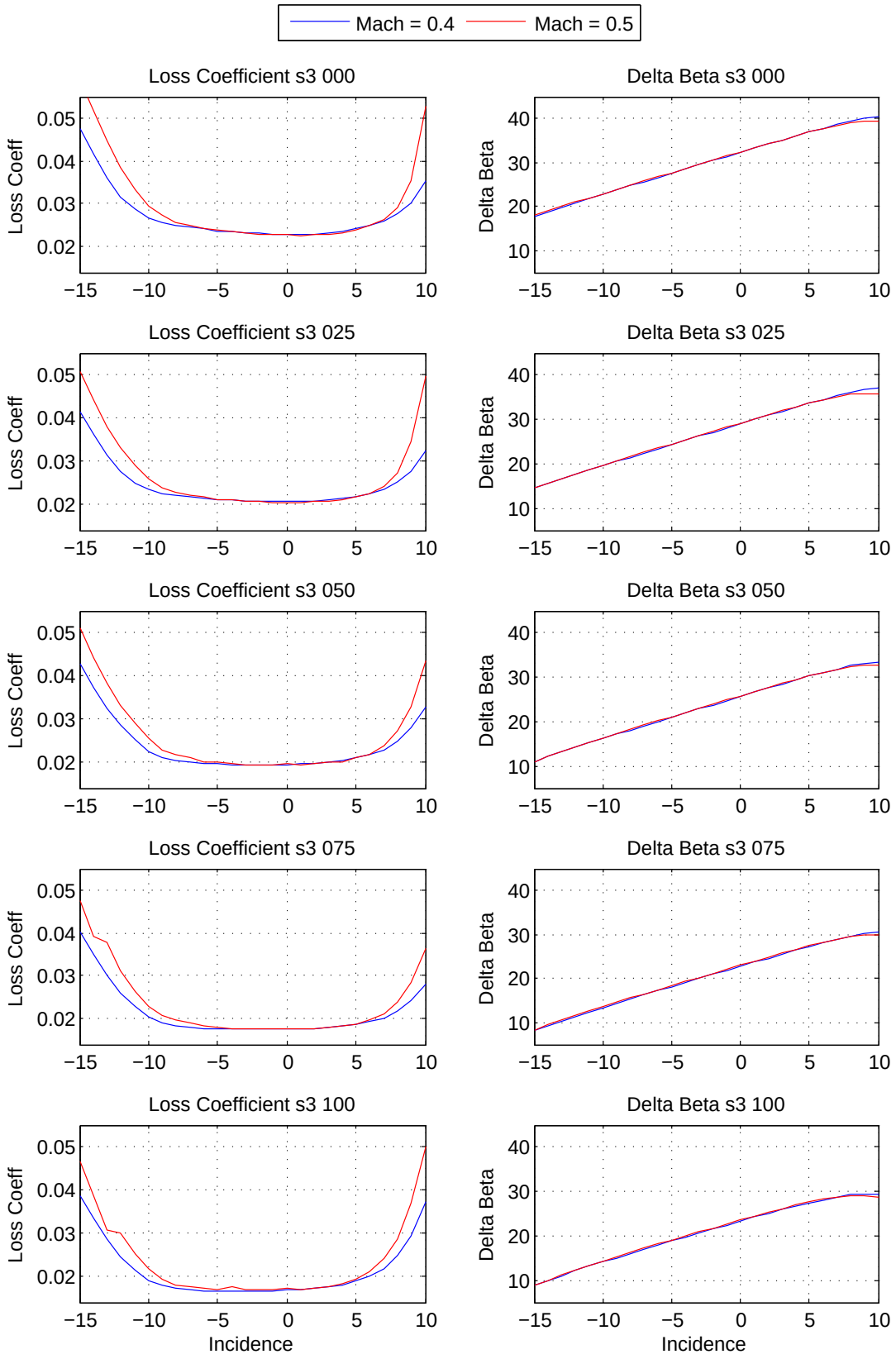

Figure 7.21: Summary of the results for the third stator blade (s3). From up to down, the profiles are neatly reported from hub to shroud. On the right side there are the graphics for the total pressure loss coefficient, while on the left there are the deflection trends.

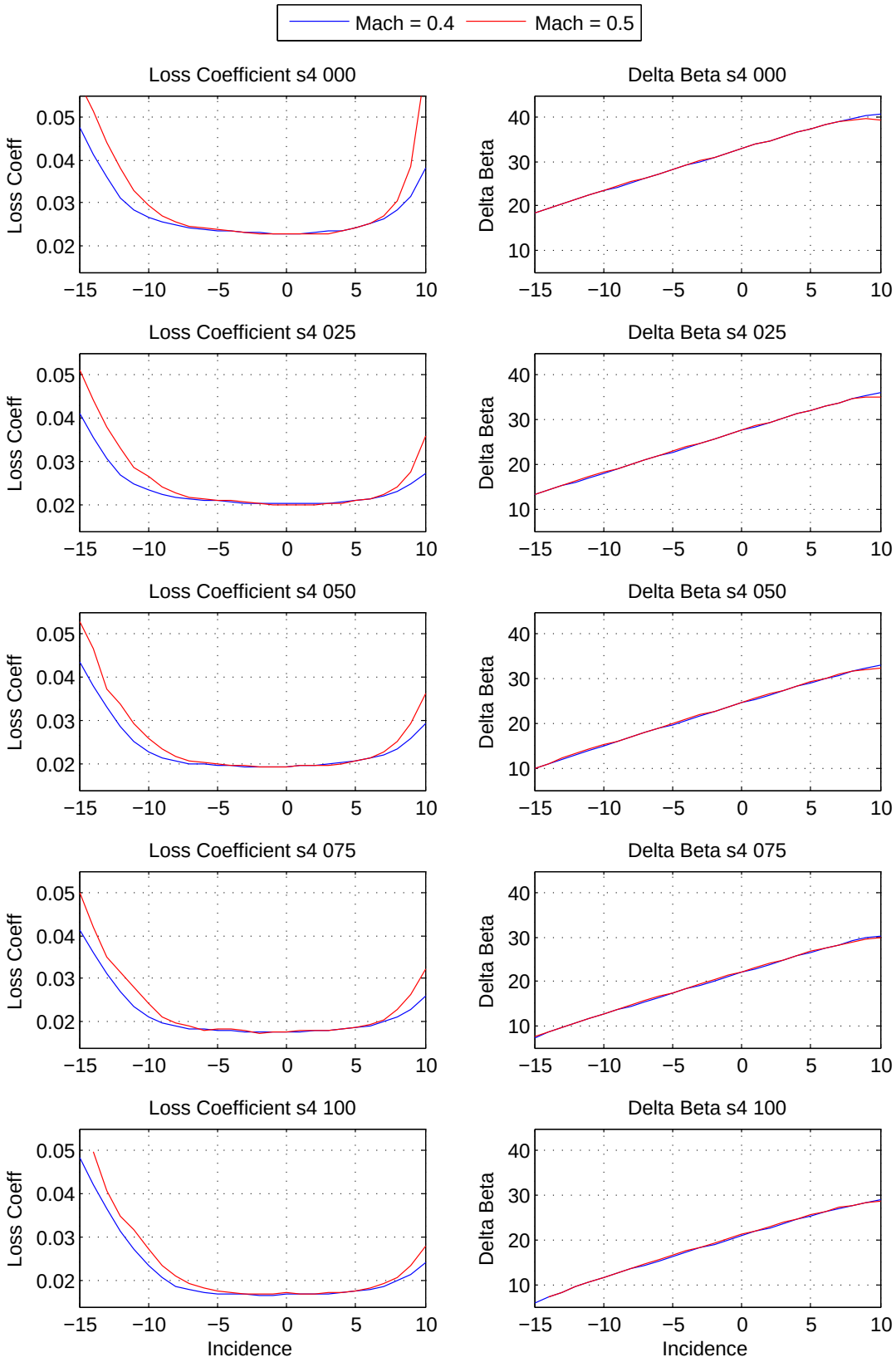

Figure 7.22: Summary of the results for the fourth stator blade (s4). From up to down, the profiles are neatly reported from hub to shroud. On the right side there are the graphics for the total pressure loss coefficient, while on the left there are the deflection trends.

7.2 Two-Phase Flow Results

As stated in Chapter 6, the main purpose of wet operating condition investigation is to compare the mass fraction between Inlet and Outlet sections in order to evaluate the amount of water mass on the blade walls. This is possible through the calculation of the mass fraction at:

- Inlet section: always the same value because the number of droplets injected into the domain is fixed at 150 (10 injection points with 15 diameter group each)
- Outlet section: it changes every time and this is in function of the number of droplets which can reach the Outlet surface in function on the Mach and Incidence angles as well

This investigation (primary evaluation) has been carried out by tracking the droplet paths inside the domain through a Lagrangian approach without resolving the flow field again and without considering the evaporation condition.

The investigation starts from the dry condition file results of hub profile of the first rotor blade and as stated in Chapter 6 by setting the expert parameters it is possible to add the wet investigation on the previous flow field. In this way the simulations take few seconds for the calculations and no interrupting criteria or max/min number of iteration definitions are required.

Different conditions of Mach number and Incidence angle have been investigated and in particular:

- M1=0,4 -15°<i<+11°
- M1=0,5 -15°<i<+10°
- M1=0,6 -12°<i<+10°
- M1=0,7 -5°<i<+8°

One graph for each Mach number condition will be extracted at the end with all the incidence specifications and a comparison of the normalized accumulated mass fraction will be reported.

7.2.1 Diameter size influence

As stated before for each injection point, 15 different diameter groups have been injected at the Inlet zone between upper and lower surfaces:

$$1,\ 2,\ 3,\ 4,\ 5,\ 10,\ 20,\ 30,\ 40,\ 50,\ 60,\ 70,\ 80,\ 90,\ 100\ [\mu m] \tag{7.3}$$

As it is possible to see in the picture (fig. 7.23), a totally different behaviour between smaller (<60 μm) and bigger droplets has been analyzed. Indeed, the smaller ones can easily adjust their paths in function of the direction of the main flow (air). Instead for big particles the iteration with the air flow decreases and the possibility to achieve or not the outlet surface is in function of the Mach number and, as it will be shown below, of the incidence angle as well.

However, as it is possible to imagine, a big diameter means big mass fraction (because it is in function of the volume of the droplet) and thus the final investigation can be influenced by this effect. Indeed, until a big diameter is present at the Outlet, it is not possible to investigate the iteration of the small particles in different conditions. Hence for further investigations it is better to decrease the droplet maximum size in order to obtain more information about the small particles.

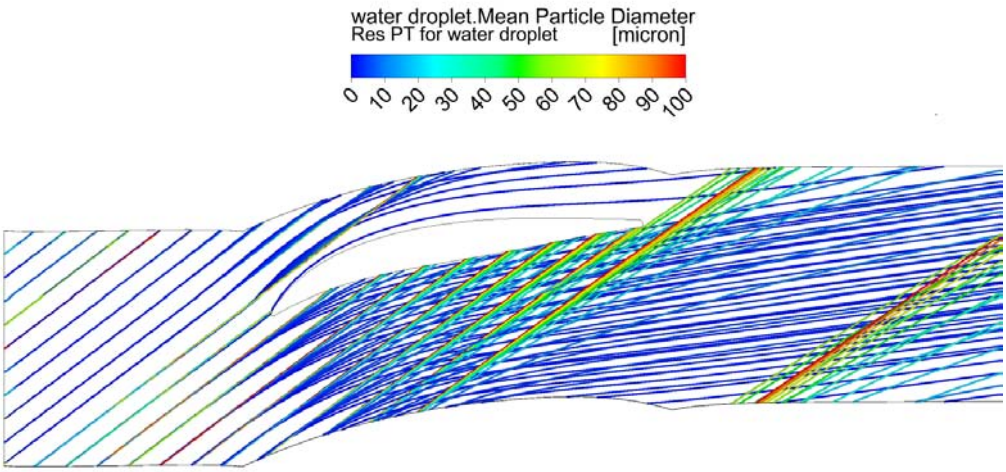

Figure 7.23: Particle paths into the domain in function of the diameter size

7.2.2 Incidence angle influence

The focus of this study is to compare the water mass fraction between Inlet and Outlet regions, on leveraging a normalized accumulated distribution of it (Chapter 6). The equation used for this investigation is here reported:

$$m_{di} = \frac{4}{3} * \pi * (\frac{d_i}{2})^3 * (\rho) * (n) \tag{7.4}$$

where it is possible to observe the influence of the droplet diameter, water density and number of particles for each diameter group at the Outlet (for Inlet surface the condition is always the same). The number of particles, which can go through the domain, is very different and it depends on the direction of the flow, hence on the incidence value as well.

This effect can be better understood by looking at the pictures below, where only one injection region is reported inside the domain in two different incidence conditions (it is also possible to understand the meaning of negative and positive specification of the incidence).

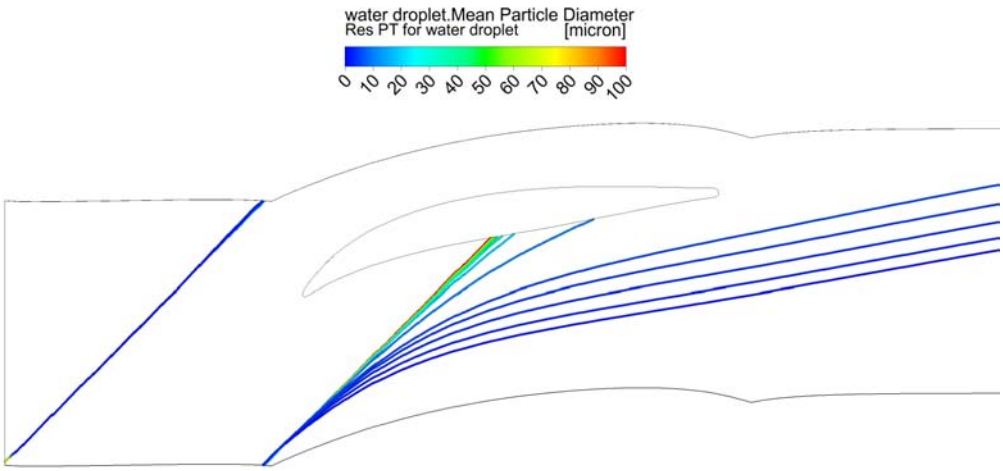

Figure 7.24: Particle paths of one injection region at M1=0,6; i=+8°

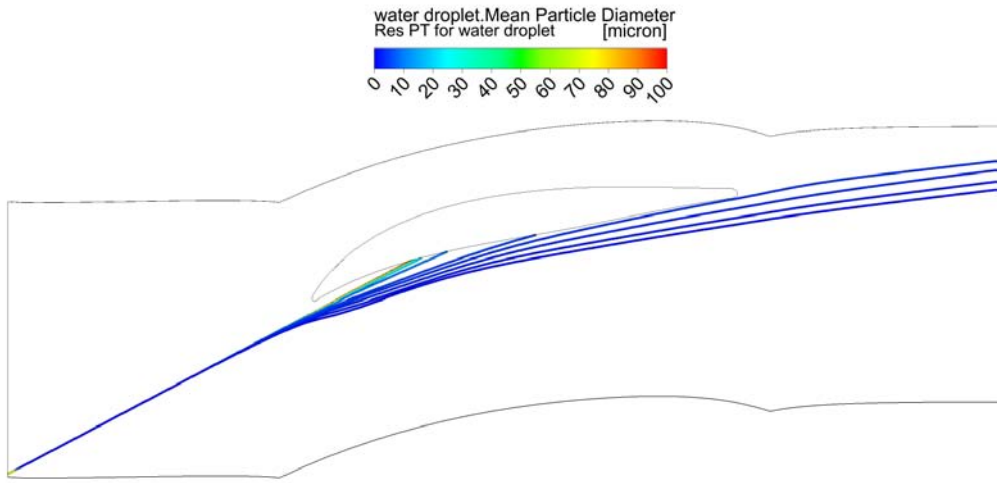

Figure 7.25: Particle paths of one injection region at M1=0,6; i=-10°

In these pictures (fig. 7.24 fig. 7.25) it is possible to investigate a totally different interaction of the droplets on the blade walls by changing the incidence value. For a positive definition of it the particles collide easier the blade because of their orientation. It is also possible to investigate again the influence of the diameter size, indeed mostly the small droplets can achieve the Outlet section in many different incidence conditions.

The final comparison of the normalized accumulated distribution of mass fraction in function of the droplet diameter is reported in the following graphics for all the Mach number conditions. From those graphs it is possible to evaluate the different behaviour of the water particles in function of the incidence. It is possible to observe a small difference between Inlet and Outlet mass fraction in negative conditions of incidence and it means that a lot of droplets (small and big) can reach the Outlet surface without colliding the blade. Moreover for a positive definition of the angle there is a big gap between Inlet and Outlet situations because of the direction, indeed the particles with a big diameter are not able to adjust their directions because the interaction with the main flow is lower than that one for the smaller droplets. Thus if the incidence is very high, the bigger particles from all the injection region can collide the blade.

The small differences between Outlet mass fraction distribution with negative incidence angle and Inlet one is caused by the big variation range given to the droplet size. Because, as it has been written before, one droplet with $100\mu m$ has the value of the mass fraction 100 times more than the one with $1\mu m$, hence until there will be at least one big particle, the influence of the small one is not considered and all the curves are very close to each other.

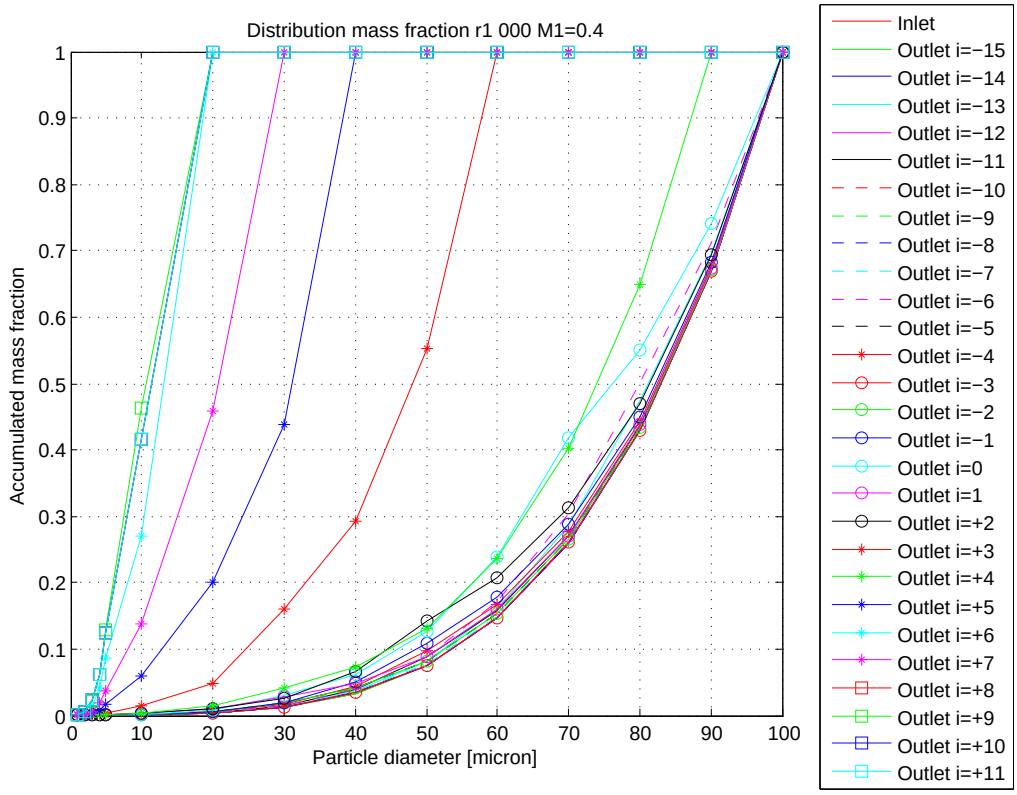

Figure 7.26: Normalized and accumulated mass fraction distribution for M1=0,4 in every incidence configuration

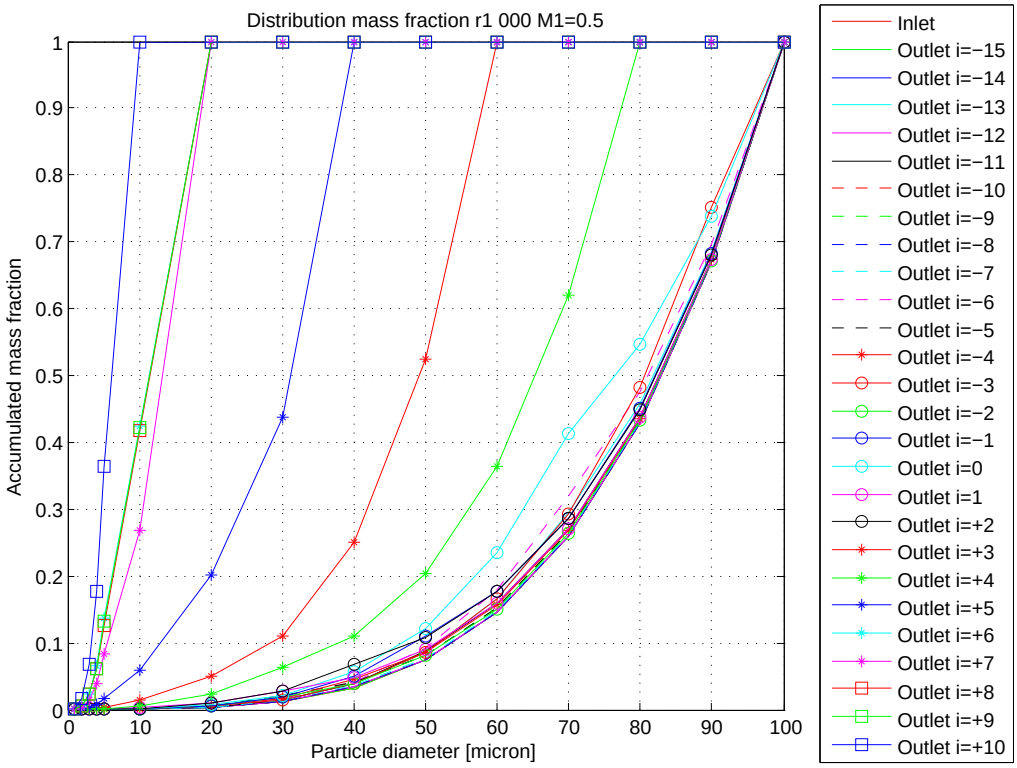

Figure 7.27: Normalized and accumulated mass fraction distribution for M1=0,5 in every incidence configuration

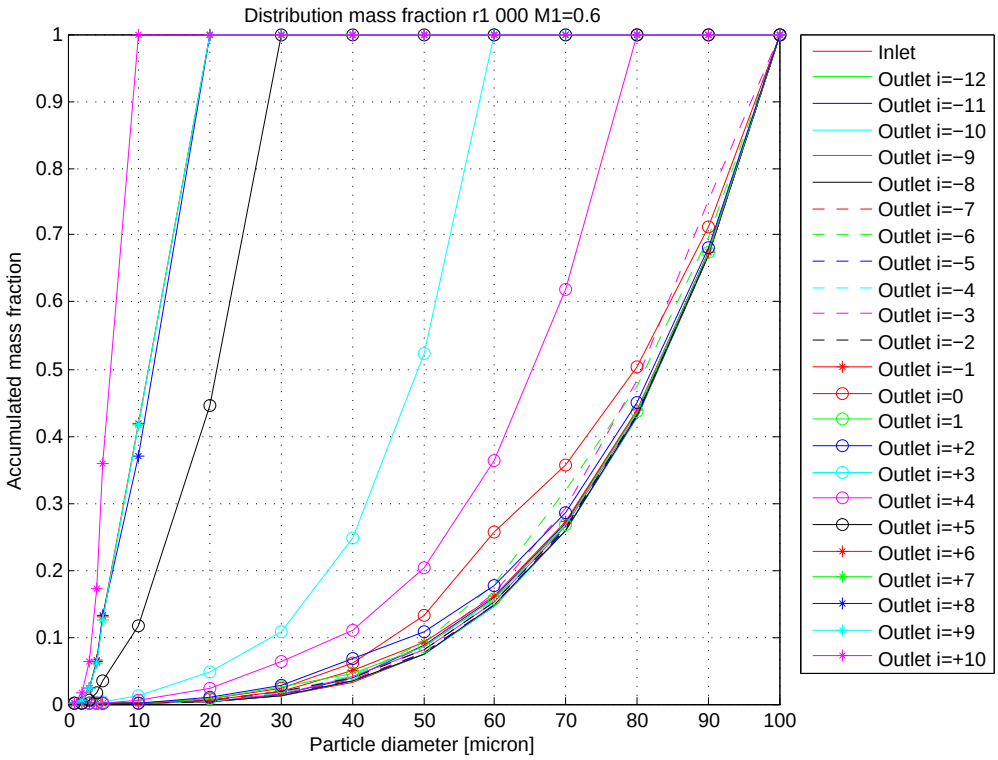

Figure 7.28: Normalized and accumulated mass fraction distribution for M1=0,6 in every incidence configuration

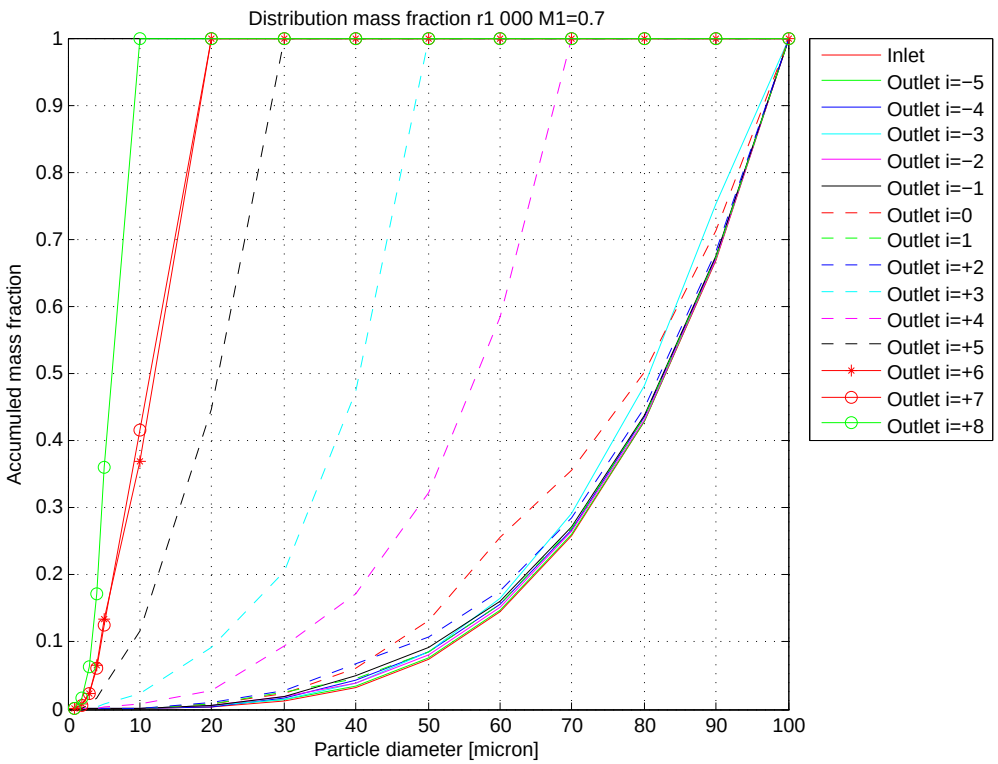

Figure 7.29: Normalized and accumulated mass fraction distribution for M1=0,7 in every incidence configuration

7.2.3 Mach number influence

Another comparison is here reported in order to investigate the behaviour of water droplets in function of the Inlet Mach number. In the final graphics (fig. 7.31 and fig.7.30) two different comparisons are reported, the first one (fig. 7.30) analyzes the differences between Mach number 0,4 and 0,7 and the second one reports a comparison between Mach 0,5 and 0,6 in order to understand the influence of the velocity. Only two different incidence configurations are reported, one in on-design condition (i=0°) and the other in off-design with a positive incidence value of angle (i=+4°). This value of incidence has been chosen because, as stated in the previous paragraph, there is not appreciable difference between Inlet and Outlet mass fraction distribution with negative angle.

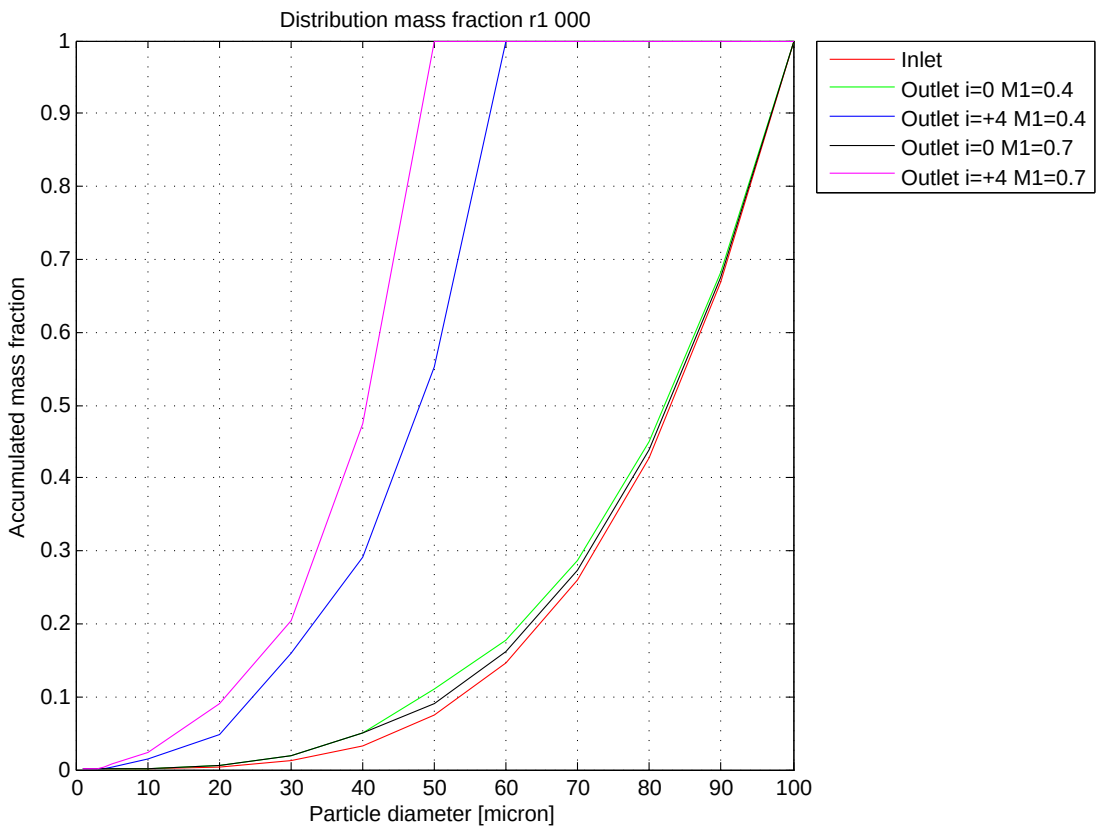

Figure 7.30: Comparison of mass fraction distribution in on and off design condition with M1=0,4 and M1=0,7

As it is possible to see in the picture (fig.7.30) there is not appreciable difference between two different Mach number conditions especially for on-design situation. Instead for off-design condition there is a gap between two different Outlet distributions of mass fraction in a same definition of incidence.

There are two principal reasons to explain this different behaviour in off-design:

- big difference of Mach number values and especially for this kind of profile M=0,7 it is very high (look at the results of dry condition) and the profile has not a good performance in this situation
- when the Mach number increases the time to adjust the direction of the flow (for a water droplet) decreases especially for the bigger ones, hence more particles can

collide the blade wall, thus the mass fraction at Outlet decreases.

In order to better understand these conditions, another comparison is here reported with a smaller gap of Mach number (fig. 7.31), it means M1=0,5 and M1=0,6, but with the same configurations of incidence angle as before. Here the difference in off-design condition is not appreciable, indeed the curves collapse almost in one, because the velocity is not so different and the behaviour is quite the same.

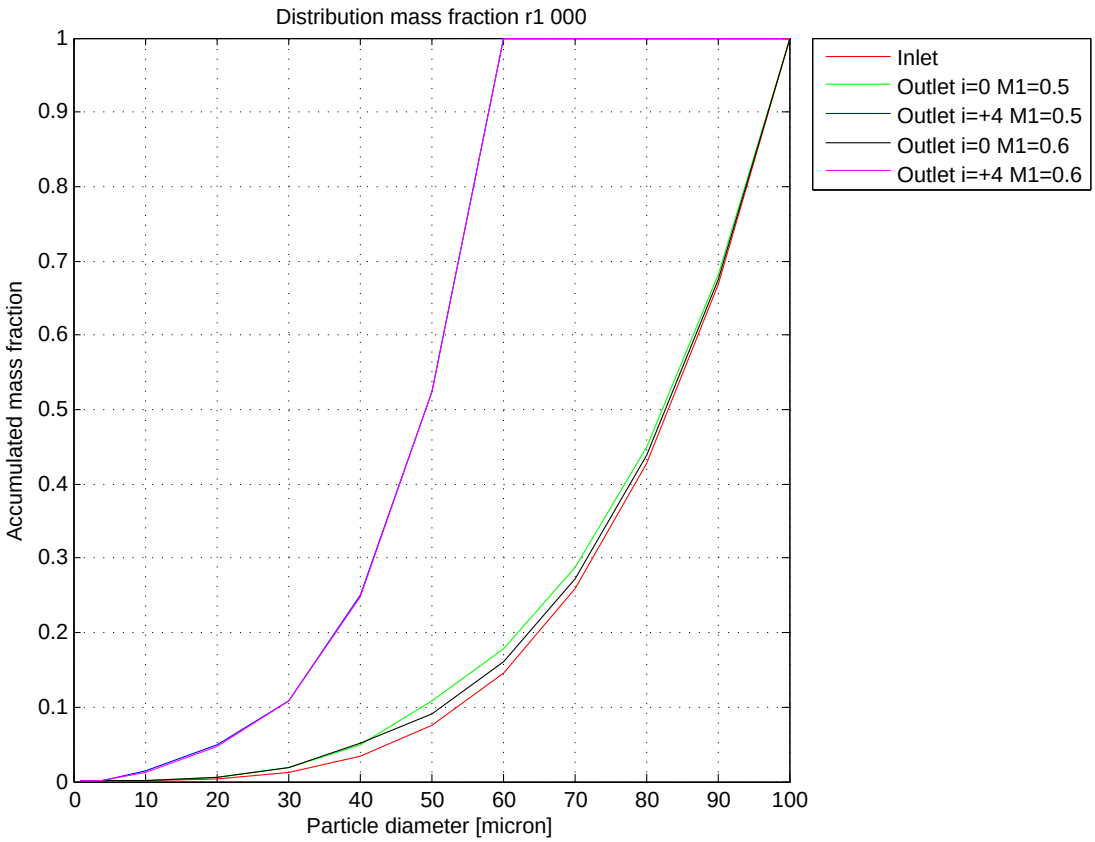

Figure 7.31: Comparison of mass fraction distribution in on and off design condition with M1=0,5 and M1=0,6

As it is possible to see in these pictures, in a design condition not an appreciable difference is investigated (i=0°) and this is because the water droplet in different velocity conditions can adjust its path better than the off-design before investigated for the influence of the presence of the blade. Because of it the particle has two possible ways: goes to the pressure side or to the suction side, in function of the pressure condition on the blade, but the collision can be avoided for a wide range of droplet size.

Chapter 8

Discussion and Conclusion

8.1 Conclusion

In this research a multi-stage axial compressor has been taken under exam in order to study the blade profile characteristics in dry and wet operating conditions. The main focus of this work is to introduce the final reports for both conditions in a new concept streamline curvature program, in order to investigate the performances of the entire compressor in a two-dimensional approach because it can save simulation time in some investigation process with the respect of the three-dimensional evaluation. For the dry condition all profiles have been examined in many different configurations of Mach number and incidence angle in order to define the total pressure loss coefficient for each profile (each span of the blade) and the deflection of the flow by comparing Inlet and Outlet flow angles. Instead of the wet condition a primary CFD investigation has been examined in order to define the behaviours of the water droplets inside the domain in function of the diameter size and the influence of Incidence angle and Mach number on the mass fraction.

The entire simulation process, started from extracting the profile points, setting the CFX-Pre Solver and the CFD-Post Processing, has been processed through different automatic Matlab scripts. With the first scripts it is possible to build the geometry profile and mesh the domain in Turbogrid, hence to obtain the final mesh file. The second Matlab script writes the session file for ANSYS CFX Pre and Post-Processing for dry condition. At the end of the first evaluation it is possible to start the second investigation of wet operating condition, given an automatic Matlab script again, in order to set the ANSYS CFX Pre and Post-processing phases starting from the dry condition results.

The automating scripting of the investigation is necessary for the high number of the different investigations present in this research and it can be used for further examinations which follow the same operative scheme (Mach number and Incidence angle like independent variables).

The final reports come from dry operation condition of every simulation situation ($\sim$ 4000) has been calculated, but not all of them have been reported in the final graphs because of a problem of convergence. Indeed through the passage channel M1=0,9 for rotor and M1=0,6 for stator blades are impossible to achieve because of the chocking conditions. It means that when the velocity increases too much the trough area decreases and the mass flow remains fixed at one value. Hence sometimes the simulation does not arrive at the convergence or if it is achieved the results are not reliable for further investigations. The final results which have been stated in the graphs of loss coefficient and flow deflection are comparable with those in literature but sometimes the variation range of the Incidence angle is not large enough in order to investigate the operating range of the profile taken

under exam especially for the stator blade in the last stage (shroud profile).

The simulations give as the most important results a wide regulation range for the IGV blades, it means that the flow can be adjusted in several directions remaining inside the operation range (without stall problems). The investigations lead to understand the importance of the profile bending especially for the first rotor blade at hub, where a high deflection leads to a high loss coefficient value in design condition. This is so high also because of the high velocity present at the hub profiles for the blocking of the blades, indeed the area decreases for the cylindrical development of the machine and the velocity increases. The same considerations are valid also for the stator blade profiles but the influence of the big curvature is not so important because the role of these blades is only to direct in a right way the flow to the next stage and this is one of the reason of the lower loss coefficient values present in those blades.

A numerical interpolations of the results (loss coefficient or defection) between two consecutive spans of one blade in the same operating condition is not possible. This is because some physical parameters like height or chord of the blade or AVDR value should be considered in order to create a general correlation for every condition, hence a polynomial or cubic interpolation is not enough.

The evaluation of wet operating condition has been carried out by leveraging the Euler-Lagrangian method (Euler for the air flow calculation and Lagrangian to track the particles paths inside the domain), without solving the flow field again but starting from the dry condition results. By following this approach it is possible to fix some injection regions exactly in a desired point and it is also possible to specify a number of droplets to injected in each region. The final evaluation is a comparison between Inlet and Outlet mass fraction distribution, in order to calculate the amount of the mass fraction which collides the blade hence without reaching the Outlet surface. This investigation does not consider the evaporation process, but this should be investigated in future research to declare the real number of droplets present at Outlet in order to find a right setting for the streamline curvature program in wet operating condition. Thus it is possible to fix into that software the percentage of water present stage by stage, and obviously it changes because of the collision with the blade and the evaporation process.

The simulations show a bigger influence of mass fraction distribution with the respect of the incidence angle (positive and negative) and the Mach number. Also the diameter size of the droplet has an important role in the investigation, because the smaller particles can adapt their flow following the air direction, instead the bigger ones can collide easier the blade walls. Moreover the variation range of the diameter should be decreased in order to better investigate the behaviours of the smaller droplet and analyze their influence on the mass fraction distribution.

Bibliography

[1] *Gas Turbine Engineering Handbook*. Elsevier Inc., fourth edition edition, 2012.

[2] E. Benini. *Slide Progetto di Macchine*. A.A. 2012/13.

[3] D. Borello, K. Hanjalic, and F. Rispoli. Computational of tip-leakage flow in a laminar compressor cascade with a second-moment turbulence closure. *International journal of Heat and Fluid Flow*, 28:587–601, 2007.

[4] S. Clauss, J. Schitzler, B. Barabas, P. Nagabhushan, F. Benra, and H. Dohmen. Tets ring design to explore water droplet behavior in a four stage axial compressor. *International Mechanical Engineering Congress and Exposition*, IMECE2013:13–21, 2013.

[5] S. L. Dixon and B.Eng. *Fluid Mechanics and Thermodynamics of Turbomachinery*. ELSEVIER, fifth edition edition.

[6] N. Falck. Axial flow compressor mean line design. Master's thesis, Lund University,Sweden, 2008.

[7] M. Hoeger, N. Sievers, and M. Lawerenz. On the performance of compressor blades with contoured endwalls.

[8] A. Inc. *ANSYS CFD-Post User's Guide*, November 2011. Release 14.0.

[9] A. Inc. *ANSYS CFX-Pre User's Guide*, November 2011. Release 14.0.

[10] A. Inc. *ANSYS CFX Reference Guide*, November 2011. Release 14.0.

[11] A. Inc. *ANSYS CFX-Solver Manager User's Guide*, November 2011. Release 14.0.

[12] A. Inc. *ANSYS CFX-Solver Modeling Guide*, November 2011. Release 14.0.

[13] A. Inc. *ANSYS TurboGrid User's Guide*, November 2011. Release 14.0.

[14] J. R. Khan and T. Wang. Implementation of a non-equilibrium heat transfer model in stage-stacking scheme to investigate overspray fog cooling in compressor. *International Journal of Thermal Sciences*, 68 (2013):63–78, 2013.

[15] U. Koller, R. Monig, B. Kusters, and H. Schreiber. Development of advanced compressor airfoils for heavy-duty gas turbine- part 1: Design and optimization. *Journal of Turbomachinery*, 122:397–405, 2000.

[16] U. Koller, R. Monig, B. Kusters, and H. Schreiber. Development of advanced compressor airfoils for heavy-duty gas turbine- part 2: Experimental and theoretical analysis. *Journal of Turbomachinery*, 122:406–415, 2000.

[17] R. I. Lewis. *Turbomachinery Performance Analysis.* Elsevier Science and Technology Books, May 1996.

[18] C. B. Meher-Homji. The historical evolution of turbomachinery. 2000.

[19] B. Ober. Experimental investigation on the aerodynamic performance of a compressor cascade in droplet laden flow. Master's thesis, Hamburg, 2013.

[20] D. Pizzo. Progetto di un compressore assiale monostadio. Master's thesis, University of Padova,Italy.

[21] M. Sanjosè, J. Senoner, F. Jaegle, B. Cuenot, S. Moreau, and T. Poinsot. Fuel injection model for euler-euler and euler-lagrange large-eddy simulations of an evaporating spray inside an aeronautical combustor. *Elsevier*, 2011.

[22] J. Schnitzler, I. von Deschwanden, and S. Clauss. Experimental determination of a four stage axial compressor map operating in wet compression. *Turbo Expo 2014*, GT-2014-26807:16–20, 2014.

[23] B. Song and W. F. Ng. Influence of axial velocity density ratio in cascade testing of supercritical compressor blade. *American Institute of Aeronautics and Astronautics*, 2004.

[24] T. Sonoda, Y. Yamaguchi, T. Arima, M. Olhofer, B. Sendhoff, and H. Schreiber. Advanced high turning compressor airfoils for low reynolds number condition- part 1: Design and optimization. *Journal of Turbomachinery*, 126:350–359, 2004.

[25] T. Sonoda, Y. Yamaguchi, T. Arima, M. Olhofer, B. Sendhoff, and H. Schreiber. Advanced high turning compressor airfoils for low reynolds number condition- part 2: Experimental and numerical analysis. *Journal of Turbomachinery*, 126:350–359, 2004.

[26] Y. Takahashi, C. Myoren, B. Barabas, and K. Kawamura. Axial compressor and gas turbine having axial compressor. *Hitachi Ltd.*, 2013.

Appendix A

Geometry construction and Mesh definition

A.1 General Script

```
%% GENERAL FILE
% Blades definition
global mode;
mode = 'igv';       %inlet guide vane
mode = 'r';         %rotor
mode = 's';         %stator
% definition of Span position
span = ['000'; '025'; '050'; '075'; '100'];
%%%%%%%%%%%%%%%%%%%%%%%%%%%%%%%%%%%%%%%%%%%%%%%%%%%%%%%%%%%%%%%%%%
%% ATT. the number of the blade changes for rotor, stator or igv
% Zigv = 29;
% Zr = 31;
% Zs = 33;
%%%%%%%%%%%%%%%%%%%%%%%%%%%%%%%%%%%%%%%%%%%%%%%%%%%%%%%%%%%%%%%%%%

% n° of the blades
Z = 33;           %real number different for each case
Z1 = 360;         %boundary conidititon for Turbogrid
% Script for IGV blades
if strcmp(mode,'igv')
    for i = 1:5
    sp = span(i,:);

    %% Create Profile IGV
    [r(i),R(i),M2,M3,r_min_h,r_max_h,r_min_s,r_max_s] = \...
        Profile_point_IGV(Z1,Z,sp);

    %% Create mesh IGV
    Create_mesh_refine_IGV(M2,M3,r_min_h,r_max_h,\...
                r_min_s,r_max_s,Z1,sp);

    end

% Script for Rotor and Stator
elseif strcmp(mode,'r') || strcmp(mode,'s')
for stg = 1:4
```

```
   path = [pwd,'\',mode,num2str(stg)];
    if ~isdir(path)
        mkdir(path);
    end
    for i = 1:5
        sp = span(i,:);

        %% Create Profile Rotor or Stator
        [r(i),R(i),M2,M3,r_min_h,r_max_h,r_min_s,r_max_s] = \...
            Profile_point(Z1,Z,sp,stg);

        %% Create mesh Rotor or Stator
        Create_mesh_refine(M2,M3,r_min_h,r_max_h,\...
                r_min_s,r_max_s,Z1,sp,stg);

    end
end
end
```

A.1.1 Extraction profile points

```
% Export profile points and Turbogrid file definition
function [r,R,M2,M3,r_min_h,r_max_h,r_min_s,r_max_s] = \...
    Profile_point_IGV(Z1,Z,sp)

global mode;
% example for IGV blades the same is for Rotor and Stator
%% WRITE PROFILE FROM .IGS FILE
% setup for the variables
% extract only the coordinate numbers
% search and read file .IGS
filename = horzcat(pwd,'\',mode,'\',mode,'_',sp,'_pro_span.igs');
file_check = fopen(filename);
    s = textscan(file_check,'%q');
fclose(file_check);
% extract only the x,y and z coordinates
for i = 4:7
    m = strcat('406,1,',num2str(i),'HPNT');
    r = size(s{1,1});
    r = r(1);
    for k = 1:r
        a = strncmp(m,s{1,1}(k),10);
        if a == 1
            j = k;
            x = strcat(s{1,1}(j+3,1));
            st = x{1,1};
            xi = str2num(st);
            point(k,:) = [xi(1,2) xi(1,3) xi(1,4)];
        end
    end
end

%% create matrix for "hub" profile
% delete unnecessary points
T = [0 0 0];
nz = length(T);
```

```
e = size(point,1);
M1 = point(:,:);
o = 0;
q = zeros(1,nz);
for i = 1:e
    if M1(i,:)== T(1,:)
    o = o+1;
    q(o) = i;
    end
end
point(q(1:o),:)=[];
% write first profile
M2r = point;

%% radius moltiplication
% the solidity must be the same
% calculate from number of blades the new value of radius

r = M2r(1,3);
R = ((Z1*r)/Z);
M2 = [M2r(:,1) M2r(:,2) (M2r(:,3)+R-10-M2r(:,3))];

%% create matrix for profile "shroud"
M3 = [M2(:,1) M2(:,2) M2(:,3)+2.3+20];

%% create a unique file_profile
% write in a unique txt file the coordinates of the two profiles

%% create "hub.curve" domain

LEh = M2(r_min_h,:);
TEh = M2(r_max_h,:);
INLETh = [LEh(1,1)-25 0 LEh(1,3)+10];
OUTLETh = [TEh(1,1)+100 0 TEh(1,3)+10];
HUB = [INLETh; OUTLETh];
filename2=strcat(pwd,'\',mode,'\',mode,'_',sp,'\GEOM\hub.curve');
dlmwrite(filename2,HUB, 'delimiter', '\t', 'precision', 6);

%% create "shroud.curve" domain

LEs = M3(r_min_s,:);
TEs = M3(r_max_s,:);
INLETs = [LEs(1,1)-25 0 LEs(1,3)-10];
OUTLETs = [TEs(1,1)+100 0 TEs(1,3)-10];
SHROUD = [INLETs; OUTLETs];
filename3=strcat(pwd,'\',mode,'\',mode,'_',sp,'\GEOM\shroud.curve');
dlmwrite(filename3,SHROUD, 'delimiter', '\t', 'precision', 6);

%% create file .INF for create the solid domain
filename4=strcat(pwd,'\',mode,'\',mode,'_',sp,'\GEOM\',mode,'.inf');
fid = fopen(filename4,'w');
import=strcat('!======  ANSYS BladeGen Export  ======== \r\n',...
                'Axis of Rotation: X \r\n',...
                'Number of Blade Sets:  ',num2str(Z1),' \r\n',...
                'Number of Blades Per Set: 1 \r\n',...
                'Blade Loft Direction: Streamwise \r\n',...
```

```
                 'Geometry Units: MM \r\n',...
                 'Coordinate System Orientation: Righthanded \r\n',...
                 'Blade 0 LE: EllipseEnd \r\n',...
                 'Blade 0 TE: EllipseEnd \r\n',...
                 'Hub Data File: hub.curve \r\n',...
                 'Shroud Data File: shroud.curve \r\n',...
                 'Profile Data File: file_profile.curve \r\n');
fprintf(fid,import);
fclose(fid);
end
```

A.1.2 Mesh Definition

```
%% CREATE MESH
% Writting state file for TurboGrid to define the mesh specification
function Create_mesh_refine_IGV(M2,M3,r_min_h,r_max_h,\...
                r_min_s,r_max_s,Z1,sp);
global mode;
% Set parameters for Mesh
GSF = 1.9;        % Global Size Factor
NESW = 3;         % Number of Elements Spanwise
FEO = 0.04;       % First Element Offset
ES1 = 1.5;        % Factor Edge Split 1
ES2 = 2.5;        % Factor Edge Split 2
ES3 = 2.5;        % Factor Edge Split 3
ES4 = 1;          % Factor Edge Split 4
ES5 = 2.5;        % Factor Edge Split 5
ES6 = 1;          % Factor Edge Split 6
ES7 = 2.5;        % Factor Edge Split 7
ES8 = 1;          % Factor Edge Split 8
%% Write file for TGRID (state file)
% definition
filename = horzcat(pwd,'\',mode,'\',mode,'_',sp,'\TGRID\',\...
                     mode,'_',sp,'.tst');
fid = fopen(filename,'w');
import = strcat('BOUNDARY:HIGHBLADE \r\n',...
                  'Apply Instancing Transform = On \r\n',...
                  %% general state file where the initial setting
                   % and the definitions for the Matlab function
                   % can be written
                  'Update Units to Preferred = Off \r\n',...
                 'END \r\n');
fprintf(fid,import);
fclose(fid);
% writting of a session file in order to save the final .GTM file
% required from ANSYS CFX
filename2 = horzcat(pwd,'\',mode,'\',mode,'_',sp,'\TGRID\',\...
                     mode,'_',sp,'.tse');
fid = fopen(filename2,'w');
import = strcat('% running the state file and saving the .GTM file
fprintf(fid,import);
fclose(fid);
end
```

Appendix B

ANSYS Pre and Post Processing

B.1 General Script

```
%% GENERAL FILE CFX CREATOR
% this is an example of ANSYS CFX Pre definition, but the same
% scheme is for the Post Processing setting (the name of the
% function change)
% span position definition
span = ['000'; '025'; '050'; '075'; '100'];
% CREATE FILE BATCH
filename = horzcat(pwd,'\batch.bat');
batch = fopen(filename,'w');
%% Rotor script definition
% loop valid also for Stator and IGV blades
% definition of the number of the stage
for stg = 1:4
%% ROTOR
mode = 'r';
% loop for all Mach number
    for M1 = 0.4:0.1:0.6
        if M1 == 0.4
            % variation range of incidence
            LB = -15;
            UB = 11;
            % selection of the span
            for i = 1:5
                sp = span(i,:);
                % launch function with the setting specification
                CFX_Pre_ROTOR (mode,stg,sp,M1,LB,UB,batch)
            end
        elseif M1 == 0.5
            LB = -15;
            UB = 10;
            for i = 1:5
                sp = span(i,:);
                CFX_Pre_ROTOR (mode,stg,sp,M1,LB,UB,batch)
            end
        else % M1 == 0.6
            LB = -12;
            UB = 10;
            for i = 1:5
```

```
                sp = span(i,:);
                CFX_Pre_ROTOR (mode,stg,sp,M1,LB,UB,batch)
            end
        end
    end
    for M1 = 0.7:0.1:0.8
        if M1 == 0.7
            LB = -8;
            UB = 8;
            for i = 1:5
                sp = span(i,:);
                CFX_Pre_ROTOR (mode,stg,sp,M1,LB,UB,batch)
            end
        else %M1 == 0.8
            LB = -6;
            UB = 6;
            for i = 2:5
                sp = span(i,:);
                CFX_Pre_ROTOR (mode,stg,sp,M1,LB,UB,batch)
            end
        end
    end
end
fclose(batch);
```

B.1.1 ANSYS CFX Pre Setting

```
%% FILE CFX PRE (for Rotor but the same is for Stator and IGV blades)
function CFX_Pre_ROTOR (mode,stg,sp,M1,LB,UB,batch)
% CHARACTERIZATIO VARIABLES
% read the external file with the angles specifications
filename = horzcat(pwd,'\',mode,num2str(stg),'\',mode,num2str(stg),\...
                '_',sp,'\GEOM\',mode,num2str(stg),'_',sp,'.txt');
Angle_inlet = importdata(filename);
% angle of Camber line
BetaMetalIn = Angle_inlet(1,1);
% Pressure side angle at Leading edge
LE_PS = Angle_inlet(1,2);
% Suction side angle at Leading edge
LE_SS = Angle_inlet(1,3);
% SOLVER VARIABLES
LTF = 15;        % local timescale factor
MAXIter = 800;   % maximum number of iterations
MINIter = 350;   % minimum number of iterations
RMS = 1.E-5;     % Residual limit for convergence
Conv = 1.E-9;    % Interrupting criteria
%% define incidence zero (simulation run without previous file .res)
inc = 0;
% writing session file for ANSYS CFX Pre setting
    import = strcat('COMMAND FILE: \r\n',...
                        'CFX Pre Version = 14.0 \r\n',...
                % sessione file where write the solver varialbes,
                % eqautions and initial conditions for the entire
                % simulations
                    '> update \r\n');
    fprintf(fid,import);
```

```
    fclose(fid);
% running the session file in order to obtain the .DEF file
% writing the batch file in the external text format file

%% Script for the others positive incidence conditions
% (the same is for negative)
for inc = 1:UB
    import = strcat('COMMAND FILE: \r\n',...
                        'CFX Pre Version = 14.0 \r\n',...
                    % sessione file where write the solver varialbes,
                    % eqautions and initial conditions for the entire
                    % simulations
                        '> update \r\n');
    fprintf(fid,import);
    fclose(fid);
% running the session file in order to obtain the .DEF file
% starting from the result file of the previous simulations.
% Writing the batch file in the external text format file
% with the specification of the interpolation criteria
% in order to start the new simulation from the old one
end
end
```

B.1.2 ANSYS CFD Post Processing

```
%% CFX POST ROTOR
% the same is for Stator and IGV blades
function CFX_Post_ROTOR (mode,stg,sp,M1,LB,UB)
% check if the simulations converge or not
inc1 = (LB:UB);
for inc = LB:UB
    v=find(inc1==inc);
    path1 = % check if the result's folder exist or not
    % if not exist
    if isdir(path1)
        Incidence1(v,1) = NaN;
        Loss_Coeff5_n(v,1) = NaN;
        Loss_Coeff6_n(v,1) = NaN;
        Delta_Beta1(v,1) = NaN;
        Beta_1ref(v,1) = NaN;
        Beta_2ref(v,1) = NaN;
        % else check the residual values of convergence
    elseif ~isdir(path1)
        % read the output file of the results and check
        % the domain imbalances
        m = strcat('%:');
        r = size(s{1,1});
        r = r(1);
        for k = 1:r
            a = strncmp(m,s{1,1}(k),2);
            if a == 1
                j = k;
                Perc = strcat(s{1,1}(j+1,1));
                DI = Perc{1,1};
                DIn = str2num(DI);
                DIa = abs(DIn);
```

```
                % good convergence if domain imbalance
                % DI < 0.1
                if DIa > 0.1
                    break
                end
            end
        end
        % if bad convergence
        if DIa > 0.1;
            Incidence1(v,1) = NaN;
            Loss_Coeff5_n(v,1) = NaN;
            Loss_Coeff6_n(v,1) = NaN;
            Delta_Beta1(v,1) = NaN;
            Beta_1ref(v,1) = NaN;
            Beta_2ref(v,1) = NaN;
        % if good convergence
        elseif DIa < 0.1;
        % create a session file for Post-Processing
            import = strcat('COMMAND FILE: \r\n',...
                              'CFX Post Version = 14.0 \r\n',...
                            % session file where write the eqautions
                            % in order to evaluate the final results
                            % in a tabular form and export all the
                            % reports in a text format
            fprintf(fid,import);
            fclose(fid);
            % read the external text file and extract
            % the different results like incidence,
            % loss coefficient, delta beta and flow
            % angles (following exampple for incidence)
            for i = 1:6
                m = strcat('Incidence');
                r = size(A{1,1});
                r = r(1);
                for k = 1:r
                    a = strncmp(m,A{1,1}(k),9);
                    if a == 1
                        j = k;
                        x = strcat(A{1,1}(j+1,1));
                        I = x{1,1};
                        Incidence = str2num(I);
                    end
                end
            end
            % write the final results in a matricial form
            Loss_Coeff5_n(v,1) = Loss_Coeff5;
            Loss_Coeff6_n(v,1) = Loss_Coeff6;
            Delta_Beta1(v,1) = Delta_Beta;
            Beta_1ref(v,1) = Beta_1;
            Beta_2ref(v,1) = Beta_2;
        end
    end
end
end
```

Appendix C

Wet condition ANSYS Pre

C.1 ANSYS CFX Pre Setting

```
%% FUNCTION FILE FOR PRE SOLVER (the general file for launch this
%function is the same wrote for dry condition Appendix B)
%% FILE CFX PRE
% only for hub profile of first rotor blade M1=0,6 at different
% incidence conditions
function CFX_Pre_wet (mode,stg,sp,M1,LB,UB,batch)
%% data from previou calculations
radius = #####; %[m] % middle radius between upper and lower surf.
teta = #####; %[degree] % opening angle
% writing session file for ANSYS CFX Pre seetting
for inc = LB:UB
        import = strcat('COMMAND FILE: \r\n',...
                          'CFX Pre Version = 14.0 \r\n',...
                        % session fie where write the initial
                        % conditions and set the expert parameters
                        '> update \r\n');
        fprintf(fid,import);
        fclose(fid);

% running the session file in order to obtain the .DEF file
% writing the batch file in the external text format file
end
end
```